EDITORIAL STAFF

R. J. McKay, Chairman, Publication Committee

Cecil V. King, Editor

Norman Hackerman, Technical Editor

Ruth G. Sterns, Managing Editor

U. B. Thomas, News Editor

H. W. Salzberg, Book Review Editor

Natalie Michalski, Assistant Editor

DIVISIONAL EDITORS

W. C. Vosburgh, Battery

J. E. Draley, Corrosion, I

R. T. Foley, Corrosion, II

John J. Chapman, Electric Insulation

Abner Brenner, Electrodeposition

H. C. Froelich, Electronics

D. H. Baird, Electronics—Semiconductors

Sherlock Swann, Jr., Electro-Organic

John M. Blocher, Jr., Electrothermics and Metallurgy, I

A. U. Seybolt, Electrothermics and Metallurgy, II

W. C. Gardiner, Industrial Electrolytic

C. W. Tobias, Theoretical Electrochemistry, I

A. J. de Bethune, Theoretical Electrochemistry, II

REGIONAL EDITORS

Howard T. Francis, Chicago

Joseph Schulein, Pacific Northwest

J. C. Schumacher, Los Angeles

G. W. Heise, Cleveland

G. H. Fetterley, Niagara Falls

Oliver Osborn, Houston

Earl A. Gulbransen, Pittsburgh

A. C. Holm, Canada

J. W. Cuthbertson, Great Britain

T. L. Rama Char, India

ADVERTISING OFFICE

Jack Bain, Advertising Manager
545 Fifth Avenue, New York 17, N. Y

ECS OFFICERS

Norman Hackerman, President
University of Texas, Austin, Texas

Sherlock Swann, Jr., Vice-President
University of Illinois, Urbana, Ill.

W. C. Gardiner, Vice-President
Olin Mathieson Chemical Corp., Niagara Falls, N. Y.

R. A. Schaefer, Vice-President
Cleveland Graphite Bronze Div., Clevite Corp., Cleveland, Ohio

Lyle I. Gilbertson, Treasurer
Air Reduction Co., Murray Hill, N. J.

Henry B. Linford, Secretary
Columbia University, New York, N. Y.

Robert K. Shannon, Assistant Secretary
National Headquarters, The ECS, 1860 Broadway, New York 23, N. Y.

Journal of the
Electrochemical Society

DECEMBER 1957 **VOL. 104 • NO. 12**

CONTENTS

Editorial

Dielectric Materialism 247C

Technical Papers

Anodization of Lead and Lead Alloys in Sulfuric Acid. *J. Burbank* 693

Disintegration of Lead Cathodes, II. *L. W. Gastwirt and H. W. Salzberg* 701

Polarization Capacity at Solid Electrodes and True Surface Area Values. *R. J. Brodd and N. Hackerman* 704

Reaction of Hydrogen with Preoxidized Zircaloy-2 at 300° to 400°C. *E. A. Gulbransen and K. F. Andrew* 709

Effect of Current Drains on Cadmium Standard Cells. *G. D. Vincent* 712

Electroluminescence of Zinc Sulfoselenide Phosphors with Copper Activator and Halide Coactivators. *I. J. Hegyi, S. Larach, and R. E. Shrader* 717

Heat Treatment of Silicon Using Zone Heating Techniques. *H. C. Theuerer, J. M. Whelan, H. E. Bridgers, and E. Buehler* 721

Electrolytic Extraction of Thorium from Fused Salts. *L. Abraham, E. L. Thellmann, and J. L. Wyatt* 724

Principles of Very Low Power Electrochemical Control Devices. *R. M. Hurd and R. N. Lane* 727

Impedance and Polarization Measurements in Fused Lithium Chloride-Potassium Chloride. *H. A. Laitinen and H. C. Gaur* 730

Technical Note

The Influence of Surface Pretreatment on the Atmospheric Oxidation of 2S (U. S. Alloy 1100) Aluminum. *P. M. Aziz and H. P. Godard* 738

Technical Review

Electroluminescence and Field Effects in Phosphors. *H. F. Ivey* 740

Discussion Section 749

Current Affairs

News Notes in the Electrochemical Field 249C

Now Available the 1955 Issue of Semiconductor Abstracts 250C

Division News 251C

Section News 251C

New Members 252C

Personals 253C

Letter to the Editor 254C

Book Reviews 254C

Employment Situation 256C

Published monthly by The Electrochemical Society, Inc., from Manchester, N. H., **Executive Offices, Editorial Office** and **Circulation Dept.** at 1860 Broadway, New York 23, N. Y., **Advertising Office** at 545 Fifth Ave., New York, N. Y., combining the JOURNAL and TRANSACTIONS OF THE ELECTROCHEMICAL SOCIETY. Statements and opinions given in articles and papers in the JOURNAL OF THE ELECTROCHEMICAL SOCIETY are those of the contributors, and The Electrochemical Society assumes no responsibility for them. Nondeductible subscription to members $5.00; subscription to nonmembers $18.00. Single copies $1.25 to members, $1.75 to nonmembers.

Copyright 1957 by The Electrochemical Society, Inc.

Entered as second-class matter at the Post Office at Manchester, N. H., under the act of August 24, 1912.

SARGENT Polarographs*

*Trademark Reg. U. S. Pat. Off.

MODEL III

Designed and Manufactured by E. H. Sargent & Co. for all Polarographic Applications in Research and Control Analysis

MODEL XXI POLAROGRAPH—S-29303—Pen Recording, Potentiometric. The complete automatic programming, the combined visual indicator and chart recorder, and the wide flexibility in controls make it most convenient for both research studies and routine analytical applications.

MODEL XII POLAROGRAPH—S-29301—Photographic Recording, Indicating. An adaptation of the original Sargent-Heyrovsky Micro Polarograph, Model X. Recommended for use in routine analyses and research procedures where the step form departs from the theoretical, simple shape and is complicated by maxima, complex formation, presence of several different ions, irreversible reactions, etc. and where it is consequently necessary to have a continuously plotted polarogram.

MODEL III POLAROGRAPH—S-29290—Manual, Indicating. Recommended for use in those routine analyses where only one substance is determined and where the step shape approximates a pure form, characteristic of reversible reactions involving simple ions in fairly substantial concentrations. Also useful in the performance of amperometric titrations and for instructional purposes in educational institutions.

MODEL XXI

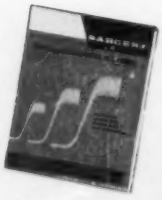

Write for our booklet on Polarographs and Accessory Equipment

MODEL XII

SARGENT

SCIENTIFIC LABORATORY INSTRUMENTS • APPARATUS • SUPPLIES • CHEMICALS

E. H. SARGENT & COMPANY, 4647 W. FOSTER AVE., CHICAGO 30, ILLINOIS
MICHIGAN DIVISION, 8560 WEST CHICAGO AVENUE, DETROIT 4, MICHIGAN
SOUTHWESTERN DIVISION 5915 PEELER STREET, DALLAS 35, TEXAS
SOUTHEASTERN DIVISION, 3125 SEVENTH AVE., N., BIRMINGHAM 4, ALA.

Editorial

Dielectric Materialism

THE Electric Insulation Division is the smallest Division of The Electrochemical Society, with 87 members at the last report. It may be predicted that the Division has a promising future and will almost certainly grow in numbers. Industrial and military requirements are rapidly expanding for insulating and dielectric materials of far more rigorous specifications than ever before. Present and projected applications indicate the need for both theoretical and experimental research as well as practical development.

The sessions held by the Division in Washington last May were eminently successful. There was much of interest to manufacturers, to electric and electronic equipment designers, and to such users of finished products as the military agencies. Only a few of the papers presented have been, or will be, published in this JOURNAL, since much of the time was devoted to reviews and discussions and general stock-taking, or dealt with practical applications. Some of the material has been published elsewhere. The magazine *Electrical Manufacturing* ran a ten-page resumé and evaluation of the contents of the program.

A panel discussion of high temperature capacitors drew especial attention. The Air Force is, of course, intensely interested in developing electronic equipment for use in supersonic aircraft and guided missiles, under conditions such that the temperature may go very high. This could be especially necessary for unusually fast "homing" missiles which must have the sensing apparatus in a temperature-vulnerable position. In some applications, equipment which could operate for long periods of time at 200°C or 300°C might be satisfactory; in other cases, even brief operation up to 500°C might be the goal.

General Electric prides itself on the manufacture of ceramic-and-metal radio tubes which can operate at 500°C. High temperature transistors are mentioned. Resistors may not be too much of a problem, and the same is true of capacitors in the micromicrofarad range. Capacitors in the 1 to 5 microfarad range, to operate at 100 to 3000 volts up to 500°C, small in keeping with the need for miniaturization, with low and stable power factor, are the present goal, and they require new materials and new ideas.

Nothing similar to electrolytic capacitors has been mentioned. The search is for stable insulating materials which can be used reliably in very thin layers, and for materials of very high dielectric constant along with other suitable properties. Certain ceramics do have exceptionally high values of dielectric constant, but they are likely to conduct too well, have a high temperature coefficient of conductance, or undergo irreversible changes at high temperatures.

Even if all components were readily available, there is still the problem of mounting, with suitable circuitry and suitable insulation. Even the problem of connecting components to each other and to the rest of the equipment becomes a serious one.

We have not heard of a symposium on batteries to operate at 500°C.

—CVK

FUTURE MEETINGS OF
The Electrochemical Society

New York, N. Y., April 27, 28, 29, 30, and May 1, 1958

Headquarters at the Statler Hotel

Sessions will be scheduled on
Electric Insulation, Electronics,
Electrothermics and Metallurgy, Industrial Electrolytics,
and Theoretical Electrochemistry (including a symposium
on "Electrokinetic and Membrane Phenomena")

* * *

Ottawa, Canada, September 28, 29, 30, October 1, and 2, 1958

Headquarters at the Chateau Laurier

* * *

Philadelphia, Pa., May 3, 4, 5, 6, and 7, 1959

Headquarters at the Sheraton Hotel

* * *

Columbus, Ohio, October 18, 19, 20, 21, and 22, 1959

Headquarters at the Deshler-Hilton Hotel

* * *

Chicago, Ill., May 1, 2, 3, 4, and 5, 1960

Headquarters at the Lasalle Hotel

* * *

Houston, Texas, October 9, 10, 11, 12, and 13, 1960

Headquarters at the Shamrock Hotel

* * *

Papers are now being solicited for the meeting to be held in New York, N. Y., April 27-May 1, 1958. Triplicate copies of each abstract (*not exceeding 75 words in length*) are due at the Secretary's Office, 1860 Broadway, New York 23, N. Y., *not later than January 2, 1958* in order to be included in the program. *Please indicate on abstract for which Division's symposium the paper is to be scheduled.* Complete manuscripts should be sent in triplicate to the Managing Editor of the JOURNAL at 1860 Broadway, New York 23, N. Y.

Anodization of Lead and Lead Alloys in Sulfuric Acid

Jeanne Burbank

U. S. Naval Research Laboratory, Washington, D. C.

ABSTRACT

The anodic lead dioxide coatings formed on lead and selected alloys in sulfuric acid were examined by electron and x-ray diffraction and by electron and light microscopy; the self-discharge of the dioxide films on the metals was followed by time-potential curves; the relation between anodic attack, self-discharge characteristics, and the microstructures of the metals are reported.

Anodically formed dioxide coatings on lead and the alloys comprise a mixture of two polymorphic forms of PbO_2 at the metal-coating interface, and common tetragonal lead dioxide at the solution-coating interface. Discharge of these dioxide coatings indicates that βPbO_2 discharges more rapidly than αPbO_2. The potential of a discharging surface is determined by these relative rates as well as by the physical structure of the dioxide layers. This in turn is determined to some extent by the microstructure of the metal.

The metals were shown to be preferentially attacked at grain boundaries and in interdendritic areas depending on the nature of the segregated material and structural discontinuities. A discussion of some of the crystal chemistry of the lead compounds, potential-*p*H diagram, and the lead acid cell is included.

Corrosion of the positive grid in the lead acid cell is a limiting factor in useful cell life, and examination of such processes includes a study of the anodic coatings formed on grid metals under cell environments. This paper is a continuation of studies reported earlier (1, 2) concerning the anodic coatings formed on Pb and its alloys in H_2SO_4, and their electrochemical and physical characterization. The experimental work comprised (*a*) determination of the self-discharge characteristics of the coatings, (*b*) determination of the relation between anodic attack of the metals and their microstructures, (*c*) identification of the anodic products by electron and x-ray diffraction, and (*d*) the microscopic examination of the anodic coatings formed on Pb and its alloys. Where possible such studies have been related to the corrosion rates of the alloys reported by Lander (3). To eliminate the possibility that preparation for electron diffraction examination caused changes in the nature of the anodic products, several experiments are reported on electrochemical preparations of the oxides deposited on Pt, and on bulk oxides.

Two crystal forms of PbO_2 have been reported, the common tetragonal variety, and an orthorhombic form (4-6). For purposes of this report the alpha form of PbO_2 is accepted as a second polymorphic form of the dioxide; however, despite the crystallographic studies devoted to this material, only very incomplete information on its stoichiometry has been published (5).

Experimental

Time-potential studies.—Alloys having the nominal compositions shown in Table I were prepared by melting weighed quantities of the pure metals in Pyrex tubes, and casting in Al molds. Specimens of each of the alloys, prepared in the same manner as previously used for pure Pb (1), were anodized above the $PbO_2/PbSO_4$ potential to develop a coating of PbO_2, and then allowed to self-discharge. The electrolyte was 1.210 sp gr H_2SO_4. The polarization and open circuit self-discharge were followed with a Hg, Hg_2SO_4 reference electrode in the same cell

Table I. Relation of microstructure to corrosion topography and rate in Pb alloys

Alloy additions wt % Ca	Sb	Sn	Relation of corrosion topography to microstructure	Corrosion rate penetration (3) cm/year
0.05	—	—	Intergranular penetration with undercutting subgrain crystallographic pitting	4.6×10^{-3}
0.09	—	—	Intergranular penetration and secondary interdendritic attack	
0.15	—	—	Severe intergranular and interdendritic penetration	
—	12	—	Severe intergranular and interdendritic penetration	
—	0.5	—	Intergranular penetration and secondary interdendritic attack	
—	2	4½	Intergranular penetration and secondary interdendritic attack	2.3×10^{-3}
—	—	4½	Intergranular attack, V notch type	
0.05	—	4½	Intergranular penetration, V notch type	
0.09	—	4½	Intergranular penetration, V notch type	
0.15	—	4½	Primarily intergranular attack with secondary interdendritic penetration	
	0.01		The relation of microstructure and corrosion in the Pb-Sb alloys has been reported (2).	
	1			
	6			
	9½			

and in precisely the same fashion used in the previous work.

A freshly polished metal specimen was used in most instances, but several specimens were reused after stripping the anodic products in NH_4Ac (saturated ammonium acetate solution) and rinsing.

Microstructure and Corrosion.—Portions of each of the alloy castings used by Lander (3) for corrosion rate determinations in the 40-week cycling test were examined at the end of the test to show the relation of corrosion to their microstructures. The corrosion products were stripped by soaking in NH_4Ac followed by rinsing and drying. Faxfilm[1] replicas were made of the corroded surfaces. A portion of each specimen was milled, polished, and etched in acetic acid, hydrogen peroxide solution to develop the microstructure. Photomicrographs were made of the replicas and metallographic specimens.

Corrosion products and special preparations.—The anodic corrosion products formed on alloys used in this study were examined by reflection electron diffraction. Specimens were prepared by polishing, etching, rinsing in NH_4Ac, and distilled water. They were anodized in H_2SO_4 above the $PbO_2/PbSO_4$ potential for varying lengths of time up to 8 hr. Specimens were blotted dry with tissue, and electron diffraction patterns taken.

Rolled Pb sheet annealed at 100°C for six weeks was cleaned by etching, rinsing in NH_4Ac and distilled water. The sheet was then anodized above the $PbO_2/PbSO_4$ potential in H_2SO_4 for various periods of time up to 30 days. The surface was blotted dry. Similarly prepared specimens were allowed to self-discharge to near the $Pb/PbSO_4$ potential, and the surfaces blotted dry. These charged and discharged surfaces were examined by reflection electron and x-ray diffraction. Anodic products were freed from such surfaces by soaking in NH_4Ac and gently lowering the specimen through a water surface. The floating residues were picked up on film-coated specimen screens for electron microscope and diffraction examinations. A similar discharged specimen was mounted in casting plastic (7), sectioned, polished, and photomicrographs made under polarized light.

Similarly prepared specimens of pure Pb sheet were anodized at constant potentials below the $PbO_2/PbSO_4$ potential, at this potential, and at gassing. The electrode products were examined by electron and x-ray diffraction.

Chemical replicas of 1% and 9½% Sb-Pb alloys were prepared and photographed (8).

Lead dioxide was deposited on Pt foil electrodes from divalent lead solutions, under conditions described by Zaslavskii, *et al.* (6), to give deposits of known crystal form. The structures were verified by x-ray diffraction. Such electrodes were rinsed in distilled water and used in these subsequent studies: *(a)* soaked in 1.250 sp gr H_2SO_4 for three days; *(b)* anodized in 1.250 sp gr H_2SO_4 above the $PbO_2/PbSO_4$ potential up to one week against a Pt cathode; *(c)* discharged cathodically against a Pt cathode in 1.250 sp gr H_2SO_4 followed by anodization above the $PbO_2/PbSO_4$ potential to reform the dioxide; *(d)* anodized in 3N NaOH solution using a Pt cathode for as long as three days.

The anodic products from this series of tests were examined by x-ray and electron diffraction and electron microscopy. The microscope specimens were prepared by soaking in NH_4Ac, floating on water, and mounting on film-covered specimen screens.

Chemically prepared tetragonal PbO_2 (9) and reagent grade PbO_2 were pressed onto lead sheets and soaked or anodized above the $PbO_2/PbSO_4$ potential in 1.250 sp gr H_2SO_4 for varying periods up to one week. The materials were then examined by x-ray and electron diffraction. After treating with NH_4Ac and floating on water, the materials were mounted on screens for electron diffraction and microscope examination.

Electron diffraction patterns and micrographs were obtained with an RCA EMU 2, and the x-ray patterns were made with Phillips or General Electric direct recording spectrogoniometers. Free use was made of the optical microscope to examine sur-

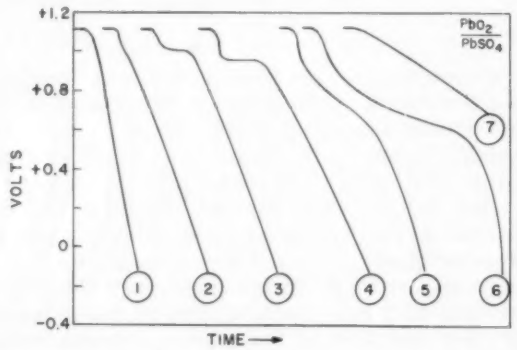

Fig. 1. Self-discharge of PbO_2 coatings on Pb alloys in H_2SO_4 vs. Hg_2SO_4/Hg electrode. The curves are numbered and were obtained with the following alloys (composition indicated is nominal weight per cent): curve 1, 4½ Sn 2 Sb; 4½ Sn; 0.15 Ca; 0.01 Sb; 12 Sb (first run); curve 2, 0.05 Ca; 9½ Sb; curve 3, 0.09 Ca; 0.05 Ca; 1 Sb; curve 4, 0.15 Ca 4½ Sn; 0.15 Ca; 12 Sb (second run); curve 5, 6 Sb; curve 6, 12 Sb (third run); curve 7, 0.09 Ca 4½ Sn; 0.05 Ca 4½ Sn.

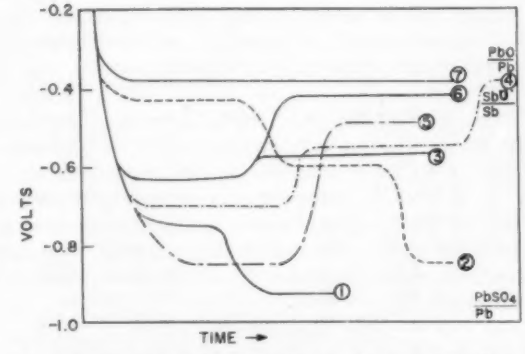

Fig. 2. Prolonged self-discharge of PbO_2 coatings on Pb alloys in H_2SO_4 vs. Hg_2SO_4/Hg electrode. The curves for the several alloys are numbered according to the following order: curve 1, 4½ Sn; 0.09 Ca 4½ Sn; curve 2, 0.09 Ca; 0.09 Ca 4½ Sn; 0.15 Ca 4½ Sn; curve 3, 4½ Sn 2 Sb; curve 4, 0.05 Ca; curve 5, 0.15 Ca; 6 Sb; curve 6, 0.09 Ca 4½ Sn; 0.01 Sb; curve 7, 12 Sb; 0.15 Ca; 0.05 Ca 4½ Sn; 1 Sb; 9½ Sb.

[1] The Faxfilm Co., 1220 W. Sixth St., Cleveland 13, Ohio.

faces during the electrochemical treatments and after removal from the electrolyte.

Results and Discussion

Time potential studies.—The self-discharge of thin coatings of anodically formed PbO_2 on the Pb alloys used in this study are shown in the schematic time-potential curves of Fig. 1 and 2. The general shape of the curves is considered, and this is not a comparison of the time intervals. It is seen that the slope of the discharge curves from the $PbO_2/PbSO_4$ potential arrest varies over wide limits and may exhibit well-defined arrests. These intermediate arrests are real in that cathodic or anodic pulses of current do not destroy them; however, they are not thought to correspond to thermodynamic equilibrium potentials, but rather to mixed potentials caused by physical changes of the anodic coatings. These physical changes are induced at least in part by the nature of the metal itself. Random metallographic cuts of a cast alloy may be expected to give rise to variation in discharge characteristics because the relative amount of segregated material exposed on a given small surface area will vary. For example, three types of discharge curve were observed for a specimen of 12% Pb-Sb alloy. These were developed by reusing the same specimen, stripping the corrosion product, rinsing, and anodizing, omitting the resurfacing or metallographic polishing between runs. Type curves numbered 1, 4, and 6 were obtained from a single specimen. The freshly prepared and polished specimen (curve 1) was found to discharge after barely pausing at the $PbO_2/PbSO_4$ potential by falling rapidly to an arrest near that of the Sb electrode. Reuse of the same area after cleaning and rinsing resulted in curve 4, and curve 6 was obtained on the third run. The change in the discharge curves is attributed to the relative amounts of segregated Sb present in the metal surface. Antimony is preferentially leached from the metal during anodization; thus reuse of a specimen causes a progressive depletion but not elimination of Sb from the surface, and produces a progressively less steep discharge curve. It is doubtful whether the Sb may be completely leached from the surface of alloys containing 1% or more, as the interdendritic canals of segregated Sb are continuous.

When clear-cut arrests appear near the $PbO_2/PbSO_4$ potential, it is believed that a fixed but limited pore area is induced in the anodic film by solution of the segregated metal phase. The potential of the surface will then be determined by simultaneous electrochemical processes, the resultant being a mutually polarized potential. This mixed potential of the surface gives rise to thermodynamically unexpected anodic products (1, 10) owing to depletion of hydrogen ion in the pore areas and polarization of the surface by PbO_2. When Pb is anodized to develop a coating of PbO_2 and allowed to stand on open circuit, it exhibits the reversible $PbO_2/PbSO_4$ potential. Scratching to expose bare metal causes a lowering of potential, but a rapid restoration occurs on termination of the disturbance. The scratch marks remain bright and clean. Such a phenomenon is considered to be healing of the anodic film by sulfation of the exposed metal. In those cases where the anodic films discharge with a steep slope, it is believed that a large pore area rapidly develops on the surface once the film becomes porous at all, and that the pores do not become sealed. When the discharge curve shows a lower slope it is thought that the pores develop continuously at a slow rate. In those instances where well-defined intermediate arrests occur, the film becomes porous, but the pores remain open and constant in area during the time of the arrest. A soluble alloy component acts as a pore generator and tends to keep the pores open. A similar effect would be expected when the specific volume of the anodic products of the alloying metal differs markedly from those of Pb. The positive plate discharge reactions take place simultaneously with the physical destruction of the coating. The ultimate materials present on a "discharged" surface depend on the relative rates of the processes. Thus it is possible to observe residual undischarged PbO_2 on the surface after complete apparent discharge (1). The tendency of the metal to develop and maintain porosity in the anodic film influences the apparent efficiency of the discharge process at the reversible $PbO_2/PbSO_4$ potential.

Prolonged self-discharge of the anodized surfaces of the several alloys shows the series of curves in Fig. 2. In some cases the discharge terminated at −0.38 v relative to the Hg, Hg_2SO_4 electrode, and others fell to the $Pb/PbSO_4$ potential only to rise again toward more positive values as sulfation was completed. These curves are similar to those reported for static passivation (11-13), and if sufficient time had elapsed, they would probably all have leveled off near the value −0.4 v. In these cases the porosity of the sulfate film is considered to be the controlling factor in the time required for total passivation as suggested by the several investigators. Here again thermodynamically unexpected materials occur because of acid depletion at the metal interface (1, 11).

Microstructure and corrosion.—The anodic corrosion of Pb alloys is related to their microstructures and usually proceeds by grain boundary attack, or a combination of grain boundary and interdendritic penetration (2). The alloys used in this study showed three types of corrosion topography. Examples of each of the categories are shown in Fig. 3, 4, and 5; results are summarized in Table I.

The relation of corrosion and microstructure in the Pb-Sb alloys has been described earlier (2). The cause of the preferential attack at the grain boundaries in the lower alloys is attributed to discontinuities in the segregated Sb at low concentrations. The higher alloys, however, have a greater degree of continuity between the material segregated at grain boundaries and in the interdendritic network as shown in Fig. 6. These microphotographs show chemical replicas (8) of two grain boundary areas of 1% and 9½% Pb-Sb alloys. The spheroidal segregation in the low alloys is less continuous than the eutectic segregation of the higher wherein the grain boundary area is not markedly different from the interdendritic.

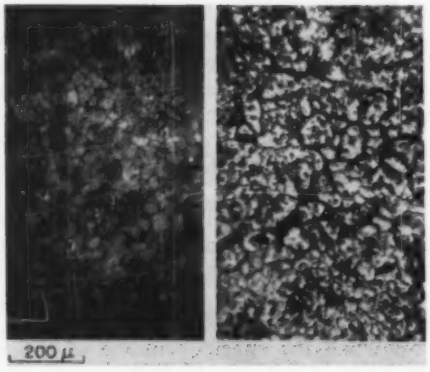

Fig. 3a. (left) 0.05 Ca-Pb binary alloy as-cast structure; Fig. 3b. (right) Replica of the corroded surface of 0.05 Ca-Pb binary alloy after removal of the corrosion products showing penetration at the grain boundaries, and areas where whole grains were undercut.

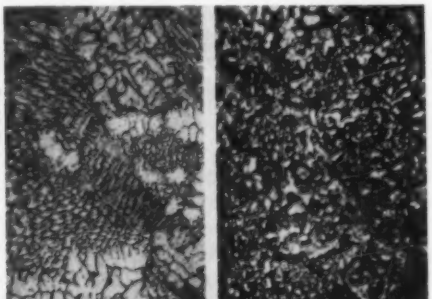

Fig. 4a. (left) 0.15 Ca-Pb binary alloy as-cast structure; Fig. 4b. (right) Replica of the corroded surface of 0.05 Ca-Pb binary alloy showing interdendritic and intergranular penetration.

The binary Pb-Ca alloys showed a behavior similar to that of the Pb-Sb system. The alloy containing 0.05% Ca corroded preferentially at the grain boundaries, and the sub-grain attack took the form of small crystallographic etch pits as seen in Fig. 3. In addition there are numerous areas where entire grains have been completely undercut. A metallographic specimen of the alloy is also shown in the photograph. In alloys of 0.09% Ca, the attack resulted in primary grain boundary penetration and secondary interdendritic attack. Fig. 4 shows the microstructure of 0.15% Ca alloy, typical of as-cast binary structures; and the corroded surface that shows deep penetration in both grain boundary and interdendritic areas.

The binary Pb-Sn alloy showed preferential attack of the V-notch type at the grain boundaries similar to that seen on pure Pb (2).

The ternary Sn, Ca, Pb alloys resembled the Pb-Sb series in their corrosion topography. Those with 0.05 and 0.09% Ca showed intergranular V-notch attack, and that with 0.15% Ca showed primarily intergranular with secondary interdendritic attack.

The microstructure of the ternary alloy with 2% Sb and 4½% Sn showed a mixture of large and small grains of different compositions (Fig. 5). The

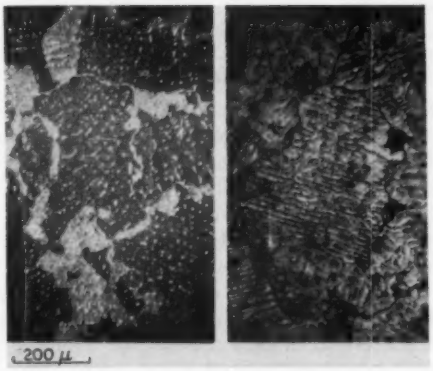

Fig. 5a (left) 2 Sb 4½ Sn-Pb ternary alloy as-cast structure showing pseudobinary structure; Fig. 5b. (right) Replica of the corroded surface showing preferential attack of the segregated eutectic material.

Fig. 6a. Chemical replica of 1% Sb-Pb alloy showing spheroidal Sb particles and discontinuity at the grain boundary region. The light areas are primary Pb dendrites, and the dark areas are segregated Sb.

smaller grains lie at the boundary areas of the larger, and it is apparent that this alloy is a pseudobinary structure, indicating that the liquidus attains the ternary eutectic composition during freezing (14). The anodic attack is primarily in the areas of the segregated ternary eutectic material as shown in the photograph of the corroded surface.

It is possible to correlate the corrosion rates with the physical pattern of the anodic attack. Lander's (3) corrosion rate determinations on these same alloys showed that the Sn binary and ternary alloys had lower rates than the alloys without Sn additions. The higher rates were associated with simultaneous attack at the grain boundaries and subgrain structures, and with deep intergranular attack, whereas the lower rates were associated with moderate grain boundary penetration and only secondary attack in the body of the grain.

Corrosion products.—The identification and characterization of the anodic corrosion products on Pb and the alloys was accomplished by electron and x-ray diffraction examination. Identification by diffraction techniques of the several anodic oxides on Pb has been effected by holding the specimens at

Fig. 6b. Chemical replica of 9½% Sb-Pb alloy showing typical as-cast structure with eutectic segregation continuous at the grain boundaries and interdendritic areas. Light areas are primary Pb dendrites and dark material is segregated Sb.

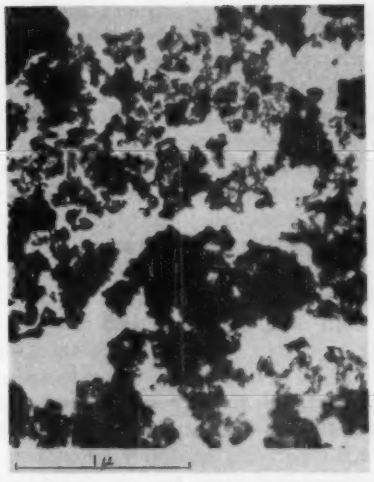

Fig. 7. Electron micrograph of αPbO_2 particles after isolation from the anodic surface.

selected potentials for sufficient time to produce coatings heavy enough to give strong clear patterns in the low theta region.

Earlier work (1) indicated the presence of an unidentified species on Pb anodes in H_2SO_4. This material has been identified as αPbO_2 in the present study. Fig. 7 is an electron micrograph of αPbO_2 after isolation from the other anodic products and the base metal. The particles exhibit no holohedral forms, and are approximately 0.1μ in diameter. This is the same size range reported by Feitknecht and Gaumann (15), and observed in this study for electrolytic tetragonal PbO_2.

Alpha PbO_2 is commonly prepared by anodic oxidation of plumbites, by extraction of plumbates, and it is the form of PbO_2 occurring on Pb in alkaline solutions at elevated potentials. The appearance of α and β PbO_2 as anodic corrosion products on Pb in acid solutions indicates that the oxidation proceeds by formation of tetravalent Pb in two ionic configurations—the so-called plumbic and plumbate.

Alpha PbO_2 has been observed in battery research in at least four independent investigations by Kameyama and Fukumoto (4), Bode and Voss (16), Ruetschi and Cahan (17), and at this Laboratory.

Anodization of Pb in acid at potentials immediately below the reversible $\beta PbO_2/PbSO_4$ potential produces a deposit of PbO_2 (1, 10) that may exhibit a preferred orientation with (110) parallel to the substrate. This causes the d = 2.81 line to be the strongest in the pattern. The pattern for $PbSO_4$ is present at certain potentials but does not occur if the potential of anodization is sufficiently near that

Table II. Some typical diffraction patterns of anodic corrosion products on Pb

βPbO_2*		βPbO_2		PbO_2		$\alpha+\beta$ PbO_2		αPbO_2		αPbO_2		αPbO_2	
H_2SO_4** x-ray†		H_2SO_4 electron diffraction		H_2SO_4 x-ray		H_2SO_4 x-ray		H_2SO_4 x-ray		H_2SO_4 electron diffraction*		KOH x-ray	
d	I‡	d	I	d	I	d	I	d	I	d	I	d	I
3.50	vvs	3.50	s	3.12	s	3.83	w	3.82	mB	3.80	w	3.82	mB
2.79	s	2.80	vvs	2.81	vvs	3.50	w	3.12	vvvs	3.11	vvvs	3.12	vvs
2.46	vs	2.46	m	2.51	vw	3.14	vvs	2.97	w	2.74	m	2.97	w
1.85	m	1.86	s	1.87	m	2.79	s	2.73	mB	2.60	m	2.74	mB
1.75	m	1.69	s	1.68	mB	2.74	m	2.61	mB	2.23	vvwB	2.61	mB
1.68	m	1.56	mB	1.406	w	2.60	m	2.23	w	2.00	wB	2.21	w
1.556	w	1.48	mB	1.218	m	1.85	sBB	1.89	w	1.81	vsB	2.01	w
1.519	w	1.28	m	1.077	m	1.687	w	1.84	mB	1.64	m	1.84	mB
1.486	m	1.22	m			1.550	w	1.81	mB	1.53	s	1.81	mB
1.387	w	1.15	mB			1.520	m	1.80	mB	1.42	w	1.64	m
1.273	m	1.123	mB			1.510	m	1.64	w	1.22	wB	1.55	w
1.238	w	0.996	m			1.257	w	1.54	mB	1.205	wB	1.53	mB
1.214	w							1.27	wB	1.155	wB		
1.152	w							1.23	wB	1.087	wB		
								1.19	wB	1.038	mB		
								1.15	wB				

* Identification on the basis of pattern shown.
** Electrolyte in which anodization was carried out. H_2SO_4 signifies 1.250 sp gr H_2SO_4. KOH signifies 3*N* KOH.
† Diffraction technique used.
‡ Estimated intensities: v = very; s = strong; m = medium; w = weak; B = broad peak; BB = very broad.
* Residue from extracted film by transmission electron diffraction; all other patterns shown were obtained by reflection.

of $PbO_2/PbSO_4$. Upon subsequent anodization of the same specimen immediately above the reversible potential, the pattern of βPbO_2 appears, and the strong pattern for PbO_t persists. Only the pattern for βPbO_2 is observed by reflection electron diffraction from such a surface while that of PbO_t is the stronger in the x-ray pattern. If anodization is continued at the elevated potential, the diffraction pattern for PbO_t diminishes gradually; the pattern for βPbO_2 increases in intensity simultaneously. The length of anodic time required to observe these effects depends on the amounts of the several materials present on the surface, and if an initial layer of $PbSO_4$ is heavy enough, its pattern and subsequently that of βPbO_2 will be the only ones observed by electron or x-ray diffraction. Superficial coatings of $PbSO_4$ and βPbO_2 may be removed by wiping the surface vigorously with dry lens tissue. It must be emphasized that the detection of PbO_t and αPbO_2 depends on the presence of limited amounts of $PbSO_4$ or βPbO_2. This is one reason why work at this Laboratory has employed constant potential anodization, as the development of the electrode product is limited to a single material characteristic of the selected potential. Anodization of cleaned lead surfaces at potentials above the $PbO_2/PbSO_4$ potential (gassing O_2) produces a deposit of αPbO_2 having a strong clear x-ray pattern in the low theta region.

Table II shows some typical diffraction patterns observed for anodic coatings on Pb. Standard comparison patterns are available in the literature, although definitive readings are best made by comparison of standards recorded on the same equipment.

As on pure Pb, the alloys of this study developed PbO_2 coatings in H_2SO_4 that were shown by electron diffraction to be laminates of βPbO_2 at the solution interface, and a composite of α and βPbO_2 at the metal surface. The greatest attention was devoted to the anodic products on pure Pb owing to the fact that the alloying agents used in the study have diffraction patterns that introduce certain difficulties. For example, Sb gives an x-ray pattern resembling that of a mixture of lead oxides, and rather strong patterns are obtained for Sb in the Pb alloys. In addition it is likely that the oxides of certain alloying agents form mixed crystals with the lead oxides, and have similar structures. The possibilities of mixed oxide formations must rest with future investigation.

The PbO_2 deposits formed on the alloys listed in Table I were variable in appearance. All were dark brown to black in color, but their textures ranged from smooth, hard, brittle, glossy adherent coatings to flaky, porous, friable, lusterless, loose deposits. In general, the alloys exhibiting low corrosion rates (Table I) produced smoother deposits. These ultimately fracture and part from the metal in large brittle concave flakes suggesting that when attached to the metal the oxide is under compression. At the base of the fracture fissures shiny base metal was visible, and on occasion the oxide flakes pulled metal away from the surface. The loose scaly deposits came away from the metal as powder; however the porosity of the deposit appeared greater in areas corresponding to the segregated phase of the metal structure.

The earlier report (1) described an unidentified anodic product on pure Pb having a body-centered tetragonal lattice with the parameters a_o 3.54, c_o 5.86 kX units. The orientation determination and parameters were calculated from reflection cross grating electron diffraction patterns of anodized surfaces. These patterns may be of normal twinned crystals, or of distorted lattices caused by compression while in contact with the metal. As mentioned above there is evidence that the anodic deposit is under compression while attached to the metal surface. The c_o value of 5.86 observed by electron diffraction is in reasonable agreement with b_o reported for αPbO_2 of 5.93 from x-ray studies. The parameter $a_o = 3.54$ would then correspond to that of 3.668 of the [101] of αPbO_2. This oxide appears to be deformed into this tetragonal lattice when attached to the metal, and to assume its normal parameters after separation from the influence of the Pb surface by fracture or by growing to sufficient depth. The stresses exerted by such a deformed lattice growing epitaxially on the Pb may be the primary cause of growth of pure Pb grids in cell use.

Special preparations.—Special preparations were undertaken to determine the nature and origin of αPbO_2 in the anodic corrosion product. It was suggested by Bode and Voss (16) that solid phase oxidation of PbO_t formed αPbO_2. Similarly it was possible that αPbO_2 had formed during some of the treatments applied to the corrosion products in this study. Alpha and beta PbO_2 could be expected to be different in their electrochemical behavior: would αPbO_2 discharge to $PbSO_4$? If so, would this sulfate anodize to αPbO_2? What significance could then be attached to the familiar $\beta PbO_2/PbSO_4$ electrode? These questions among others prompted a few special preparations and preliminary studies.

X-ray diffraction examinations showed that coatings of αPbO_2 on Pt discharged in H_2SO_4 to form $PbSO_4$. When reanodized in H_2SO_4 βPbO_2 was the solid product. Therefore, formation of αPbO_2 may be considered an irreversible electrode process when it occurs in the positive plate of the lead acid cell, and it is necessary to differentiate between studies of reversible systems such as reported by Beck, Lind, and Wynne-Jones (18) and of irreversible systems such as grid corrosion.

Chemically pure βPbO_2 was treated with solutions of H_2SO_4 and NH_4Ac in contact with metallic Pb and $PbSO_4$. The extracted residues showed only βPbO_2 by electron diffraction. Therefore αPbO_2 is not formed by chemical reaction nor during subsequent treatments of the corrosion products used in this study. The isolation of αPbO_2 from the other anodic products eliminated the possibility that x-ray patterns obtained by reflection from the anodic material *in situ* arise from oriented $PbSO_4$ and PbO_t.

Lead sheet anodized above the $PbO_2/PbSO_4$ potential in H_2SO_4 was allowed to self-discharge to

Fig. 8. Plastic mounted section of discharged PbO_2 coating on Pb showing $PbSO_4$ and heavy layer of αPbO_2. Magnification 1000x before reduction for publication.

near the Pb/$PbSO_4$ potential. The specimen appeared gray and totally discharged; x-ray diffraction examination of the surface showed only $PbSO_4$. Extraction with NH_4Ac removed the heavy sulfate coating leaving considerable residue of dark brown material. This residue was shown by electron diffraction to be αPbO_2 of very high purity. The two materials, $PbSO_4$ and αPbO_2, are visible in the micrograph of the cross section of the discharged sheet shown in Fig. 8.

The fact that discharged films are composed chiefly of these two materials indicates that the two forms of PbO_2 discharge at different rates. On the specimen, Fig. 8, the discharge has taken place at discontinuities in the αPbO_2 layer and across the surface, precisely where the βPbO_2 appears, indicating that βPbO_2 discharges more readily than αPbO_2.

It is clear that the efficiency of the discharge of PbO_2 coatings on Pb and its alloys in H_2SO_4 is governed by the physical nature of the films (porosity, stress, alloying metals); the morphology of the crystalline phases present; and the rates and mechanisms of discharge of the two forms of PbO_2.

Crystal Chemistry and Thermodynamics

The formation of the anodic corrosion products of Pb in H_2SO_4 is considered to take place by three crystallization mechanisms summarized succinctly by Feitknecht (19): (*a*) by way of the free solution; (*b*) by boundary nucleation and growth; and (*c*) by solid phase transformation. These three mechanisms may be applied equally well to the cycling processes of the active material, and interpreted in terms of the crystal chemistry of the lead oxides, and the thermodynamic equilibria of the system summarized by Delahay, Pourbaix, and Van Rysselberghe (20) in the potential-*p*H phase diagram. For convenience part of the diagram has been reprinted in Fig. 9, with the solid phases indicated. The reactions and numeration are retained from the original presentation.

Lead sulfate is in equilibrium under conditions defined by lines 51 and 52 with βPbO_2. During anodization of sulfate crystals they were observed by

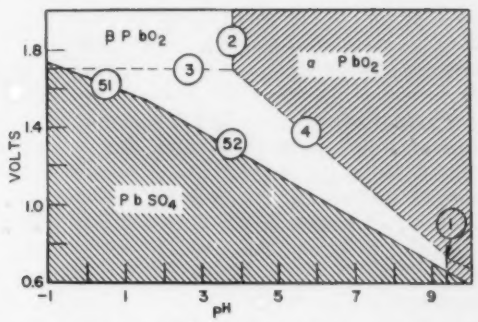

Fig. 9. Portion of the potential-pH diagram of Pb in H_2SO_4 with solid phases indicated. The reactions indicated by the original numerations are:

1. $HPbO_2^- + 3H^+ = Pb^{++} + 2H_2O$
2. $PbO_3^= + 6H^+ = Pb^{+4} + 3H_2O$
3. $Pb^{+4} + 2e^- = Pb^{++}$
4. $PbO_3^= + 6H^+ + 2e^- = Pb^{++} + 3H_2O$
51. $PbO_2 + HSO_4^- + 3H^+ + 2e^- = PbSO_4 + 2H_2O$
52. $PbO_2 + SO_4^= + 4H^+ + 2e^- = PbSO_4 + 2H_2O$

The equilibrium between the two forms of PbO_2 remains to be verified by experiment in the region of line 4. Potentials are shown vs. standard hydrogen electrode.

optical microscope to become colored dark brown. A single crystal of sulfate may be part clear sulfate, part opaque brown, and the conversion appears to take place as a solid phase transformation. The complete conversion to βPbO_2 of the sulfate crystal occurs because the transformation liberates H_2SO_4, and the interior of the crystal does not suffer a depletion of acid. The transformation is best described as a boundary nucleation and growth phenomenon, rather than a solid phase oxidation. The direction of growth is toward the Pb-rich interior of the crystal, and the holohedry of the sulfate crystal is sometimes maintained by the mass of small βPbO_2 crystals.

Microscopic observation of the discharge of a coating of βPbO_2 on Pb indicates that the sulfate forms by way of the free volume of solution as dendritic crystals grow out into the solution. However, they are anchored in the dioxide coating and probably originate from nuclei in the boundary layer and grow outward into the sulfate-rich solution. If such crystals are knocked off the surface, it may be seen that the hole in the PbO_2 coating is an intaglio of the base of the sulfate crystal. These dendritic sulfate crystals are smoothly reconverted to βPbO_2 upon anodization.

Prolonged discharge results in a heavy layer of congealed rhomboidal sulfate crystals in which the dendritic crystals are embedded. These larger crystals are reconverted to βPbO_2 with difficulty because they frequently lose contact with the anodic surface owing to gas formation in the interstices where βPbO_2 first forms in such coatings (15).

The diagram of Fig. 9 shows that in solutions of *p*H 9.4 and higher, βPbO_2 would not be expected to form reversibly at any potential, whereas below this pH, βPbO_2 can be expected as the dominant phase in certain potential ranges. The area where αPbO_2 would be expected approaches the $PbSO_4$ do-

main at pH 9.4 and higher; therefore, αPbO_2 and $PbSO_4$ may comprise a reversible system at this area unless compounds not shown on the diagram intervene.

In an area near lines 4 and 2 an eutectic of both phases of PbO_2 could occur, and may be expected to transform reversibly by proper choice of environment.[2] But this change is not rapid as coatings of αPbO_2 and βPbO_2 on Pt do not transform upon anodization in H_2SO_4 and NaOH, respectively, for as long as three days as shown by x-ray diffraction examination.

It is now evident why the anodic corrosion products formed on Pb above the $PbO_2/PbSO_4$ potential and the active material paste of a charged cell (16) exhibit the same lamellar formation: the solution interface shows only tetragonal PbO_2, the stable phase in acid of battery strength at positive plate potentials. At the anodic surface water and/or hydroxyl ions are being discharged. At the metal surface and inner layers of the active material, the potential and pH may lie within the domain of αPbO_2, or at least in the area where mixtures of the two phases are formed. At constant high potential, once the βPbO_2 coating forms, it may increase in thickness only by deposition of Pb ion in solution or by conversion of the underlying material. The heavy layer of αPbO_2 (Fig. 8) indicates that corrosion of the underlying metal at elevated potentials takes place to a considerable extent by migration of the oxygen species into the surface. The occurrence of the αPbO_2 growing epitaxially on the Pb and in a deformed lattice suggests that the oxidation takes place beneath the βPbO_2 surface coating as a solid phase oxidation of the base metal, and an oxide layer progressively richer in metal toward the center of the specimen would be expected. The rate of formation of the αPbO_2 as a corrosion product must be controlled by the rate of penetration of the oxygen species through the βPbO_2 layer.

The point of zero charge on a βPbO_2 electrode is approximately 0.1 v positive to the $PbO_2/PbSO_4$ electrode in battery electrolyte (21). Anodization of Pb coated with βPbO_2 at such a potential produces a positive surface charge. At the positive interface owing to charge orientation, hydrogen ion would not be the dominant species, nor would it be able to penetrate the coating, and an increase in pH would be expected at the metal-coating interface. Therefore the thermodynamically stable phase at elevated pH and potential is formed by grid corrosion beneath the original βPbO_2 coating. If the metal ion migrated out to form PbO_2 at the solution interface, βPbO_2 would become buried in the αPbO_2, and such is not the case, as a superficial coating of βPbO_2 was always observed by electron diffraction. It was suggested by Kabanov, Kiseleva, and Leikis (21) that oxygen does penetrate the βPbO_2 lattice, and cause recrystallization and a change in crystal structure of βPbO_2. The rate of penetration of the oxygen species through the lattice would control the rate of corrosion of the underlying Pb, and would be dependent on the effective oxygen concentration at the surface. Thus a high corrosion rate of grid metal would be expected under overcharge conditions, as is well known to be the case in actual practice.

On cycling a mixture of the two forms of PbO_2, both discharge to $PbSO_4$, but owing to the difference in rates some αPbO_2 remains in the discharged mixture. Upon reconverting the $PbSO_4$ to βPbO_2 H_2SO_4 is liberated in contact with the αPbO_2 and it tends to convert to $PbSO_4$ and βPbO_2. Thus, upon cycling, αPbO_2 will gradually be consumed, and Bode and Voss (16) reported that the amount of αPbO_2 in the interior of the active material of a cell does indeed diminish with cycling. However, αPbO_2 continues to be generated by the corrosion mechanism until complete exhaustion of the free metal.

It was observed in this study that initially a conversion to βPbO_2 takes place at the surface of PbO_t crystals on anodizing in acid.[3] Formation of PbO_2 from such crystals at elevated potentials must therefore occur beneath a superficial βPbO_2 coating which prevents ready access of acid. Therefore paste materials that contain lower oxides and sulfate deficient mixtures may be expected to give rise to αPbO_2 and very slow development of full capacity. Any treatment of a cell that would shift the conditions of the positive plate away from those pertaining near lines 51 and 52 in Fig. 9 toward lines 2 and 4 would be expected to form some αPbO_2 both by grid corrosion and from active material components.

Beneficial effects of gradients in acid concentration existing in the cross section of the plate may be inferred from the diagram. The high positive polarization of the plate is fixed by the βPbO_2 surface. Areas deficient in acid would be held above their discharge potentials. At the beginning of discharge the process would be confined to the high acid surface of the plate. As this area became deficient in acid the discharge would extend into the deeper layers, and ultimately all the βPbO_2 could be converted to $PbSO_4$ provided sufficient acid were present. If such a mechanism did not apply, little capacity would be obtainable as the material immediately adjacent to the grid would discharge simultaneously with the outer surface and undercut active material.

Manuscript received May 3, 1957.

Any discussion of this paper will appear in a Discussion Section to be published in the June 1958 JOURNAL.

REFERENCES

1. J. Burbank, *This Journal*, **103**, 87 (1956).
2. J. B. Burbank and A. C. Simon, *ibid.*, **100**, 11 (1953).
3. J. J. Lander, *ibid.*, **99**, 467 (1952).
4. N. Kameyama and T. Fukumoto, *J. Soc. Chem. Ind., Japan*, **49**, 154 (1946).
5. T. Katz, *Ann. de Chim.*, 12th Ser., **5**, 5 (1950).
6. A. I. Zaslavskii, Yu. D. Kondrashov, and S. S. Toklachev, *Doklady Akad. Nauk, SSSR*, **75**, 559 (1950).

[2] The precise location of the eutectic line separating the two solid phases of PbO_2 must be determined by future investigation.

[3] The conversion of the lead monoxides to sulfate is not rapid, and several days' soaking in acid is required to produce sufficient sulfate to be detectable by x-ray diffraction. In anodizing the PbO_t crystals in acid, a βPbO_2 coat[illegible] was observed by electron diffraction during the period when x-[illegible] diffraction showed only unconverted PbO_t. The open circuit potential of such a specimen was that of the $PbO_2/PbSO_4$ electrode.

7. A. C. Simon and E. L. Jones, *This Journal*, **102**, 279 (1955).
8. J. Burbank, *J. Metals*, **5**, 55 (1953).
9. M. P. Applebey and R. D. Reid, *J. Chem. Soc.*, **1922**, 2129.
10. J. J. Lander, *This Journal*, **98**, 213 (1951).
11. W. J. Muller and W. Machu, *Korr. u. Met.*, **16**, 187 (1940).
12. E. J. Casey and K. N. Campney, *This Journal*, **102**, 219 (1955).
13. H. E. Haring and U. B. Thomas, *Trans. Electrochem. Soc.*, **68**, 163 (1935).
14. W. Hofmann, "Blei und Bleilegierungen," p. 75 ff., Julius Springer, Berlin (1941).
15. W. Feitknecht and A. Gaumann, *J. Chim. Phys.*, **49**, 135 (1952).
16. H. Bode and E. Voss, *Z. Elektrochem.*, **60**, 1053 (1956).
17. P. Ruetschi and B. D. Cahan, *This Journal*, **104**, 406 (1957).
18. W. H. Beck, R. Lind, and W. F. K. Wynne-Jones, *Trans. Faraday Soc.*, **50**, 147 (1954).
19. W. Feitknecht, *Fortschr. chem. Forsch.*, **2**, 670 (1953).
20. P. Delahay, M. Pourbaix, and P. Van Rysselberghe, *This Journal*, **98**, 57 (1951).
21. B. N. Kabanov, I. G. Kiseleva, and D. I. Leikis, *Doklady Akad. Nauk, SSSR*, **99**, 805 (1954).

Disintegration of Lead Cathodes, II

L. W. Gastwirt[1] and H. W. Salzberg

Chemistry Department, City College, New York, New York

ABSTRACT

In continuation of previous work, the disintegration of lead cathodes at high current densities at 25°C was studied. The solutions were acid, basic, and neutral combinations of sulfuric and phosphoric acids and ammonium and alkali sulfates, chlorides, and phosphates. The results support the hydride mechanism and contradict the alkali alloy hypothesis. The data are interpreted to indicate that water molecules are reduced at current densities below those needed for visible disintegration and that the surface is saturated with adsorbed hydrogen atoms at the start of disintegration.

Bredig and Haber (1) reported disintegration of cathodes of Pb, As, Sb, Sn, and other metals and ascribed it to the formation of an alkali alloy which reacted with the solution and disintegrated. They were at a loss to explain disintegration in acid solutions. Salzberg (2) studied the disintegration of Pb cathodes at high current densities in alkaline, neutral, and slightly acidic solutions, and suggested that the phenomenon was due to the formation of an unstable volatile hydride of Pb with the empirical formula PbH_n. This hypothesis was confirmed qualitatively by Pourbaix and Van Muylder (3) who reported that the standard free energy of formation of the compound was $+69.5 \pm 4.5$ kcal/mole, which would explain its instability and the high cathodic voltage needed for its formation.

However, Angerstein (4) stated that he was not able to obtain disintegration in molar and tenth molar acids in the absence of alkali metal cations at current densities of 10-100 ma/cm^2 and that he was not able to reproduce the results in dilute acids reported previously (1, 2). He therefore reiterated the alkali-alloy hypothesis in preference to a hydride mechanism.

The purposes of the present work were to check the results Angerstein stated that he could not duplicate and to obtain data using solutions that did not contain alkali cations.

Apparatus, Method, and Materials

An apparatus described previously (5) was simplified to facilitate removal of the cathode between runs. The cathodes were replaceable lead washers, usually 7-8 mm in diameter and about 1 mm thick, held between polyethylene washers on an iron shaft with a teflon sleeve. All work was done at 25°C.

Cathodes were prepared as in previous work (2). The materials were C.P. grade except for CsCl and RbCl. All solutions were pre-electrolyzed before use and frequently between runs. Whenever results were low or erratic either the solution or the cathode or both were cleaned or replaced. Checks were run using samples from different lots of material and sometimes using solutions prepared by different methods from different starting materials.

In spite of these precautions, reproducibility was poor. Consequently data were considered reliable only when obtained using different washers in several samples of each solution and reproduced in successive runs. Whenever cleaning or replacing the cathode or solution increased the rate, the lower result was discarded when preparing the graph.

Results

The dissolution rates were independent of time and the graphs of rate vs. current density were straight lines intercepting the current density axis. The intercept, i_o, varied with the solution. The slopes were of the correct theoretical value if, starting at i_o, one equivalent of divalent Pb left the electrode with each Faraday of current. Disintegration was observed in neutral, acid, and alkaline solutions in the presence of alkali cations, ammonium ions, and hydronium ions, either separately or in combination. No differences were noted between results in chloride, sulfate, and phosphate solution, at the same ionic strengths. Impurities caused lower and more erratic results.

[1] Present address: Princeton University, Princeton, N. J.

Table I.

H_2SO_4 Molarity	Current density	Dissolution rate
0.001	94 ma/cm²	0.1 mg/cm²-min
0.01	535	0.2
0.1	630	0.1

Acid inhibits the reaction. Table I shows a lack of appreciable disintegration in acid solutions containing no salt. Fig. 1 shows that in the presence of salt there is disintegration but that it falls off with increasing acidity. Note that until the acid concentration is about 0.05M, the slopes of the curves are unchanged, although the i_a's are increased.

Fig. 2 shows the same type of inhibition in ammonium sulfate solution. Here, however, there is an anomaly. In the concentrated salt solution a small increment of acid increases the rate, although a large increment, as usual, decreases the rate. A comparison of Fig. 1 and Fig. 2 show that the rates in ammonium salt solution are much lower than in sodium sulfate solution.

Salt effect.—Fig. 3 shows that, in the absence of acid, in dilute solution the disintegration rate is the same in all of the alkali salt solutions, but in concentrated solutions differences do show up. In molar salt solution the rates were higher in sodium sulfate than in potassium sulfate. In all cases the rates in ammonium salt solutions were less than in alkali salt solutions. Obviously, there is some inhibition due to ammonium ions.

In the presence of acid the (ungraphed) results were somewhat uncertain. The curves for each separate alkali salt solution were within the experimental error of each other and conceivably all the points could fall on the same curve. However, there did seem to be a trend indicating that the rates in Li solution were the highest, the rates in Na, K, and Rb solutions were all about the same, and those in Cs solution were significantly lower. The rates in ammonium salt solution were the lowest of all.

Conclusions and Discussion

The results are in qualitative and quantitative agreement with those previously published (2). Angerstein failed to obtain disintegration in acid solutions because his current densities were too low.

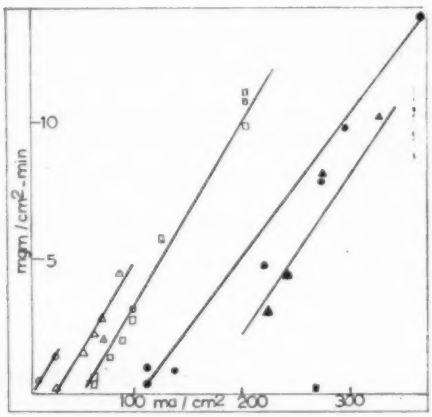

Fig. 2. Acid and NH_4^+ effects. Open circle, 0.01M $(NH_4)_2SO_4$ + 0.001M H_2SO_4; open triangle, 0.01M $(NH_4)_2SO_4$ + 0.01 H_2SO_4; closed square, 0.01M $(NH_4)_2SO_4$ + 0.1M H_2SO_4; closed circle, 0.1M $(NH_4)_2SO_4$ + 0 H_2SO_4; open square, 0.1M $(NH_4)_2SO_4$ + 0.01M H_2SO_4; closed triangle, 0.1M $(NH_4)_2SO_4$ + 0.1M H_2SO_4.

In 0.1-1M H_2SO_4 without added salt his maximum current density was 100 ma/cm², whereas Fig. 1 shows that even in 0.1M sodium sulfate it is necessary to go to at least 200 ma/cm² to get disintegration. In the absence of salt much higher current densities are needed.

The alkali-alloy hypothesis cannot be correct because: *(a)* as previously reported (2) the addition of alkali cations, in the absence of acid, decreased the disintegration rate instead of increasing it; *(b)* disintegration was observed when there was no alkali cation present (Table I, Fig. 2, 3); (c) this mechanism would require a positive temperature coefficient, whereas the temperature coefficient actually is negative (2); and *(d)* when alkali alloys do form, as at mercury cathodes, they are not volatile and, although they react with water, this reaction does not produce disintegration of the surface with formation of colloidal mercury.

Other than the work of Paneth (6), there is still no direct proof of the formation of volatile lead hydride, due to the instability of the hydride at room temperature. However, the indirect evidence seems to be rather conclusive. Work is now in prog-

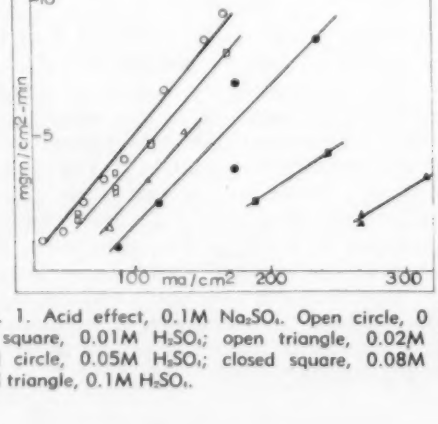

Fig. 1. Acid effect, 0.1M Na_2SO_4. Open circle, 0 H_2SO_4; open square, 0.01M H_2SO_4; open triangle, 0.02M H_2SO_4; closed circle, 0.05M H_2SO_4; closed square, 0.08M H_2SO_4; closed triangle, 0.1M H_2SO_4.

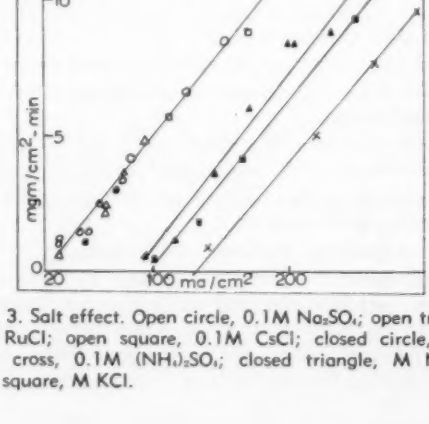

Fig. 3. Salt effect. Open circle, 0.1M Na_2SO_4; open triangle, 0.1M RuCl; open square, 0.1M CsCl; closed circle, 0.1M K_2SO_4; cross, 0.1M $(NH_4)_2SO_4$; closed triangle, M Na_2SO_4; closed square, M KCl.

ress at lower temperatures in an attempt to obtain lead hydride in the gases leaving the cell.

The surface hydronium ion concentration must be slight at and below the critical current density, i_o. The high free energy of formation of Pb would require a high potential. The reduction of hydronium ion obviously takes place at a much lower potential than that of the water molecule, and so only when the surface hydronium ion concentration is too low to support the current would water molecules be reduced. If the potential needed for hydride formation is greater than that needed for hydronium ion reduction, there would be no hydride formed until the surface hydronium ion concentration was depleted and water molecules were reduced, with an attendant rise in potential. Therefore, addition of acid would increase the current density required to start water reduction and hydride formation. Addition of alkali cations which would displace the hydronium ion from the surface would therefore decrease i_o.

Since the experimental data seem to support these ideas, it follows that, at and above i_o, water molecules are being reduced. However, the situation below i_o is still not understood. Schuldiner's results (7) indicate that water reduction may commence at potentials of about 0.1-0.2 v, which is certainly below that needed for the formation of lead hydride. Also, even in alkaline solutions with practically no hydronium ion (2) there is a large i_o, showing that even after the start of water reduction there must be an appreciable increase of current to build up the potential to the required value. So, although the point at which water reduction commences is not yet known, it seems safe to say that, even in acid solutions, water discharge commences below the onset of cathode disintegration.

The surface is largely covered with hydrogen atoms, even below i_o. Since PbH_2 contains two hydrogen atoms, the mechanism of its formation must involve the production of two high energy atoms near enough to each other to produce a hydride molecule before the activation energy is dissipated to the electrode or the solution, i.e., they must be on the same or adjacent sites. This is true whether the rate-determining step is a chemical combination of adsorbed hydrogen atoms or an electrochemical reduction of a water molecule adjacent to an adsorbed atom. So, at i_o, there must be both a high potential and a high degree of surface coverage. Below i_o either the potential factor or the surface coverage is insufficient.

If the surface is covered but the potential is too low, i_o will coincide with the attainment of a critical potential and the disintegration will therefore be an exponential function of potential. Since the over-all current density is also an exponential function of potential, the disintegration rate and the over-all current density would be linear with each other. There should be a sharp intercept of the disintegration rate-current density curve. This is actually observed.

If, on the other hand, the potential is already sufficient, the rate of disintegration at i_o would depend only on the concentration of adsorbed hydrogen atoms. Since below i_o all hydrogen leaves the surface as H_2, the concentration of hydrogen would be proportional to the square root of the current density. This means that if the rate-controlling step is the electrochemical production of a hydrogen atom adjacent to another, the disintegration rate would be proportional to the concentration of hydrogen atoms and would be linear with the square root of current density. This is not the case on Pb although it is observed on Sn (8). If the rate-controlling step in hydride production is the chemical combination of adsorbed atoms, then under these irreversible conditions (at about 1 v overvoltage) the surface would have to be saturated with hydrogen atoms, anyhow.

The effect of ammonium ion is probably to inhibit the disintegration by being itself reduced at potentials below those needed for hydride formation. This opinion is based on the following:

The rates in ammonium salt solution are lower than in corresponding solutions of the alkali metal cations (Fig. 2, 3). Addition of ammonium ions to solutions of sodium salts decreases the rate markedly, indicating that there is a specific inhibition. Addition of small increments of acid to concentrated ammonium salt solutions increased the rate slightly, probably by decreasing the amount of ammonium ion migrating to the surface (hydronium ion has a higher transference number than ammonium ion). Finally, a lead cathode in ammonium salt solutions undergoes a change in appearance from a shiny brightness to a dull, almost velvet-like blackness. This black coating is a nonadherent deposit of lead characteristic of the decomposition of a surface compound analogous to the mercury ammonia compound forming at a mercury cathode. Further work is now in progress on this subject

Acknowledgment

This work was done under the sponsorship of the Office of Naval Research. The authors wish to thank J. C. White and Sigmund Schuldiner, both of the Naval Research Laboratory, for their advice and help with the theoretical end of the work and Saul Berman, of the Office of Naval Research, for his aid in administrative matters.

Manuscript received Nov. 13, 1956.

Any discussion of this paper will appear in a Discussion Section to be published in the June 1958 JOURNAL.

REFERENCES

1. G. Bredig and F. Haber, *Berichte*, **31**, 2741 (1898); F. Haber, *Trans. Electrochem. Soc.*, **2**, 190 (1904).
2. H. W. Salzberg, *This Journal*, **100**, 146 (1953).
3. M. Pourbaix and J. Van Muylder, Cebelcor Rept. #14 (1954).
4. H. Angerstein, *Bull. Acad. Polon Sci.*, **3**, 447 (1955).
5. A. Andreatch and H. Salzberg, *This Journal*, **101**, 528 (1954).
6. F. Paneth, *Z. Elektrochem.*, **24**, 298 (1918).
7. S. Schuldiner, *This Journal*, **99**, 488 (1952).
8. H. Salzberg and F. Mies, To be published.

Polarization Capacity at Solid Electrodes and True Surface Area Values

Ralph J. Brodd[1] **and Norman Hackerman**

Department of Chemistry, University of Texas, Austin, Texas

ABSTRACT

The polarization capacities of Pt, Ni, Cr, Fe, Ta, Al, Cu, and Pb in 1M Na_2SO_4 were evaluated from charging and decay curves obtained by imposing a 2 cps signal on a cell containing one of these metals and a large nonpolarizable electrode. These values are compared to surface areas for the metals determined by Kr adsorption at 78°K in a very small volume adsorption apparatus. For some of the metals the electrochemical method is suitable for routine surface measurements. The use of the parallel procedures provided some additional insight into electrical double layer phenomena at solid electrodes.

The need for a convenient method for measuring actual surface areas of solids often arises. For small areas, as with metals, the gas adsorption method is difficult and often not feasible. The use of charging curves for electrode area measurements was described by Bowden and Rideal (1) and a somewhat more satisfactory procedure was given by Wagner (2) more recently. These methods depend on the proposition that the electrical double layer (edl) capacity at any electrode at which the hydrogen reduction potential is being approached is about 20 $\mu F/cm^2$. However, the quantity in question is actually the differential capacity C, which is a function of the potential of the electrode (3). C is believed to be relatively insensitive to potential in the region considerably cathodic to the zero point of charge (zpc) but short of the hydrogen discharge potential (reversible hydrogen potential plus hydrogen overpotential under the experimental conditions employed), a range comprising probably no more than 200-300 mv at best. Thus, to use a constant C the measurement must be restricted to the range indicated. There is no comparable insensitive region on the anodic side of the zpc. In fact, such curves of C vs. E as are available for solid electrodes suggest that the insensitive region on the cathodic side is small or lacking, in contrast to the case for mercury.

Pegues (4), following Wagner's method, measured the areas of a number of metal electrodes. These depended on assessing the capacity of a mercury surface of known area and comparing to the capacity of a solid electrode of known projected area. The values obtained were satisfactorily reproducible but suffered from lack of suitable calibration because leakage of solution between the mercury pool and its glass container made the "known" mercury surface area uncertain.

For these reasons it was decided to obtain charging curves of each metal at whatever potential it exhibited in the solution used, and to use gas adsorption areas of the metals for comparison purposes. In other words, the electrode was not polarized by applied current except to the extent caused by the input signal, and the total capacity could be compared to the total area determined by an accepted standard procedure. Thus, if the ratio of capacity to area is constant for a variety of sample sizes of the same metal under the same conditions, the method provides reproducible information. Then it becomes necessary only to decide on a value for C in order to calculate surface areas from capacities thereafter. For this purpose the differential capacity curves for mercury [using largely the data of Grahame (3)] were used as guides.

The important assumptions required are: *(a)* the edl capacity can be measured by charging curves; *(b)* the area seen by solution species and by adsorbing gas does not differ by more than the errors inherent in either method—and differ by a constant amount under all conditions; and *(c)* the values of C for mercury are not markedly different from those for other metals under the same conditions. The last implies a lack of specific interaction between the metal and solution species.

Experimental

The charging curve method was used here because it is capable of measuring larger capacities than is the inherently more accurate bridge method. At constant current, I, the capacity, C, is given by

$$C = I(dt/dV) \qquad (I)$$

where (dt/dV) is the reciprocal of the slope of the charging curve. This assumes that I remains constant as the electrode interfaces become charged, and that the slope to be measured is unequivocally recognizable. If either or both of these assumptions do not hold, the method is of little use in so far as C is concerned. Nevertheless so long as conditions are reproduced it can be a useful, empirical area measuring procedure.

The circuit shown in Fig. 1 contained a Dumont model 304-H oscilloscope and a Hewlett-Packard model 202-A function generator. A large area plati-

[1] Present address: National Bureau of Standards, Washington 25, D. C.

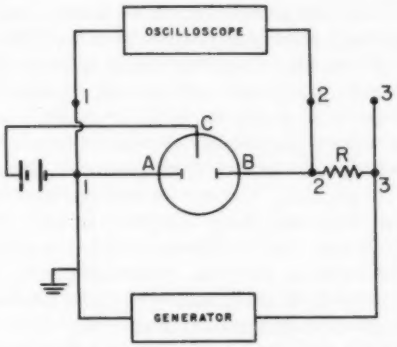

Fig. 1. Circuit diagram: A—lead to test electrode; B—lead to platinized platinum electrode; C—auxiliary electrode for polarizing purposes; R—standard resistor; 1, 2, 3—oscilloscope connections.

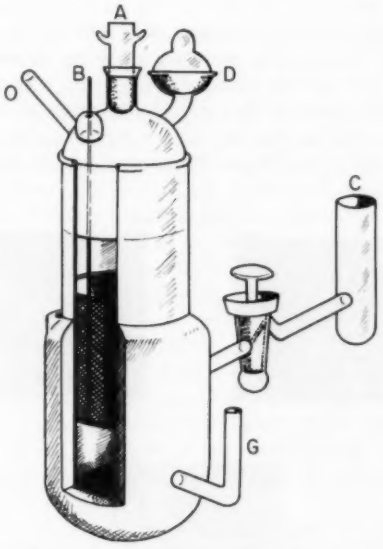

Fig. 2. Polarization cell: A, B, C as in Fig. 1; O—gas inlet; G—gas outlet.

nized platinum electrode, B, served as a nonpolarizable mate for the electrode under study and an auxiliary lead, C, was available for polarizing purposes. The current was determined with the aid of the standard resistor R.

The cell is shown diagramatically in Fig. 2. The solution could be boiled in place by means of a nichrome wire heater in the asbestos casing around the cell. Bureau of Mines grade A helium (their assay showed 99.997% purity with less than 10^{-4}% of either oxygen or water vapor) was bubbled through the cell during the boiling period and during a 20-hr pre-electrolysis treatment.

In all experiments the solution was 1M Na_2SO_4. This was prepared from analytical reagent grade material and doubly distilled water (specific conductance less than 1.5×10^{-6} mho/cm). Organic material was removed from the water by carrying out the second distillation from alkaline permanganate.

The test electrode was introduced through A, Fig. 2, and current from the generator was adjusted to give a total voltage increment on the test electrode

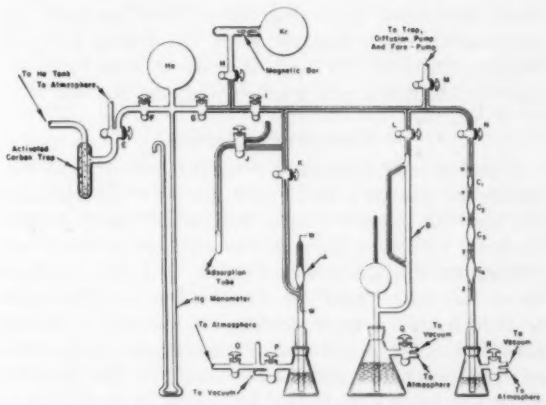

Fig. 3. Small surface area gas adsorption apparatus. E-R, vacuum stopcock; W, tungsten leads; A, high pressure McLeod gauge; B, low pressure McLeod gauge; C_1—C_4, calibrated bulbs; u, v, x, y, z, calibration marks.

of not more than 20 mv. The function used was a 2 cps [2] square wave and the current through the cell was adjusted by means of the auxiliary polarizing circuit so that the square wave current went equally on either side of zero. A picture was taken of the polarization and decay trace on the oscilloscope after allowing for equilibration between electrode and solution. The current was obtained from a picture of the trace of the potential drop across the standard resistor. The capacity was then calculated from an analysis of the photographs, using Eq. (I). It was independent of oscilloscope calibration. The temperature of the cell was maintained at 30°±1°C.

The small surface areas were measured by adsorption of Kr at 78°K (5). The low vapor pressure of Kr at this temperature minimizes dead space corrections. In addition the adsorption apparatus (Fig. 3) was made of 2 mm tubing throughout to reduce the total volume and the total glass area. The free volume was about 14 cc and the dead space about 0.8 cc, varying slightly each time the adsorption chamber was sealed onto the system. A modified McLeod gauge (6) of very small internal volume was used. Because of the small areas involved, it was necessary to correct for adsorption on the walls of the system. It was assumed that the roughness factor (ratio of B.E.T. surface area to projected geometric area) of the glass did not change with use of the system since the walls were subjected to treatment no more drastic than adsorption and desorption of krypton (and perhaps a little water vapor when the system was opened). More complete details of the krypton adsorption unit are given by Joncich (7).

Platinized Pt, Ni, and Cr electrodes were prepared by electrodeposition on Pt, Ni, and Cu, respectively, by standard plating procedures for each. The deposits ranged in thickness from a tenth up to several millimeters. Cu (from Malin & Company) Fe, Ta, Pb (from A. D. MacKay Company), and Al (from Alcoa) were used in the form of wire. The electrodeposited electrodes were washed thoroughly with 1M Na_2SO_4 before being placed in the cell. The

[2] Chosen so as to permit polarizing large area electrodes.

wire electrodes were degreased with benzene. In addition Cu was washed with 7M H_2SO_4 and 1M Na_2SO_4, while Fe, Pb, and Al were cleaned cathodically in 7M H_2SO_4 and washed with 1M Na_2SO_4.

Discussion of Results

Frumkin (8) suggested a useful relationship between the zpc of a metal and its work function. At the zpc the potential drop across the solution side of the interface is zero in the absence of adsorbed species on the electrode surface. If a cell is made up of two such "null" electrodes, the potential difference between them should be also the junction potential difference between the metals. This is the contact potential difference between the metals, which, in turn, equals the difference in work functions. Corroboration of this deduction is supplied by the fact that for Ag (9), Pb, Te, Cd (10), and Pt (11) differences in potential between their zpc and that of mercury (the electrocapillary maximum in this case) are approximately equal to the differences in work function.

By obtaining the zpc of each metal using the indirect method just described and knowing the potential of each electrode while it is being polarized it becomes possible to make comparisons with mercury at equivalent displacements from the zpc. Also, it is possible to suggest whether cations or anions predominate in the inner Helmholtz layer.

It should be remembered that accurate prediction is not possible because *(a)* a truly null electrode is unlikely on the basis of specific metal-solution species interaction and *(b)* the work function values in the literature for most metals show considerable variation. A recent discussion of the relationship is pertinent (12). Table I lists the work functions and the approximate zpc potentials relative to the saturated calomel electrode (SCE) for all of the metals used in this work, using Frumkin's relation between work function and zpc and based on the experimental zpc of mercury for Na_2SO_4 solutions (3).

In the following results the gas adsorption surface area of the actual electrode was determined wherever possible. Otherwise measurements were made on relatively long lengths of wire and the surface area of the electrode itself was calculated from the ratio of lengths. Potentials were determined relative to SCE and were also rationalized and are given also relative to the zpc of the metal.

Platinum.—Fig. 4a is a picture of a trace produced on imposing the 2 cps square wave on a cell containing a Pt test electrode and a nonpolarizable electrode. The capacity was measured on 6 separate samples and was found to be 20.1 ± 0.7 $\mu F/cm^2$ (Table II).

Robertson (11) obtained 19 ± 1 $\mu F/cm^2$ for smooth Pt in 1*N* HCl at the zpc. Other values reported (13, 14) are 25 and 30 $\mu F/cm^2$. Since the electrodes in this work were at 0.2 v relative to SCE, or about −0.2 v relative to the zpc, cations populated the Helmholtz layer. Robertson's comparable value was

Table I. Calculated zero point of charge

Metal	Work function* (ev.)	Estimated zpc (v on SCE scale)
Mercury	4.5	−0.45
Platinum	5.3	+0.4
Nickel	4.6	−0.4
Chromium	4.0	−1.0
Iron	4.4	−0.6
Tantalum	4.2	−0.8
Aluminum	4.2	−0.8
Copper	4.6	−0.4
Lead	4.0	−1.0

* C. J. Smithells, "Metals Reference Book," Vol. 2, p. 668, Interscience Publisher Inc., New York (1955).

Table II. Platinum electrodes*

Electrode	Surface area by Kr adsorption, cm^2	Capacity in μF by polarization	Capacity in $\mu F/cm^2$
1	56.7	1210	21.4
2	271	5900	21.8
3	615	10600	17.3
4	407	8750	21.5
5	80.3	1460	18.2
6	23.9	494	20.7
		Average	20.1 ± 0.7

* The surface area of each electrode was measured.

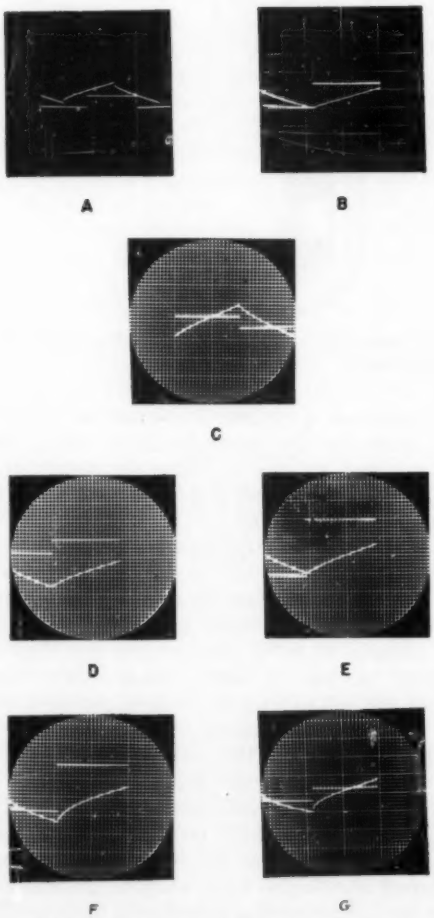

Fig. 4. Polarization traces: A—Pt; B—Ni; C—Cr; D—Fe; E—Ta; F—Cu; G—Pb. Horizontal traces, current input; angular traces, cell output or charging curves.

22 $\mu F/cm^2$. Incidentally, his measured zpc for Pt in 0.01*N* HCl was 0.35 v relative to SCE in satisfactory agreement with the estimated value here. Because of some doubt concerning the surface areas of the electrodes leading to the highest two values cited above, it may be concluded that there is reasonable agreement and that the most likely value is closer to 20 than 25 $\mu F/cm^2$.

There is no regular variation in polarization capacity per unit area with total area of the electrodes used. Thus it is possible to use this method as a means of determining the surface area of Pt or Pt black. The "roughness factors" of the electrodes used here varied from 3,900 to 20,000.

Nickel.—A typical polarization curve is given in Fig. 4b. The average value of the polarization capacity of 7 Ni electrodes was 28.8±0.5 $\mu F/cm^2$ (Table III).

The potential of the Ni electrodes was −0.4 v relative to SCE, or just about at zpc. This compares satisfactorily with values of 28 $\mu F/cm^2$ in 0.01*N* HCl, 37 $\mu F/cm^2$ in 0.1*N* HCl, 41 $\mu F/cm^2$ in 1*N* HCl, 22 $\mu F/cm^2$ in 0.006*N* NaOH, and 27 $\mu F/cm^2$ in 0.12*N* NaOH (15). Rakov, Borisova, and Ershler (16) reported 22-27 $\mu F/cm^2$ in 1*N* NaOH.

The potentials of the Ni electrodes lie near the zpc (see Table I) and applying Grahame's differential capacity curve (3) to Ni, the predicted capacity of the Ni electrode is about 27 $\mu F/cm^2$. This value and the experimental value agree satisfactorily.

There is no trend in polarization capacity with total area of the electrodes. This indicates that the polarization capacity may be used to estimate the surface area of a Ni electrode. The roughness factor of the plated Ni electrodes varied from 80 to 175.

Chromium.—A picture of a polarization curve for a Cr electrode is given in Fig. 4c. The average value of the polarization capacity of 6 Cr electrodes was 9.7±0.6 $\mu F/cm^2$ (Table IV).

The potential of the Cr electrodes was −0.1 v relative to SCE or 0.9 v relative to zpc. The experimental value of 9.7 $\mu F/cm^2$ may be compared to the value of 10 $\mu F/cm^2$ found by Powers (17) for Cr electrodes. However, the capacity expected from a consideration of the work function and the differential capacity curve of Grahame (3) is 39 $\mu F/cm^2$.

Most Cr plate has an elaborate crack network and is therefore quite porous. The outer surface projections probably shield the interior of the cracks and pores from any electrochemical reaction. Therefore, only a small fraction of the total surface as seen by gas adsorption may be expected to participate in a buildup of the edl. Thus, this method is not useful in studying the edl at a Cr surface unless the true area is known; it gives too low a capacity. It would be useful as an area measuring method only if the relation between the thickness and porosity of plate were constant for all samples. An alternate explanation of the experimental results could be based on the postulation of an oxide film on the electrodes.

Iron.—A typical polarization curve is shown in Fig. 4d. The average polarization capacity of the edl at 7 Fe electrodes was 35.9±0.8 $\mu F/cm^2$ (Table V). The potential of these electrodes was about −0.8 v relative to SCE or −0.2 v relative to zpc.

The polarization capacity predicted from a consideration of the work function and Grahame's differential capacity curves of Hg (3) is about 22 $\mu F/cm^2$. The polarization capacity of a Hg surface at which there is adsorption of anions is about 40 $\mu F/cm^2$ (3). It has been shown that sulfate ions adsorb irreversibly on Fe (18). It has also been shown that specific adsorption of iodide ions on Hg shifts the zpc as much as −0.4 v (3, 19). Thus, it is possible that sulfate ions adsorbed specifically on the Fe electrodes at the potential and caused the polarization capacity to be higher than would be predicted in the absence of specific adsorption.

The polarization capacity at Fe electrodes showed no definite trend with total surface area. Thus, it may be used to determine the extent of an Fe surface. The roughness factor of the Fe electrodes was 9.3, probably somewhat high.

Tantalum.—A typical polarization curve for a Ta electrode is shown in Fig. 4e. The average polarization capacity of the edl at 9 Ta electrodes was 4.61 ± 0.1 $\mu F/cm^2$ (Table VI). The potential of the

Table III. Nickel electrodes*

Electrode	Surface area by Kr adsorption, cm^2	Capacity in μF by polarization	Capacity in $\mu F/cm^2$
1	119	3350	28.0
2	134	3670	27.4
3	183	5400	29.4
4	118	2985	26.4
5	63	1930	30.5
6	100	3035	30.4
7	139	4075	29.3
			Average 28.8 ± 0.5

* The surface area of each electrode was measured.

Table IV. Chromium electrodes*

Electrode	Surface area by Kr adsorption, cm^2	Capacity in μF by polarization	Capacity in $\mu F/cm^2$
1	128	1390	10.9
2	36	412	11.1
3	56	640	11.5
4	116	1450	8.8
5	275	2150	7.8
6	225	1750	7.8
			Average 9.7 ± 0.6

* The surface area of each electrode was measured.

Table V. Iron electrodes*

Electrode	Surface area by Kr adsorption, cm^2	Capacity in μF by polarization	Capacity in $\mu F/cm^2$
1	23.1	785	34.0
2	20.2	795	39.4
3	17.9	575	37.9
4	16.7	525	31.4
5	14.6	510	35.0
6	10.7	392	37.6
7	10.2	369	36.2
			Average 35.9 ± 0.8

* The surface area was measured on 6 meters of wire. The surface area of each electrode is a proportionate part of the total area.

Table VI. Tantalum electrodes*

Electrode	Surface area by Kr adsorption, cm²	Capacity in μF by polarization	Capacity in μF/cm²
1	3.58	15.4	4.23
2	4.08	20.5	5.26
3	4.52	21.2	4.76
4	5.30	27.5	5.40
5	6.25	27.7	4.47
6	7.64	33.0	4.36
7	8.86	37.7	4.23
8	9.95	43.1	4.38
9	10.1	45.7	4.18
			Average 4.59 ± 0.11

* The surface area was measured on 6 meters of wire. The surface area of each electrode is a proportionate part of the total area.

Ta electrodes was −0.2 v relative to SCE, or 0.6 v relative to zpc. The polarization capacity expected from a consideration of the work function and the differential capacity curves of Hg (3) is about 40 μF/cm².

The low value of the polarization capacity is thought to be due to the oxide film on the surface of the electrodes. A similar low value of 7 μF/cm² for an oxide film on the surface of an electrode was found by Ershler *et al.* (16). The presence of the oxide film on the surface lowers the charge density on the surface of the electrode. This produces an increase in the thickness of the edl, and, as a result, decreases the capacity. The lower capacity may also be thought of as being caused by an increase in distance between plates of the condenser formed by the electrode and the solution.

It should be noted that the results, while low, are consistent, and may be used to determine the extent of the surface of oxide-coated Ta electrodes. The roughness factor of the Ta electrodes was 3.3.

Aluminum.—Problems wtih Al were manifold. The portion of the charging curve from which to take the slope was usually in doubt. Also there appeared to be a frequency dependence which resisted clarification. About all that can be said at this time is that "capacity" was not a function of the total (gas) surface area available. Therefore, the method is applicable to Al provided a firm value can be obtained for C. Work on this system is continuing.

Copper.—A typical polarization curve for Cu electrodes is given in Fig. 4f. The average polarization capacity of 10 Cu electrodes was 32.9 ± 0.8 μF/cm² (Table VII). This may be compared to 32 μF/cm² found by Bockris and Pentland (20) and to 23 μF/cm² obtained by Wiebe and Winkler (21) on cathodic charging. The potential of the Cu electrodes was −0.2 v relative to SCE, or 0.2 v relative to zpc. The capacity expected from a consideration of the work function and the differential capacity curves of Hg (3) is about 30 μF/cm². This is in fair agreement with the experimental value, but here again there was some question about choice of the applicable slope.

The polarization capacity of the Cu electrodes is fairly constant over the range of surface areas studied. The roughness factor of the Cu electrodes was 1.5.

Table VII. Copper electrodes*

Electrode	Surface area by Kr adsorption, cm²	Capacity in μF by polarization	Capacity in μF/cm²
1	4.54	125	28.5
2	5.0	155	31.0
3	5.12	159	31.1
4	5.6	195	34.8
5	6.59	243	36.9
6	6.8	246	36.2
7	7.57	265	35.0
8	8.3	240	28.9
9	9.1	315	34.6
10	10.7	344	32.2
			Average 32.9 ± 0.8

* The surface area was measured on 6 meters of wire. The surface area of each electrode is a proportionate part of the total area.

Table VIII. Lead electrodes*

Electrode	Surface area by Kr adsorption, cm²	Capacity in μF by polarization	Capacity in μF/cm²
1	14.1	690	47.7
2	12.3	650	52.7
3	9.81	527	62.1
4	8.3	460	55.4
5	6.54	326	50.0
6	4.65	221	47.5
			Average 52.6 ± 1.7

* The surface area was measured on 6 meters of wire. The surface area of each electrode is a proportionate part of the total area.

Lead.—A typical polarization curve for a Pb electrode is shown in Fig. 4g. The average polarization capacity at 6 Pb electrodes was 52.6 ± 1.7 μF/cm² (Table VIII). The potential of the Pb electrodes was −0.6 v relative to SCE, or 0.4 v relative to zpc.

The expected polarization capacity for Pb electrodes at this potential from a consideration of the work function and the differential capacity curves of Hg (3) is about 45 μF/cm², but the estimated capacity is not very accurate as the capacity curve of Hg rises rapidly at this potential. Kabanov and Jofa (22) found a polarization capacity of 30 μF/cm² at a potential of −0.70 v relative to SCE and the polarization capacity rose rapidly to about 40 μF/cm² as the potential was changed to −0.68 v relative to SCE. The high value of the polarization capacity suggests that sulfate ions are adsorbed on the surface. Subject to the indicated limitations the roughness factor of the Pb electrodes was 5.6.

Conclusions

The polarization capacity appears to be a satisfactory measure of the extent of the surface of an electrode (*a*) if the value of the polarization capacity is actually known, or (*b*) if a standardized procedure is worked out for each case. The measurement of the polarization capacity is fast, relatively accurate, and is made easily and quickly in contrast to the more tedious measurement of surface area by gas adsorption techniques. The method appears to be applicable to Pt, Ni, Fe, Ta; less so to Cr, Cu, and Pb for different reasons; and inapplicable to Al so far.

The relationship of the work function to the position of the zpc first noted by Frumkin (8) and the electrocapillary behavior of Hg may be used in the absence of specific interaction or reaction to predict with fair accuracy the polarization capacity of metal electrodes. The apparent failure of these relationships in the case of Al, Ta, Cr, Fe, and Pb are believed to be due to specific adsorption of ions on the electrode, the presence of oxide layers, or the passage of faradaic current. In comparing the capacity of metal electrodes the potential relative to the zpc is a very important factor. Comparisons made at nonequivalent potentials are meaningless.

Acknowledgment

The authors are pleased to take this opportunity to express their appreciation to the Office of Naval Research for its financial support of this work. They also acknowledge helpful discussions with J. J. McMullen of this laboratory.

Manuscript received Nov. 1, 1956. This paper was prepared for delivery before the San Francisco Meeting, April 29-May 3, 1956.

Any discussion of this paper will appear in a Discussion Section to be published in the June 1958 JOURNAL.

REFERENCES

1. F. P. Bowden and E. K. Rideal, *Proc. Roy. Soc. (London)*, **120A**, 59 (1928).
2. C. Wagner, *This Journal*, **97**, 72 (1950).
3. D. C. Grahame, *Chem. Rev.*, **41**, 441 (1947).
4. Betty Pegues, M.A. Thesis, University of Texas (1951).
5. R. A. Beebe, J. B. Beckwith, and J. M. Honig, *J. Am. Chem. Soc.*, **67**, 1554 (1945).
6. C. Kenty, *Rev. Sci. Instr.*, **22**, 217 (1951).
7. M. J. Joncich, Ph.D. Dissertation, University of Texas, p. 26 (1953).
8. A. Frumkin, *Colloid Symposium Annual*, **7**, 89 (1930).
9. T. Veslovsky, *Acta Physicochim, U.R.S.S.*, **11**, 815 (1939).
10. T. Borisova, B. Ershler, and A. Frumkin, *Zhur. Fiz. Khim.*, **22**, 925 (1948).
11. W. D. Robertson, *This Journal*, **100**, 194 (1953).
12. P. Ruetschi and P. Delahay, *J. Chem. Phys.*, **23**, 697 (1955).
13. B. Ershler and M. Proskurnin, *Acta Physicochim., U.R.S.S.*, **6**, 195 (1937).
14. P. Dolin and B. Ershler, *ibid.*, **13**, 747 (1940).
15. J. O'M. Bockris and E. C. Potter, *J. Chem. Phys.*, **20**, 614 (1952).
16. A. Rakov, T. Borisova, and B. Ershler, *Zhur. Fiz. Khim.*, **22**, 1390 (1948).
17. R. A. Powers, Ph.D. Dissertation, University of Texas, p. 29 (1952).
18. N. Hackerman and S. J. Stephens, *J. Phys. Chem.*, **58**, 904 (1954).
19. O. Essin and B. Markov, *Acta Physicochim., U.R.S.S.*, **10**, 353 (1939).
20. J. O'M. Bockris and N. Pentland, *Trans. Faraday Soc.*, **48**, 833 (1952).
21. A. K. Wiebe and C. A. Winkler, *Can. J. Chem.*, **31**, 1118 (1953).
22. B. Kabanov and S. Jofa, *Acta Physicochim. U.R.S.S.*, **10**, 617 (1939).

Reaction of Hydrogen with Preoxidized Zircaloy-2 at 300° to 400°C

Earl A. Gulbransen and Kenneth F. Andrew

Research Laboratories, Westinghouse Electric Corporation, Pittsburgh, Pennsylvania

ABSTRACT

The permeability of preformed oxide films to hydrogen at 300°-400°C was studied. Two types of reactions were observed. If the oxide film was permeable, a general reaction occurred with the formation of zirconium hydride phases on the surface. If the oxide film was relatively impermeable, reaction occurred at the edges of the sample where defects probably exist in the oxide. The reaction starts at localized areas and spreads through the metal with hydride and oxide film spalling from the metal continually.

Zirconium reacts with hydrogen at temperatures up to 550°C to form stable hydrides of the metal when the hydrogen concentration exceeds the terminal solubility (1,2). The formation of a hydride phase on the surface and in the metal causes major changes in the physical and chemical properties of the metal or alloy (3).

Hydride phases can form readily at 400°C since the terminal solubility is only 1.86 at. % or 200 ppm by weight of hydrogen. One of the effective barriers to reaction of Zr at 300°-400°C with hydrogen is a surface oxide film (4).

With the development of Zr-Sn alloys for use in nuclear power reactors, it is of interest to study the permeability of several types of oxide films to hydrogen at temperatures of 300°-400°C and the effects of the hydrogen reaction on the alloy.

The mechanism of the reaction of hydrogen with pure Zr was considered earlier (4). The permeability of several types and thicknesses of oxide films to hydrogen was determined at 150°C. The results showed that the oxide film formed at room temperature on abraded and cleaned metal samples offered more resistance to hydrogen permeation than thicker oxide films formed at 250°C and higher. Oxygen and nitrogen dissolved in the metal phase had no effect on the rate of permeation when compared to an oxide-free surface. Chemically polished surfaces of Zr were impermeable to hydrogen at 150°C.

Experimental

Apparatus.—The vacuum microbalance apparatus was used (5) for preparing the oxide films and for determining the reaction with hydrogen. Details of

Table I. Chemical and spectrographic analyses of Zircaloy-2

Zircaloy-2 Foil			
Element	Wt %	Element	Wt %
Zr	Major	Hf	0.0055
Sn	1.45*	Si	——
Fe	0.135*	N	0.0038
Ni	0.055*	H	0.0020
Cr	0.100*	O	0.1400
Al	0.0045		

* Chemical.

the apparatus and method have been described (5).

Pure hydrogen was prepared by diffusing a purified grade of hydrogen through a hot Pd tube.

Samples.—Thick strips of Zircaloy-2 were obtained from the Westinghouse Atomic Power Division and rolled to strips 5 and 10 mil thick. Table I shows the spectrographic and chemical analyses of the alloy.

Samples were abraded and cleaned (6). Some of the samples were given a chemical polishing treatment in a special acid bath having the composition: 45% HNO_3, 10% HF, and 45% H_2O.

Steam reacted samples.—These were reacted with steam at 399°C for three days to weight gains of 118 to 155 $\mu g/cm^2$. Although most of the oxygen forms an external oxide film, some oxygen may dissolve in the metal.

Results and Discussion

Comparison of Initial Pretreating Procedures

Abraded and chemically polished samples of Zircaloy-2 were reacted at 400°C with pure hydrogen at 5.0 cm Hg pressure. Since the vacuum was better than 10^{-6} mm Hg, the samples showed no evidence for a pick-up of oxygen on heating to the reaction temperature.

Fig. 1 shows the time course of the hydriding reaction for both samples. Here weight gain in micrograms per cm^2 was plotted against the time in minutes. Curve A shows the time course for the abraded sample containing the room temperature oxide film. A rapid sorption of hydrogen occurs with the composition $ZrH_{0.77}$ (43 at. % hydrogen) being formed in 2 min of reaction. Although the hydrogen was evacuated at the end of 2 min, the reaction continued during evacuation until the hydrogen pressure was reduced to a value corresponding to the decomposition pressure characteristic of the hydride phase (about 10^{-4} mm Hg) (2).

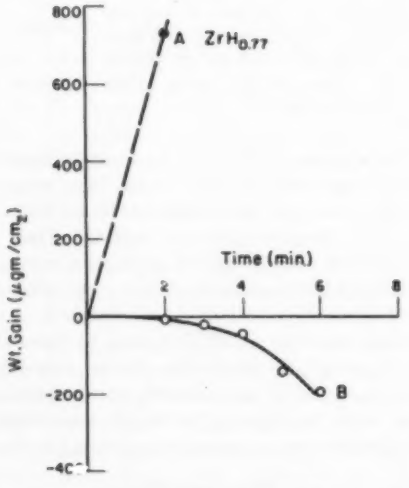

Fig. 1. Comparison of initial oxide film on hydriding Zircaloy-2, 400°C, 5.0 cm Hg of H_2. Curve A, abraded, room temperature oxide film; curve B, chemically polished oxide film.

On cooling to room temperature, the sample was found to be brittle and cracked readily into a number of pieces. Since the terminal solubility was only 1.86 at. % at 400°C, most of the hydrogen was in the hydride phase $ZrH_{1.5}$ and was concentrated in the surface layer. A rapid reaction occurred at 400°C although the room temperature oxide film limited the reaction with hydrogen at 150°C.

Curve B of Fig. 1 shows the results for the chemically polished sample. Although the chemical polishing solution removes metal from the sample, a passive type of oxide or corrosion film remains on the alloy. Curve B shows that the passive film protects the metal for 2 min of reaction time after which reaction occurs. However, as fast as hydride is formed, it spalls from the metal giving a weight loss instead of a weight gain. The rate of spalling increases steadily with time as more surface is exposed for reaction. An examination of the specimen after cooling shows that the sample edges were the only regions attacked by hydrogen.

It is concluded that chemical polishing the alloy forms a film which was nearly impermeable to hydrogen over the major portion of the surface. However, reaction occurred at the sample edges. Since the attack is highly localized, spalling of hydride occurred with a loss of weight. Curves A and B of Fig. 1 were reproducible.

Permeability of Preformed Oxide Films to Hydrogen

Zircaloy-2 samples were reacted with pure oxygen at 400°C to form oxide film thicknesses of 10, 24.5, and 73 $\mu g/cm^2$. These weight gains corresponded to 615, 1510, and 4480Å of oxide using the conversion factor of 61.5 (6) to relate Angstroms to weight gain in micrograms per cm^2.

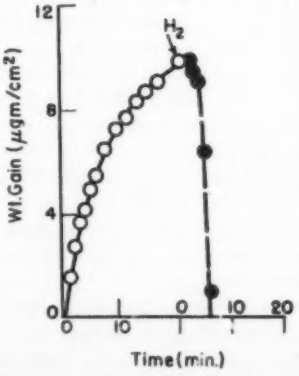

Fig. 2. Effect of thin oxide film (10 $\mu g/cm^2$) on hydriding Zircaloy-2, 400°C, 5.0 cm Hg of H_2.

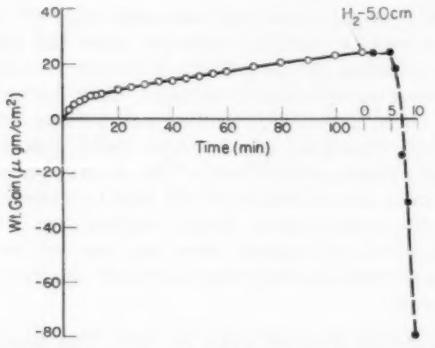

Fig. 3. Effect of thin oxide film (24.5 μg/cm^2) on hydriding Zircaloy-2, 400°C, 5 cm Hg of H_2.

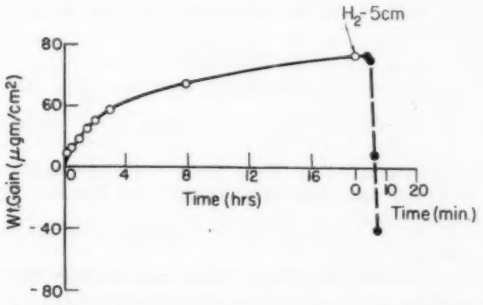

Fig. 4. Effect of thin oxide film (73 μg/cm^2) on hydriding Zircaloy-2, 400°C, 5.0 cm Hg of H_2.

These samples were reacted with hydrogen at 400°C and 5.0 cm Hg pressure. Fig. 2, 3, and 4 show the time courses for the oxidation and hydrogen reaction curves for three experiments. Hydrogen was added after removing the oxygen and evacuating to a pressure of 1 x 10^{-6} mm Hg.

The weight change-time curves for the hydrogen reaction were similar to Curve B of Fig. 1. After an induction period, reaction occurred with immediate spalling of hydride. This behavior was characteristic of a highly localized attack. On cooling, all of the samples showed a highly localized attack at the edges.

Table II summarizes the results on this series of experiments. It is concluded that the oxide films were nearly impermeable to hydrogen except at the edges where localized attack occurs with spalling of the hydride together with the oxide film.

Studies on Steam Formed Oxide Films

Six samples of Zircaloy-2 were reacted with steam at 399°C for three days to form oxide films of thicknesses between 119-155 μg/cm^2. These thicknesses were 33-44% of the 350 μg/cm^2 film thickness found by Thomas (7) for transition in the corrosion rate. The presence of hydride in the steam-reacted films before hydriding was not tested.

Samples were reacted in the as-received condition with hydrogen at pressures of 1, 2.4, and 5.0 cm Hg and at temperatures of 300°-400°C. Table III shows a summary of the oxide thicknesses, the hydrogen reaction conditions, and results.

At 300°C no reaction occurred in 20 hr for a hydrogen pressure of 2.4 cm Hg, while at 350°C reaction occurred after 62 hr for 1 cm Hg hydrogen pressure and after 12 min for 5.0 cm Hg hydrogen pressure. The 400°C experiments showed reaction in three of the four experiments. The fourth experiment would probably show reaction if the reaction time had been extended.

Fig. 5 shows a photograph of the 350°C-1 cm Hg pressure experiment. The course of the edge type of spalling is seen clearly. All of the samples which reacted with hydrogen in this group of experiments reacted at the edges as shown in Fig. 5.

To prove that the alloys having a steam-formed oxide film react with hydrogen at the edges, x-ray diffraction studies were made of the spalled material and the remaining metal phase. The steam-corroded Zircaloy-2 sample reacted with hydrogen at 400°C and 5.0 cm Hg of H_2 was studied (*see* Fig. 5).

The spalled reaction product gave an x-ray diffraction pattern characteristic of the delta-hydride phase having the composition $ZrH_{1.4-1.6}$ (1) with no evidence of a metal phase. The x-ray diffraction pattern of the remaining metal gave a pattern characteristic of Zr with no hydride reflections. Although oxide reflections may be expected, the amount was too small to detect by x-ray diffraction methods. It is concluded from these observations that spal-

Table II. Summary of results of hydrogen reaction of alloy and alloy with oxide film formed in oxygen atmospheres, hydrogen, 400°C, 5.0 cm Hg pressure

Oxide thickness μg/cm^2	Oxide thickness Å (ρ = 1)*	Color of oxide	Results
Room temp oxide		None	Adsorbed hydrogen, no spalling. Fine cracks on surface.
Chem. polished		None	Reaction at edges with spalling.
10	615	Blue-green	Reaction at edges with spalling.
24.5	1510	Pink-green	Reaction at edges with spalling.
73	4480	Gray	Reaction at edges with spalling.

* ρ = surface roughness ratio.

Table III. Summary of results on hydrogen reaction of corrosion films on Zircaloy-2 Prepared (Lustman) H_2O—3 days at 400°C

Area cm^2	Wt gain, g	Thickness μg/cm^2	Thickness Å (ρ=1)*	Hydrogen conditions Temp, °C	Hydrogen conditions Pressure cm	Results
17.42	0.0027	155	9,510	300	2.4	No reaction in 20 hr.
17.42	0.0027	155	9,510	400	5.0	Edge reaction in 6 min, spalling.
17.96	0.0023	128	7,850	400	1.0	No failure in 3 hr.
17.96	0.0023	128	7,850	400	5.0	Edge reaction in 2 hr, spalling.
18.45	0.0022	119	7,300	400	1.0	Edge reaction in 3 min, spalling.
17.35	0.0023	133	8,150	350	5.0	Edge reaction in 12 min, spalling.
18.45	0.0025	135	8,310	350	1.0	Edge reaction after 62 hr, spalling.

* ρ = surface roughness ratio.

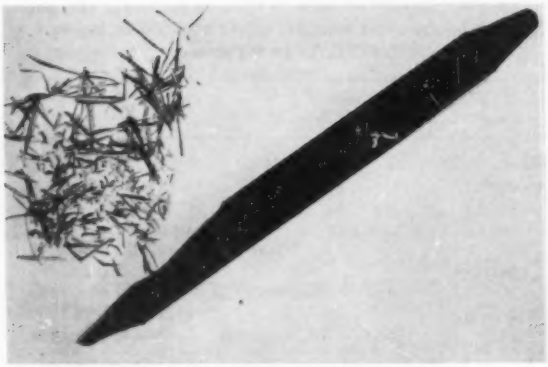

Fig. 5. Effect of hydrogen on steam-corroded Zircaloy-2; steam, 750°F, 3 days; hydrogen, 350°C, 1.0 cm Hg of H_2. Magnification, 2X before reduction for publication.

ling of the metal phase is due to the formation of the hydride phase at the sample edges and that no appreciable attack occurs through the oxide film on the flat surface.

Several additional facts can be drawn from Table III: (*A*) hydrogen reaction increases with pressure and temperature; (*B*) since the reaction occurs at the edges the results suggest a variation in reactivity due to defects in the metal at the edges such as cracks, strains, etc.

Conclusions

Two types of reaction were observed when Zircaloy-2 was exposed to hydrogen at temperatures of 400°C. If the oxide film was permeable to hydrogen, a general reaction occurred with the hydride $ZrH_{1.5}$ forming on the surface. This type of reaction was observed on abraded samples when the equilibrium room temperature film was present on the metal. If the oxide, on the other hand, was impermeable, reaction occurred at the edges where defects exist due to cracks in the metal or stresses set up in the metal during rolling, cutting, etc. The reaction starts at localized areas and spreads through the metal with the hydride continually spalling from the metal.

Manuscript received April 15, 1957. This paper was prepared for delivery before the Buffalo Meeting, Oct. 6-10, 1957.

Any discussion of this paper will appear in a Discussion Section to be published in the June 1958 JOURNAL.

REFERENCES

1. E. A. Gulbransen and K. F. Andrew, *This Journal*, **101**, 474 (1954).
2. E. A. Gulbransen and K. F. Andrew, *J. Metals*, **7**, 136 (1955).
3. W. L. Mudge, Jr., "Zirconium and Zirconium Alloys," p. 730, American Society for Metals, Cleveland (1953).
4. E. A. Gulbransen and K. F. Andrew, *This Journal*, **101**, 348 (1954).
5. E. A. Gulbransen, *Trans. Electrochem. Soc.*, **81**, 187 (1942).
6. E. A. Gulbransen and K. F. Andrew, *Trans. Am. Inst. Mining Met. Engrs.*, **185**, 515 (1949).
7. D. E. Thomas, "Metallurgy of Zirconium," by Lustman and Kerze, pp. 608-640, McGraw-Hill Book Co., New York (1953).

Effect of Current Drains on Cadmium Standard Cells

George D. Vincent

Standard Cell Department, The Eppley Laboratory, Inc., Newport, Rhode Island

ABSTRACT

Various sizes of unsaturated cadmium standard cells were subjected to current drains of from 0.5 to 12 μa (0.2 — 20 μa/cm^2). Voltages across the terminals of these cells were observed for several years. The relationship between change in voltage and time is not a linear one; an approximation of the decrease per unit area of electrode is 11 μv/coulomb cm^{-2}.

Although the use of standard cells has received considerable attention (1-3), the determination of conditions to maintain the highest accuracy and constancy has been the intent, with few exceptions (4), of previously published work. The statement appears on standard cell certificates that the maximum permissible current through a cell is 100 μa, but since it may be assumed that such current will flow for very short periods, a few seconds at most, and also that it will probably flow as often in the charging as in the discharging direction, the total effect of the current on the cell is negligible.

However, certain instruments now available, in addition to a very recently described potentiometer (5), use standard cells under conditions of current drain. The purpose of this paper is to make known the results of tests on standard cells made at intervals during the past nine years, which will be useful in estimating the error likely to arise from the use of a standard cell under conditions which draw a small current from it.

Apparatus and Procedure

The main body of observations were measurements of voltages between terminals of standard

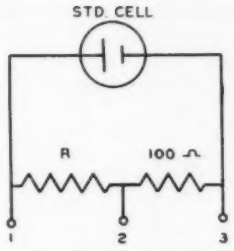

Fig. 1. Test circuit. R = 0.08—2 megohms

cells which were delivering from 0.5 to 12 μa. As indicated in Fig. 1, each cell was connected to a load resistor R of appropriate value (0.08-2 megohms) in series with a precision 100-ohm resistor, which was compared to within 0.01% against N.B.S. certified laboratory standards at the beginning and the end of the test. The voltage across points 1 and 3 is the closed circuit voltage of the cell, while the measurement of the voltage across 2 and 3 provides a means of determining the current.

Voltages were measured with a Feussner-type potentiometer (6), using as a standard a saturated cell from the working standards group of the Eppley Laboratory. This cell was maintained in an oil thermostat and was constant and accurate to within 2 ppm as determined by frequent comparison with the standards bank which is maintained at this Laboratory, and checked at six-month intervals at the National Bureau of Standards. The sum of all instrumental errors was within 0.01%. All test measurements were made at room temperature, 25° ± 3°C.

Three sizes of commercially available types of unsaturated cells were used, with cross-sectional areas of 5.5 cm^2, 1.43 cm^2, and 0.50 cm^2. All were taken from the regular production of this Laboratory. They all had 12½% cadmium amalgam as the negative electrode, purified mercury as the positive electrode, electrolytic mercurous sulfate as the depolarizer, and unsaturated cadmium sulfate solution, slightly acidified with sulfuric acid, as the electrolyte. They were hermetically sealed in H-shaped glass vessels, both limbs being the same size, and had plugs and septa (7) to hold the electrode materials in place. These plugs and septa, consisting of either cork or polystyrene (8) washers covered with linen, reduced the electrode area by the reduction of physical surface due to the area occupied by the materials comprising them, and in effect by the restriction which they imposed on free circulation of the components of the electrolyte.

Results

Four groups of cells were used in the principal test. In each of three groups were 3 cells from which no current was drawn, and 2 each from which currents of about ½, 1, 2, 5, and 10 μa were taken continuously for 52 months, or until the voltage became erratic, if that condition was reached in less than 52 months. One of the groups was composed of cells of 0.50 cm^2 electrode area, which had septa of linen held in place by polystyrene washers. The other two groups where composed of cells of 1.43 cm^2 electrode area, with linen septa held in place by treated cork washers. The fourth group, which also had linen septa and cork washers, consisted of 15 cells of 5.5 cm^2 area. In this group were 3 cells with no current drain; 2 with 1 μa; 1 with 2 μa; 1 each with 3.7, 4.2, and 4.7 μa, which are averaged together and reported as 4.2 μa; 1 each with 6.1 and 7.0 which are reported together as 6.5 μa; 1 each with 8.0, 8.7, and 8.9, reported together as 8.5 μa, and 1 with 12 μa current drain. The quotient of the current, as determined by the drop across the 100-ohm resistor (Fig. 1), divided by the electrode area is reported as the current density of the discharge currents. From the current density and the elapsed time of discharge the quantity of electricity withdrawn per unit area in coulombs/cm^2 is determined.

Throughout the discharge period, the closed circuit voltages of the cells were determined from time to time. Fig. 2, 3, and 4 show the decrease in closed circuit voltage against elapsed time.

The zero point of these curves is the closed circuit voltage at the beginning of the test, and differs from the open circuit emf of the cell by the *IR* drop due to the internal resistance. This is discussed further below. The general form of the discharge curves is similar to other battery curves, with a relatively rapid decrease in voltage at first, which becomes progressively slower until a "knee" is reached, beyond which the decrease again becomes more rapid. It appears that this knee is reached when the cell has decreased about 5 mv. The change in voltage beyond this point being sufficiently rapid and unpredictable to make the cell of little value as a standard, a decrease of 5 mv in the closed circuit voltage may be taken as the end point of the useful life of a standard cell under discharge.

The data on which Fig. 2, 3, and 4 were based then were calculated to the basis of quantity of electricity withdrawn in coulombs/cm^2, which permits the various rates of decrease in voltage in the three sizes of cells tested to be correlated. The results of this reduction of the data are listed in Table I and the average decrease in voltage as shown in

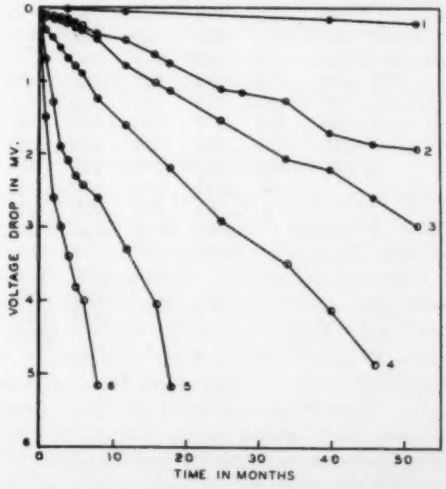

Fig. 2. Decrease in closed circuit voltage of cells with 0.5 cm^2 electrode area vs. time. 1, Controls, no current; 2, 0.5 μa; 3, 1 μa; 4, 2 μa; 5, 5 μa; 6, 10 μa.

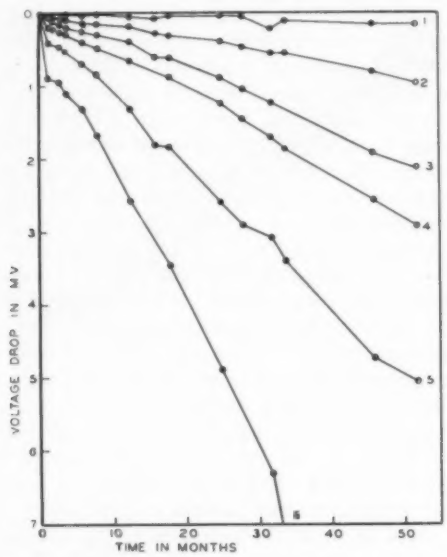

Fig. 3. Decrease in closed circuit voltage of cells with 1.43 cm^2 electrode area vs. time. 1, Control, no current; 2, 0.5 μa; 3, 1 μa; 4, 2μa; 5, 5μa; 6, 10 μa.

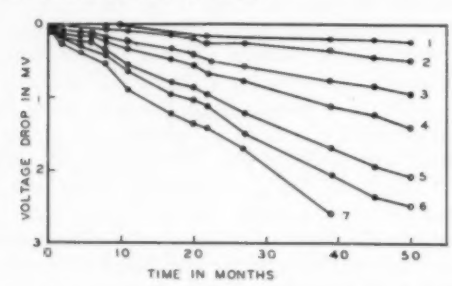

Fig. 4. Decrease in closed circuit voltage of cells with 5.5 cm^2 electrode area. 1, Controls, no current; 2, 1 μa; 3, 2 μa; 4, 4.2 μa; 5, 6.5 μa; 6, 8.5 μa; 7, 12 μa.

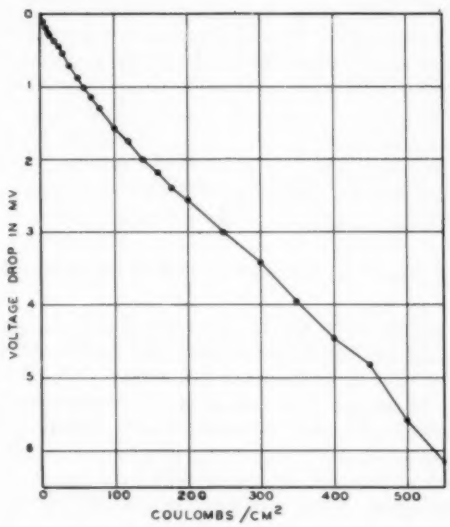

Fig. 5. Decrease in closed circuit voltage vs. total quantity of electricity withdrawn per unit area of electrode.

the last column is plotted in Fig. 5 against the total quantity of electricity per unit area.

From the data in Table I, the average rate of decrease in voltage over intervals of discharge can be calculated, as listed in Table II.

As confirmation of the above results, another separate test, similar to the above, was run with two groups, each consisting of three cells of 1.43 cm^2 electrode area. One group was discharged at a rate of 1 μa and the other at a rate of 5 μa. The decrease in voltage against time is displayed in Fig. 6.

The dashed lines in Fig. 6 represent a rate of decrease of 11 μv/coulomb cm^{-2} for the respective groups.

Table I

No. of cells:	2	4	1	4	3	2	2	4	3	2	1	4	2	4	2	2	
Area cm^2:	5.5	1.4	5.5	1.4	5.5	0.5	5.5	1.4	5.5	0.5	5.5	1.4	0.5	1.4	0.5	0.5	
μa/cm^2:	0.18	0.29	0.36	0.69	0.76	0.99	1.19	1.34	1.56	2.01	2.17	3.46	3.86	6.91	10.1	19.2	Average
Coul./cm^2									Closed circuit decrease, μv								
3		95	85	110	90	100	110	115	90	75	130	170	90	120	100	200	112
6	102	155	125	180	120	130	185	190	160	140	190	265	180	360	250	400	196
9	171	185	210	235	150	180	210	235	190	150	250	340	270	460	360	620	264
12	260	275	275	285	165	225	230	275	210	165	290	420	320	490	450	660	312
18	350	365	390	355	280	320	250	370	275	200	330	420	380	530	540	690	378
24	515	555	530	450	360	385	345	435	320	260	375	435	425	650	670	800	469
30		680	650	605	430	435	460	495	400	290	420	490	540	730	800	1000	562
40		980	810	780	575	620	615	615	570	400	505	595	680	845	1015	1280	726
50			1020	1040	740	820	745	735	720	587	645	670	800	930	1250	1500	872
60				1265	870	1030	840	855	850	750	845	750	900	1030	1480	1780	1019
70				1540	1015	1140	985	985	960	890	965	830	1120	1115	1710	1900	1166
80				1835	1150	1220	1150	1140	1035	980	1065	935	1240	1165	1910	2140	1305
100					1410	1640	1415	1510	1315	1125	1260	1160	1420	1280	2060	2600	1516
120						1860	1675	1900	1595	1430	1410	1400	1600	1440	2220	2780	1755
140						2410	1935	2230	1830	1645	1590	1625	1800	1650	2340	2950	2000
160							2130	2550	2070	1870	1800	1855	2000	1860	2440	3100	2168
180								2910	2330	2090	2065	2085	2190	2080	2500	3260	2390
200									2460	2310	2330	2320	2410	2300	2575	3710	2552
250										2715	2980	2900	2915	2820	2870	3840	3006
300												3195	3340	3335	3220	4010	3420
350												3950	3830	3845	3560	4625	3962
400												4570	4210	4365	3920	5220	4457
450												4950	4780	4875	4730		4834
500														5355	5800		5578
550														6150			6150

Table II. Rate of decrease in closed circuit voltage

Interval in coulombs/cm²	Rate of decrease in μv/coulomb cm⁻²
0-50	17.4
50-100	12.9
100-200	10.4
200-300	8.7
300-400	10.4
400-500	11.2

IR Drop

Fig. 6 was drawn to illustrate also the *IR* drop due to the internal resistance of the cell. This has been discussed by Hartshorn and Manning (4). They express the voltage of a cell which has been delivering current as

$$V = E_o - IR_o - \Delta V \qquad (I)$$

where "IR_o is the initial drop" and "ΔV is the slow change of voltage associated with chemical changes".

Some of the decrease in voltage of an unsaturated cell on closed circuit is no doubt due to formation of $CdSO_4$ and the consequent increase in the concentration of the electrolyte (9). However, it is unlikely that any gain in accuracy would result from the use of a saturated cell, because such a cell would immediately deposit solid $CdSO_4 \cdot 8/3\ H_2O$ as a result of the discharge current, which deposit would increase the internal resistance in an erratic manner, similarly increasing the *IR* drop.

Effect of Interrupted Currents

To determine whether the summed up effects of discontinuous current drains might be predicted from the continuous current drain data, 3 cells of 1.43 cm² area were discharged at 30.3 μa, one continuously, one for 16 hr continuously out of every 24, and the third for 8 hr continuously out of 24. At the end of 31 days, the closed circuit voltage of the cell on continuous discharge had decreased 740

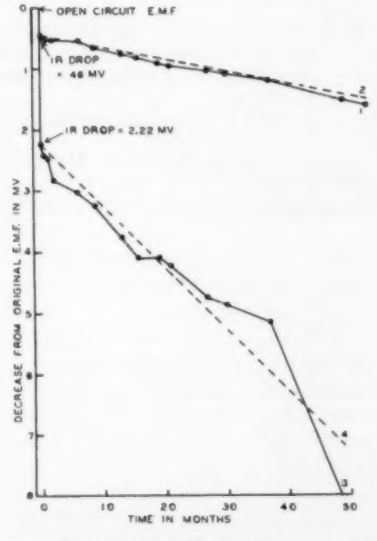

Fig. 6. Decrease in closed circuit voltage of cells with 1.43 cm² electrode area vs. time, showing IR drop immediately upon closing circuit. 1, Avg. 3 cells at 1 μa; 2, rate of 11 μv/coulomb cm² for 1μa and 1.43 cm²; 3, avg. 3 cells at 5 μa; 4, rate of 11 μv/coulomb cm⁻² for 5 μa and 1.43 cm².

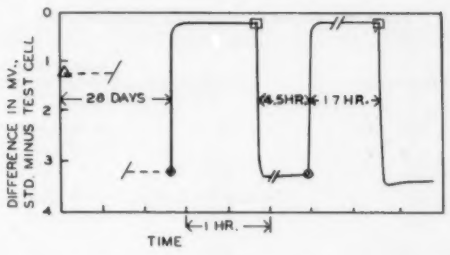

Fig. 7. Extracted from continuous strip chart recording, showing rate of return to closed circuit voltage after interruption of current. Open triangle, closed circuit voltage at beginning of discharge; open circle, circuit opened; open square, circuit reclosed.

μv, or 13.1 μv/coulomb cm⁻²; the cell on discharge 16 hr /day had decreased 600 μv, or 15.9 μv/coulomb cm⁻², and the cell on discharge 8 hr/day, 230 μv or 12.2 μv/coulomb cm⁻².

The same question was further investigated in another test, in which a cell was discharged by withdrawing about 180 coulomb/cm², and the drop in voltage continuously recorded. The cell under load was opposed by a saturated standard cell, and the difference in voltage continuously balanced and recorded by a 16 mv full scale L&N Speedomax recorder. At the beginning of the discharge period, the open circuit voltage was about 1.1 mv higher than the standard. At the end of the discharge period, when the closed circuit voltage had decreased about 2 mv, the load was removed from the cell under test for a period of 1 hr. The load was then reconnected for 4½ hr, when it was again removed, this time for 17 hr. When the load was removed, the voltage of the cell rose within 15 min to a value within 0.05% of the open circuit value to which it eventually recovered. Both times, upon reconnecting the load, the closed circuit voltage dropped immediately to the value it had when the load was disconnected. Fig. 7 is drawn from the chart curve obtained. This was repeated with two other cells, with the same results.

It appears, therefore, from the evidence in the two preceding paragraphs, that no large error is introduced by considering the effects of an interrupted current approximately the same as that of an equal quantity of electricity withdrawn in a continuous current.

Variations of Individual Cells

With the portable types of unsaturated cells such as those in this work, there is probably considerable variation in the effective electrode area, due to the effect of the septa. Although test cells made without septa would lead to better agreement in comparing the results on individual cells, the variations encountered in available types of cells must be considered in predicting the performance of instruments, and are therefore of interest.

The distribution of deviations from the average rate of closed circuit voltage decrease indicates that there is greater probability of encountering wide deviations for any individual cell on the side of higher-than-average rate. Table III lists the rate of de-

Table III. Decrease rates of 22 individual cells

Electrode area	Current	Rate of decrease at 200 coulomb/cm²
cm²	μa	μv/coulomb cm⁻²
5.5	8.0	12.7
5.5	8.9	12.6
5.5	8.9	13.4
5.5	12.0	10.4
1.43	4.8	9.3
1.43	5.0	13.8
1.43	5.0	12.4
1.43	5.0	14.6
1.43	5.0	14.2
1.43	5.1	11.0
1.43	9.5	11.7
1.43	9.6	9.9
1.43	9.9	11.2
1.43	10.6	12.8
0.5	0.9	10.4
0.5	1.0	13.1
0.5	1.9	11.3
0.5	1.9	12.2
0.5	5.0	14.8
0.5	5.1	10.6
0.5	9.4	16.2
0.5	9.8	18.0

crease in μv/coulomb cm^{-2} of 22 cells at 200 coulombs/cm², which is about the midpoint of the useful life of a discharging standard cell.

Of the 48 cells measured, the greatest rate of decrease observed after the initial rapid drop was 28.9 μv/coulomb cm^{-2} in a cell of 1.43 cm² electrode area discharging at 0.622 μa/cm², and the smallest was 9.7 μv/coulomb cm^{-2} in a cell of the same size discharging at 3.34 μa/cm².

Internal Resistance of Cells

The internal resistances of the cells used in this test were measured with a 60 cycle A. C. Bridge (L&N type 4960 Portable Electrolytic Resistance Indicator). The cells of 5.5 cm² area average about 75 ohms at 25°C; those of 1.43 cm² area, about 350 ohms, and those of 0.5 cm² area, about 750 ohms. No significant change in a-c resistance was observed throughout the test. A word of caution may be inserted here. Since the emf of a cell which has been discharging will drop quite rapidly by an amount equal to $IR_s + \Delta V$ (Eq. I), it is not possible to measure the internal resistance of such a cell by simple measurement of the voltage drop across its terminals under fixed load. A later paper will deal with this matter more completely.

Control Cells

The several cells under no current drain carried along as controls with each test group exhibited no abnormal behavior. They decreased in emf at a rate which varied for different cells from 30 to 60 μv/yr, with an average of about 45 μv/yr (10).

Summary

It is possible to use a standard cell under conditions which require the withdrawal of small currents, with the probability that it will decrease in closed circuit voltage by about 11 μv/coulomb cm^{-2}. The magnitude and duration of the current should be limited by the error which can be tolerated in the complete system. After about 450 coulombs/cm² have been withdrawn, the closed circuit voltage of the cell will have decreased about 5 mv at which point the cell becomes so unreliable that further use as a standard cell is not advisable.

Acknowledgment

The author is indebted to his colleagues at the Eppley Laboratory, where this work was performed, for valuable assistance, and especially to Marion Eppley, for guidance in many fruitful discussions.

Manuscript received May 27, 1957. This paper was prepared for delivery before the Washington Meeting, May 12-16, 1957.

Any discussion of this paper will appear in a Discussion Section to be published in the June 1958 JOURNAL.

REFERENCES

1. M. Eppley, *Elec. Eng.*, **51**, 341 (1932).
2. G. W. Vinal, "Primary Batteries," p. 212, John Wiley & Sons, Inc., New York (1950).
3. J. H. Park, *J. Research Nat. Bur. Standards*, **10**, 89 (1933).
4. L. Hartshorn and F. A. Manning, *J. Sci. Instr.*, **31**, 115 (1954).
5. W. H. Wood, *Rev. Sci. Instr.*, **28**, 202 (1957).
6. M. Eppley and W. R. Gray, *ibid.*, **2**, 242 (1931).
7. M. Eppley and G. Vincent, *Nat. Bur. Standards Circ 524*, 81 (1953).
8. M. Eppley (to The Eppley Laboratory, Inc.) U. S. Pat. 2613234, Oct. 7, 1952.
9. W. C. Vosburgh and M. Eppley, *J. Am. Chem. Soc.*, **45**, 2268 (1923).
10. W. C. Vosburgh, *J. Opt. Soc. Amer.*, **11**, 59 (1925).

Electroluminescence of Zinc Sulfoselenide Phosphors with Copper Activator and Halide Coactivators

I. J. Hegyi, S. Larach, and R. E. Shrader

RCA Laboratories, Radio Corporation of America, Princeton, New Jersey

ABSTRACT

The choice of halide coactivators in the synthesis of electroluminescent powder phosphors of the Zn(S:Se):Cu system markedly affects the spectral distribution and efficiency of the phosphors. Iodide coactivated ZnS:Cu can be prepared as a blue-emitting phosphor exhibiting no shift in spectral emission with field excitation from 20 to 50,000 cps. Several-fold increase in radiant output over the chloride coactivated ZnS:Cu phosphor is obtained by using iodide coactivator.

ZnSe:Cu phosphors, iodide coactivated, also show no shift in spectral distribution with frequency. However, the emission from Zn(S:Se):Cu materials, prepared with any of the halide coactivators, shifts to lower peak wave length with increasing frequency of excitation. A red-emitting electroluminescent phosphor can be synthesized from the (Zn:Cd):Se:Cu system by the use of bromide or iodide as a coactivator.

The role of the halide is extended from that of a randomly distributed donor to one of association with the activator, and consequences of such activator-coactivator association are discussed.

Although some references to the electroluminescence of a few particular Zn(S:Se):Cu phosphors have appeared in the literature (1-4), no systematic investigation of such materials has been published. Such an investigation has been carried out, and the following represents some of the results.

Experimental

The zinc sulfoselenide phosphors were prepared by the addition of Cu (0.1% by weight) activator (as the halide dissolved in NH_4OH) to the desired proportions of ZnS and ZnSe. Crystallizations were carried out in a nonflowing purified nitrogen atmosphere at 1075°C, with a large amount of ammonium halide (10% by weight). The amount of ammonium halide used was determined empirically for the maximum light output. As the halides sublime at temperatures under 551°C, only a small proportion is retained and incorporated into the phosphor. Deviation of lattice constants (as determined by x-ray analysis) from values to be expected from application of Vegard's law indicate that there is no significant loss of ZnSe.

The spectral emission and light intensity were examined in a capacitor-type electroluminescent (EL) cell with castor oil dielectric, using sinusoidal excitation up to 50 kc. Samples for these measurements were ground in a mortar and mixed in constant proportion with castor oil. No other treatment, such as washing, was given to the samples.

A few of the samples were analyzed for total Cu and Cu remaining after washing in KCN solution. It is assumed that Cu remaining after the cyanide wash is in solid solution in the ZnS·ZnSe host crystal, and the Cu dissolved in the cyanide is excess Cu forming a second phase of Cu_2S. This assumption is based on experimental observation that for a given composition subsequent cyanide washings failed to change the measured Cu concentration.

Chemical analysis for Cu of ZnS and 0.6ZnS:0.4ZnSe samples coactivated with the halides showed that no Cu is lost during synthesis. However, the proportion of Cu (in solid solution) remaining after KCN wash was dependent on the halide used. Table I lists the percentage of Cu in solid solution (remaining after cyanide wash) in the host crystals of ZnS and 0.6ZnS:0.4ZnSe originally containing 0.1% Cu.

The above analysis shows that the amount of Cu incorporated in the lattice is a function of both the host crystal and the halide coactivator. In general, the solubility of copper in the ZnS lattice decreases with increase in the size of the halide.

Chemical analysis for iodide content before and after cyanide wash was also made on ZnS:Cu(0.1) coactivated with iodide. The analysis for I and Cu for both unwashed and cyanide washed samples are shown in Table II.

The above data show that there are equal amounts of Cu and I by weight in solid solution in

Table I

	ZnS	0.6 ZnS:0.4 ZnSe
	%	%
Cl	88	62
Br	53	62
I	25	34

Table II

	Unwashed	Washed in Cyanide
	%	%
Cu	0.098	0.024
I	0.036	0.024

ZnS. The atomic weight ratio of I/Cu is about 2, consequently for each I there are 2 Cu atoms in solid solution.

X-ray diffraction examination of zinc sulfoselenide series synthesized at 1075°C showed that from ZnS to 0.6Zn:0.4ZnSe both cubic and hexagonal phases are present. With more than 0.4ZnSe only the cubic phase is present. The unit cell of the cubic phase expands linearly with increase in ZnSe; however, the hexagonal lattice showed no observable expansion with increase in ZnSe content. This indicates that in the two-phase region up to 0.6ZnS: 0.4ZnSe, one phase is a solid solution of ZnSe in ZnS, and the other phase, hexagonal ZnS. The amount of the hexagonal phase present is apparently not enough to give a significant deviation from Vegard's law for the cubic phase.

Results

The effect of frequency on the chloride coactivated ZnS:Cu is well known (6, 7) in that the blue-to-green ratio increases with increasing frequency. However, ZnS:Cu, coactivated with iodide, has essentially a single emission band with excitation frequencies of 20 cps to 50,000 cps. The Cu content can be varied from 0.02% to 0.2% Cu, (3×10^{-4} to 3×10^{-3} Cu/mole ZnS), with but small changes in spectral emission for all compositions.

In Fig. 1a, normalized spectral distribution curves of emission for ZnS:Cu are shown for the different halides as coactivators. The spectral distribution curve of ZnS:Cu:I shows a narrow band with peak wave length in the blue. The chloride and bromide coactivated spectral distribution curves show much broader bands whose apparent peak is at a longer wave length than the iodide curve. It is quite apparent that the spectral emission of ZnS:Cu(Cl,Br) consists of at least two emission bands of different relative intensity. The relative intensity of blue and green present in bromide coactivated materials appears to be more sensitive to amount of activator, coactivator, and processing than in chloride phosphors. The emissions of the bromide coactivated phosphors do not necessarily always peak at a longer wave length than the chloride coactivated samples, as shown in Fig. 1a. Phosphors have been prepared with almost identical spectral distribution for chloride and bromide coactivators. Curves are also shown, Fig. 1b, relating the integrated output (as observed with RCA 5217 Photomultiplier, S10 surface), and frequency of field excitation, at 280 v rms.[1] These curves show the superiority of iodide and bromide over chloride coactivated electroluminescent phosphors, for integrated output.

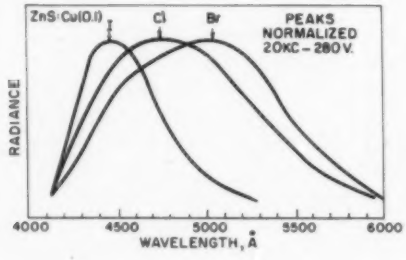

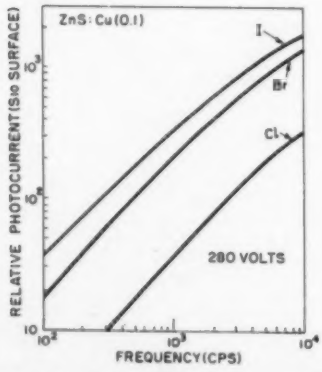

Fig. 1a. (Top) Spectral distribution curves of the electroluminescence of chloride, bromide, and iodide coactivated ZnS:Cu. Fig. 1b (Bottom) Relative radiance of chloride, bromide, and iodide coactivated ZnS:Cu EI phosphors.

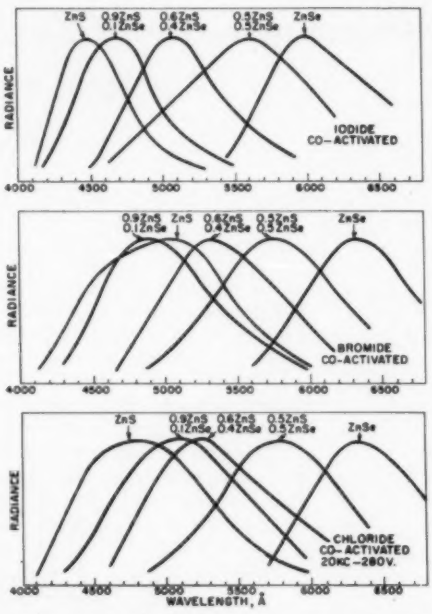

Fig. 2. Spectral distribution curves of the electroluminescence of Zn(S:Se):Cu with varying S:Se ratios, coactivated with chloride, bromide, or iodide. The S:Se ratios refer to compositions before firing.

In Fig. 2 spectral distribution curves are given for materials with varying amounts of S and Se. Curves for iodide coactivated materials peak at shorter wave length than corresponding bromide or chloride coactivated phosphors. For iodide-containing phosphors, the spectral shift with increasing Se content is monotonic and comparatively uniform with change in composition. With chloride, however, the first 10% Se produces a large color shift, which is not renewed until 20-25% Se is incorporated. The bromide coactivated phosphors with low Se content are centered at shorter wave length than corresponding chloride coactivated materials, while at increasing Se concentration the curves of chloride and bromide materials become more similar.

[1] Cell thickness was 0.002 in.

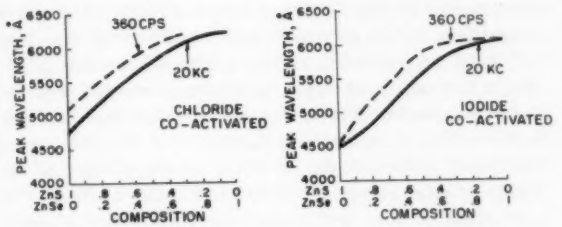

Fig. 3a. (Left) Peak wave length EL emission (at excitation frequency of 360 cps, and 20 kc) of Zn(S:Se):Cu:Cl with varying S:Se ratios. Fig. 3b. (Right) Peak wave length EL emission (at excitation frequency of 360 cps, and 20 kc) of Zn(S:Se): Cu:I with varying S:Se ratios.

In Fig. 3, peak wave length of spectral emission is plotted as a function of ZnS:ZnSe composition for copper activated iodide and chloride coactivated phosphors at two frequencies, 360 cps and 20,000 cps. With increase in frequency the iodide coactivated curve shows no change in peak wave length at the extremities (ZnS or ZnSe), but at intermediate compositions [Zn(S:Se)], the peak shifts to shorter wave lengths. The chloride coactivated materials show a shift to shorter wave length with increasing frequency for ZnS. This shift decreases in the Zn(S:Se) region, and appears to disappear for ZnSe.

In Fig. 4, curves are shown of spectral emission for the material 0.6ZnS:0.4ZnSe:Cu(0.1), iodide, bromide, and chloride coactivated, under EL excitation at 20 kc, 2 kc, and 0.2 kc. The spectral shift from 20 kc to 2 kc is largest for the chloride coactivated material, and smallest for the iodide. At frequencies of 2-0.2 kc the shift is largest for the iodide and smallest for the chloride. The bromide coactivated samples show a more linear spectral shift over the 20-0.2 kc frequency range. Relative peak intensity data are also shown. For comparison purposes, the dotted curves show the spectral distribution under excitation by 3650Å u.v. radiation.

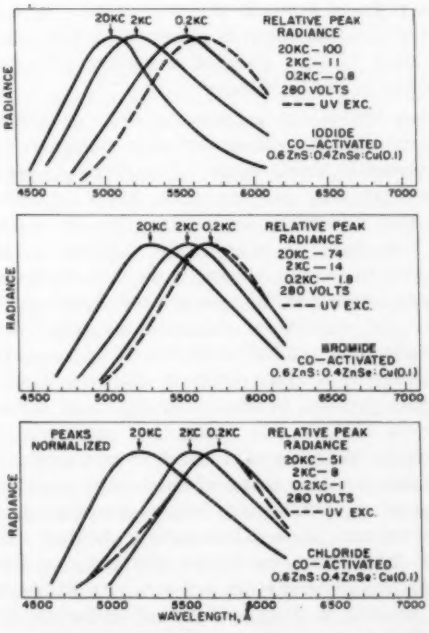

Fig. 4. Spectral distribution curves of the electroluminescence of 0.6ZnS:0.4ZnSe:Cu(0.1) coactivated with chloride, bromide, and iodide for the excitation frequencies of 20, 2, and 0.2 kc; also of the photoluminescence under excitation by 3650 Å u.v. radiation.

Fig. 5 shows the relative photoluminescent efficiencies of the three materials for Fig. 4 as a function of the exciting wave length.

The phosphor with the longest dominant wave length (ZnSe:Cu) is still subjectively red-orange. Using the same synthesis procedure but replacing some of the ZnSe with CdSe, and using either bromide or iodide as coactivator, a red-emitting phosphor can be obtained.

In Fig. 6, the peak wave length of EL from iodide coactivated (Zn:Cd) Se:Cu is plotted as a function of ZnSe/CdSe ratio. It is seen that a linear increase of peak wave length is obtained with increased amounts of CdSe.

Discussion

There are three features of this study that should be emphasized. These are: (a) the effects of the

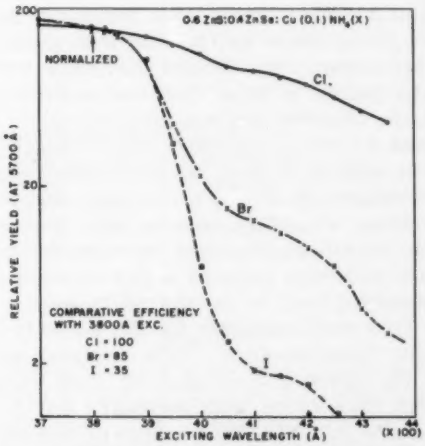

Fig. 5. Relative photoluminescent yield of the materials of Fig. 4 under excitation for radiation of various wave lengths.

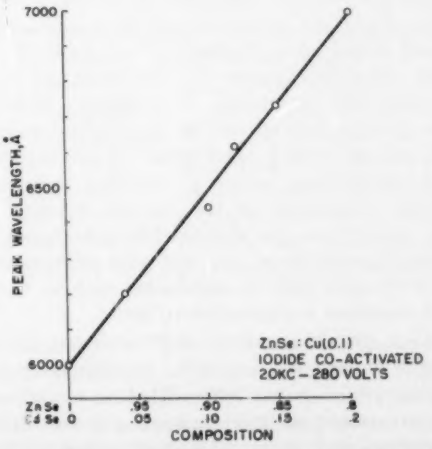

Fig. 6. Peak wave length EL emission of (Zn:Cd):Se:Cu with varying Zn:Cd ratios coactivated with iodide.

nature of the halide coactivator; (*b*) the effect of operating frequency on the emission; and (*c*) the effects of composition (S:Se ratio) on the emission under EL excitation. These aspects are interdependent, but also are complicated by the peculiar nature of EL excitation.

It is well known that ZnS phosphors with certain activators are prepared in the presence of halide. It was originally believed that the function of the halide was that of a "flux", i.e., a low melting phase to aid in recrystallization and particle growth. This view was modified when Smith (7) proposed that the halide actually was incorporated into the lattice. The function of the halide as a charge-compensating agent has been set forth by Kroger and his collaborators. The role of halide as a donor has recently been proposed (8-10). The cathodoluminescence of ZnS:Cu with chloride, bromide, or iodide coactivator, is predominantly in the blue region of the spectrum, with only traces of a green band for the materials prepared with chloride and bromide. These same materials, when excited by photons, show wide variations in their emission colors (blue/green), particularly as functions of excitation wave length and density, and operating temperature. Thus, in all three materials, emission centers giving rise either to blue or to green emissions are present, regardless of the nature of the coactivator halide. If more than one emission center exists, the observed emission of a crystallite is determined by the competitive process which exists between centers. In turn, the competitive situation is determined by the concentration distribution, temperature, excitation nature, etc. The Schon-Klasens hypothesis describes the simplest type of competitive process whereby a hole captured at one recombination level is transferred to another level of the type which accounts for the majority of the radiative recombinations. This explains qualitatively the green-to-blue shift of ZnS phosphors with low Cu content, with increasing u.v. irradiation density, in which the presence of two emission bands is easily demonstrated. Nevertheless, for photo-excitation and electroluminescence, Zn(S:Se):Cu phosphors prepared with different halide coactivators exhibit markedly different properties.

The role of the halide merely as a randomly distributed donor must, therefore, be modified or extended. One modification is to abandon the requirement that the coactivator is randomly distributed in the crystal, and to assume association exists between activator and coactivator. If activator-coactivator association exists in varying degrees, the diffusion differences of the various coupled complexes could make for distribution inhomogeneities. Further, the nature of the activator determines the density of each type of association and its distribution throughout a crystallite volume.

The phenomenon of color shift with frequency reported in this paper cannot be explained by a simple application of the Schon-Klasens hypothesis. A material excited at fixed voltage and two different frequencies may show a marked color shift. The same material operated at an intermediate frequency and at two voltages which produce the same brightness levels as previously obtained by the two different frequencies shows negligible color shift. Since the same change in over-all output results in both cases but with color shift in one case and not in the other, it must be assumed that the two cases involve a different distribution of absorbed (or, at least, emitted) energy throughout the bulk of the crystallite. If one reconsiders the hypothesis of activator-coactivator association and the probable effect on center distribution, it can be seen qualitatively how the halide effects on color shift may be explained. This is especially so if one makes the reasonable assumption that the complexes involving the large iodine ions have low volume solubility and, hence, are to be found in greater concentration near the surface. Iodine coactivated Zn(S:Se) in Fig. 4 was shown to be most frequency-sensitive.

What is still unknown is the exact nature of the complete emission center, either blue or green, and the closeness of coupling between the Cu atom or ion and the halide atom (or ion). Measurements cited show that the incorporated Cu content is definitely related to the particular halide and that the Cu-halide ratio is also affected. This further confirms the premise that not only do the different halides have different solubilities but that there are different solubilities (concentrations) of the Cu-halide complexes.

The concept of a Cu-halide complex is strengthened by the determination (11) that the blue emission band of ZnS:Cu(0.1):I is not the usual "host-crystal" blue band of ZnS:I, but is as associated with Cu as is the usual green band.

The predominance of the blue band in ZnS:Cu (0.1):I regardless of type of excitation, and in spite of the reduced amount of incorporated Cu, suggests that the Cu-I complex is closely coupled, and is the only such closely coupled complex of significant solubility in the ZnS lattice.

When the Se proportion is 40% or larger, the shape of the spectral distribution obtained for any one material and mode of excitation seemingly shows that only one emission band is significant. With this situation, an explanation of color shift with frequency is even more difficult to achieve than for the cases where interplay between two emission bands could be postulated. It is seen in Fig. 4 that u.v. excitation causes essentially identical emissions from 0.6ZnS:0.4ZnSe:Cu:X regardless of the nature of X. That there is still a marked effect of halide present is shown in Fig. 5 in which I is found to reduce the "impurity excitation band" drastically. Whether this effect is best explained by the absorption properties of the complex or by some feature of its distribution between surface and volume is not now known. It is significant that, although the relative photo-excitation efficiency of Cl-coactivation to I-coactivation is 3 to 1, the EL excitation at 20 kc is 1 to 2. The "sliding sidewise" type of color shift suggests that in the disorder present in a mixed lattice there is an effective continuum of levels separated spacewise by their distance from the EL surface barrier. Tests of this hypothesis us-

ing x-rays, C-R excitation, annealing, digestion, etc., are planned.

The first-order effects of S-to-Se ratio in the composition are, of course, expected since the band gap of the Zn:Se series shows a smooth monotonic variation from ZnS to ZnSe. What is of more interest is the way in which addition of Se to the ZnS:Cu:(x) lattice disturbs the blue-green competitive balance.

Manuscript received July 23, 1956. This paper was prepared for delivery before the San Francisco Meeting, April 29-May 3, 1956.

Any discussion of this paper will appear in a Discussion Section to be published in the June 1958 JOURNAL.

REFERENCES

1. S. Roberts, Jr., *J. Opt. Soc. Amer.*, **42**, 850 (1952).
2. U. S. Patent No. 716,159.
3. J. S. Prener, U. S. Patent No. 2,731,423.
4. A. Fisher, *Z. Naturf.*, **8a**, 756 (1953).
5. H. H. Homer, R. M. Rulon, and K. H. Butler, Jr., *This Journal*, **100**, 566 (1953).
6. P. Zalm, G. Diemer, and H. A. Klasens, *Philip Res. Repts.*, **9**, 81 (1954).
7. A. L. Smith, *This Journal*, **96**, 75 (1949).
8. F. A. Kroger, et al., *Z. Physik u. Chem.*, **203**, 1 (1954).
9. R. H. Bube and S. M. Thomsen, *J. Chem. Phys.*, **23**, 15 (1955).
10. J. S. Prener and F. E. Williams, *Phys. Rev.*, **101**, 1427 (1956).
11. R. E. Shrader and S. Larach, *ibid.*, **106**, 1899 (1956).

Heat Treatment of Silicon Using Zone Heating Techniques

H. C. Theuerer, J. M. Whelan, H. E. Bridgers, and E. Buehler

Bell Telephone Laboratories, Inc., Murray Hill, New Jersey

ABSTRACT

New insight into the mechanism for the changes in silicon with solid-state heat treatment has been obtained with the aid of the floating zone apparatus normally used to refine silicon. With this system, a liquid or solid hot zone may be caused to traverse the rod while the rest of the apparatus is kept relatively cool.

Through the use of this technique, it has been established that contaminants left on the silicon surface even after careful etching and washing procedures are a controlling factor in the observed heat treating effects. The impurities involved have high diffusivities, as is the case for copper and iron in silicon. That these impurities lower lifetime on heat treatment has been demonstrated by rubbing the silicon rod with copper or iron wires prior to zone heat treatment.

The heat treatment of Si at temperatures between 400° and 1200°C usually causes changes in carrier lifetime, resistivity (1), and in some cases conductivity type. Such changes are not, however, a necessary consequence of heating high purity Si. For example, Si has been prepared by the floating zone method (2) which can be heat treated without changes in properties if contamination is avoided. Residual impurities left on the surface after etching and cleaning procedures and the furnace environment during heat treatment are contamination sources capable of causing serious lifetime and resistivity changes. The impurities responsible for these changes must have a high diffusivity in Si, as is the case for Cu, Fe, and Au (3), since the time required to obtain the effects is short.

In heat treating studies furnace contamination can be avoided by using the floating zone apparatus in which the high purity Si is initially prepared. However, if the Si is handled prior to heat treatment, serious contamination is encountered; this is not eliminated by the usual etching and cleaning procedures. With the zone heating technique, lifetime changes may be used effectively to evaluate new etching procedures. Details of the method and results obtained in a number of experiments are given herein.

Apparatus

The apparatus used in the floating zone technique consists of a quartz tube 22 in. long and ¾ in. OD which is fitted to metal end heads. The end heads contain stainless steel chucks used to clamp quartz holders with which the Si under test is suspended axially in the apparatus. A single turn induction coil surrounds the quartz tube and is connected to a 5 MC generator for direct induction heating of the Si. Provision is made to cool the entire quartz envelope during the heating of the Si by means of a water curtain. The entire apparatus is mounted from a carriage, allowing the quartz tube to be moved through the induction coil at a controlled rate, usually 0.05 in./min in these experiments. By this means, the hot zone may be caused to traverse the entire rod. During zone treatment, the apparatus is flushed continually with pure dry hydrogen entering and leaving through ports provided in the metal heads.

Surface Contamination Studies with Liquid Zones

Extensive refining with the apparatus described above results in p-type Si with resistivities above 10,000 ohm-cm and carrier lifetimes above a millisecond. This establishes that this furnace is not a serious source of contamination and should, there-

fore, be suitable for heat treating studies. In an initial investigation to determine the effect of residual surface impurities on resistivity and lifetime, a Si rod was given four liquid zone treatments. A *p*-type rod with resistivities ranging between 25-60 ohm-cm and having carrier lifetimes between 200-250 μsec was obtained. The lifetime measurements were made by the photoconductivity decay method. The rod was then etched with the standard HF-HNO_3 mixture,[1] washed with deionized water, and dried. One additional zone pass through the rod degraded the lifetime to values of 30-40 μsec without a significant change in resistivity. A second experiment clearly established that the furnace environment was not the source of the contaminants responsible for this lifetime degradation. A rod was given 10 zone passes and was then removed from the apparatus without handling of the surface. The furnace tube, however, was cleaned in HF-HNO_3 and rinsed, as was done in the initial experiment. The Si was then remounted in the apparatus and one-half of the rod given an additional zone pass. No significant lifetime differences were observed. The control section with 10 zone passes had lifetimes between 600-300 μsec; the section with one additional pass had lifetimes between 480-330 μsec.

In addition to lifetime changes, etching a Si rod in HF-HNO_3 prior to a liquid zone pass also results in donor contamination, observed as a change in resistivity or conductivity type if the starting material is sufficiently pure. For example, after extensive zone refining, a *p*-type Si rod section had a resistivity of 3300 ohm-cm. An additional zone pass was put through the rod after sandblasting, etching in HF-HNO_3, and washing in deionized water. The Si obtained was p-type, and the resistivity in the previously measured section was now 6000 ohm-cm. Since the acceptor impurity in this Si was B, with a distribution coefficient of 0.8, the increase in resistivity could not have been due to refining by the single zone pass but must have been due to donor contamination. This was further substantiated by repeating the above surface treatment prior to a second zone pass. The rod section was now *n*-type with a resistivity of 1000 ohm-cm. From the resistivity data, the donor contamination was estimated to be about 3×10^{12} at./cm^2/treatment. Assuming that all of the contaminants were on the Si surface initially, the concentration calculated from the above value is $\approx 4 \times 10^{11}$ atoms/cm^2, which is equivalent to 0.001 of a monolayer.

[1] This mixture contains 1 part HF 48%, 3 parts HNO_3 71%.

Surface Contamination Effects in Solid Zone Studies

It is apparent from the liquid zone experiments that contaminants from the surface may degrade lifetime seriously. Similar results have been obtained in heat treating studies with solid Si. In such experiments, a hot zone at 1100°-1200°C is initiated at the end of the rod and is caused to traverse the rod by moving the system through the induction coil at a controlled rate. In this way a zone approximately ¼ in. long is maintained at 1200°C, and the material on either side of the zone for a distance of approximately 1 in. is visibly red. Using a zone velocity of 0.05 in./min the material is at 1200°C for approximately 5 min during each pass and cools to 650°C in approximately 20 min.

In initial experiments, using this method, the following questions were answered: (*a*) can Si be heat treated at 1200°C using the floating zone apparatus without deterioration of lifetime? (*b*) is water cooling of the quartz furnace tube essential to preservation of high lifetime during heat treatment? (*c*) is etching and washing the rod prior to heat treatment deleterious to lifetime?

In these experiments high lifetime Si crystals were prepared by passing 10 zones through each rod. The first 4 cm of the rods were then given three zone treatments at 1200°C leaving a 10 cm section at the end of these rods for control purposes. The experimental conditions and the results obtained are summarized in Table I. From the data of Table I, it is evident that Si can be heated in the range between 400°-1200°C without serious deterioration of lifetime, provided the quartz envelope is kept cool with an external water curtain during the heat treatment. If the furnace tube is allowed to heat by removing the water curtain, the lifetime of the Si drops drastically when heat treated in the range between approximately 400° and 1200°C. Etching and washing the Si prior to heat treatment results in serious changes in lifetime. The evidence is clear that contaminants which impair lifetime on heat treatment may be introduced from a hot quartz tube, even with the specimen freely suspended. Such contaminants may also be introduced as residual impurities left on the surface after etching and washing.

In a second group of experiments, attempts were made to establish what steps in the etching and

Table I. Variations in heat-treating procedures and their effect on the lifetime of Si

Procedure	Lifetime μsec, Distance along rod from lead end in cm						
	2	4	6	8	10	12	14
Rod grown and not removed from furnace, given three zone passes at 1200°C, quartz tube water cooled	300	150	500	600	840	700	500
Rod grown and not removed from furnace, given three zone passes at 1200°C, quartz tube not water cooled	<3	<3	<3	4	580	650	650
Rod grown and exposed to air 15 min, rod remounted, three zone passes at 1200°C, quartz tube water cooled	90	135	320	550	520	570	480
Rod etched in HF-HNO_3, washed three zone passes at 1100°C, quartz tube water cooled	5	3	10	3	7	150	180
	Section heated to 1200°C		Section heated above 400°C		Section heated <400°C		

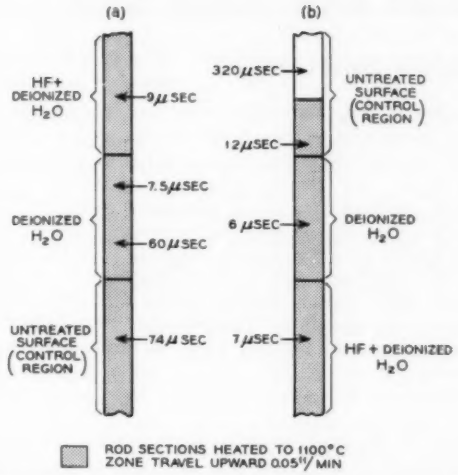

Fig. 1. Effect of surface preparation prior to heat treatment on the lifetime of Si.

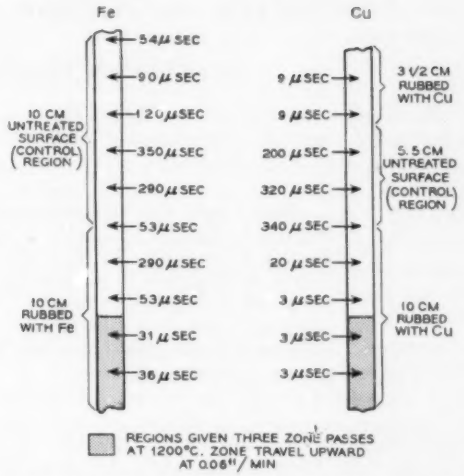

Fig. 2. Effect of surface deposits of Fe and Cu on the lifetime of Si after heat treatment.

washing technique were responsible for lifetime deterioration. In these experiments, two high lifetime crystals were prepared by passing 5 liquid zones through each rod. The rods were removed from the apparatus and given the surface treatments indicated in Fig. 1. After treatment, the rods were given a single zone pass at 1100°C using a zone velocity of 0.05 in./min. From the lifetime data of Fig. 1a, it is obvious that washing with HF followed by a deionized water rinse reduces the lifetime drastically. Although not as severe, some lifetime deterioration after heat treatment is indicated in the rod sections washed with deionized water or only exposed to air. Note also that the lifetime in the upper region of the rod section treated with deionized water had a lifetime of 7.5 μsec, whereas lower in this section the lifetime was 60 μsec. This is an indication that impurities introduced by the HF rinse diffuse into the deionized water-treated region during the zone heating process. That this occurs is shown more clearly by the results, given in Fig. 1b, for the second rod. In this case, the hot zone was passed from the section treated with HF through the section treated only with water and part way through the section which was exposed only to air. The lifetime was drastically reduced through the entire area which had been heat treated irrespective of the prior surface treatment; only in the unheated region was the lifetime preserved. This establishes that the impurities responsible for lifetime deterioration have a high diffusivity in Si.

Copper and iron, for example, are known to diffuse rapidly through Si and destroy the lifetime. This was confirmed by preparing two high lifetime rods using the floating zone method. Without other treatment, the rods were rubbed with Cu in one case and with Fe in the other at the locations indicated in Fig. 2. The lower 5 cm of the rubbed rods were then heat-treated at 1200°C by passing three zones at the rate of 0.06 in./min through these regions. As can be seen from the data, the lifetime was seriously impaired by both Cu and Fe, the damage in each case extending well beyond the 1200° hot zone. The lifetime deterioration was most severe with Cu, and surprisingly it was effective in the upper Cu-treated region of the rod which could not have been heated at temperatures much above 400°C.

Using the basic method discussed above, a number of etching and cleaning methods for the removal of surface contaminants have been investigated. Etching Si with Br_2 at elevated temperatures or with NaOH solutions is no more effective than the standard HF-HNO_3 treatment. Immersion in hot HNO_3, H_2SO_4, H_2O_2, and NaCN after etching has not led to improved lifetime after heat treatment.

Manuscript received May 23, 1957. This paper was prepared for delivery before the Washington Meeting, May 12-16, 1957.

Any discussion of this paper will appear in a Discussion Section to be published in the June 1958 JOURNAL.

REFERENCES

1. C. S. Fuller, J. A. Ditzenberger, N. B. Hannay, and E. Beuhler, *Acta Metallurgica*, **3**, 97 (1955).
2. P. H. Keck and M. J. E. Golay, *Phys. Rev.*, **89**, 1297 (1950); H. C. Theuerer, *J. Metals*, **8**, 1316 (1956).
3. C. S. Fuller, J. D. Struthers, J. A. Ditzenberger, and K. B. Wolfstein, *Phys. Rev.*, **93**, 1182 (1954); J. D. Struthers, *J. Appl. Phys.*, **27**, 1560 (1956).

Electrolytic Extraction of Thorium from Fused Salts

Lothar Abraham, Edward L. Thellmann, and James L. Wyatt[1]

Horizons Incorporated, Cleveland, Ohio

ABSTRACT

High purity thorium metal powder has been produced by fused salt electrolysis of thorium chloride by a process readily adaptable to continuous production techniques. An electrolytic cell design based on a frozen-salt crucible design concept has been evolved. Heating of the salt bath was accomplished by graphite resistance heaters immersed in the bath. Metal quality, current efficiency, and other operating characteristics of the internally heated electrolytic cell compare favorably with those experienced in smaller scale, externally heated cells.

Numerous processes for the preparation of thorium metal have been investigated, including thermal reduction of halides with Ca (1), thermal reduction of the oxide with Ca (2) or a metal hydride, and by fused salt electrolysis (3). The latter approach was considered promising and as such has merited intensive investigation.

Small-scale investigations of a chloride fused salt system, carried out by Raynes, *et al.* (4), have led to the successful development of an electrolytic process which readily lends itself to continuous operation. The process can be summarized as encompassing the electrolysis of fused anhydrous $ThCl_4$ in NaCl under an inert atmosphere. The Th is deposited as dendritic crystalline metal in a matrix of salts from which it can be separated readily by aqueous methods.

Anhydrous $ThCl_4$ is supplied to the electrolytic cell in the form of a $ThCl_4$-NaCl mixture and diluted with NaCl to obtain an electrolyte containing approximately 15% Th by weight.

A companion paper (5) describes one method for producing a suitable electrolyte.

Electrolytic Equipment

Early in the development program, fused salt electrolysis was carried out in externally heated cells which have been described previously (4). The basic design proved satisfactory for small-scale operations and served as prototype for larger capacity units.

Electrolytic Cell Scale-Up

The limitation of construction materials for the fused salt container imposed a severe problem in attempts to scale up operations, principally because of the porosity of commercial grade graphite and carbon crucibles. Crucibles up to 24 in. in diameter were evaluated, leakage invariably developing. The results of these operations clearly pointed to the necessity of developing an entirely different concept of cell design.

Prior research in a related field at this laboratory had investigated a concept of cell construction which utilized an internal graphite heater. While the work did not include Th, the principles appeared to be applicable to any fused salt system. Accordingly, a program was initiated to apply these approaches to the production of Th. This program was primarily an engineering development effort, and no particular efforts were made to produce high quality Th metal. For example, cells were opened frequently to allow observation of various cell components during operations; of necessity, therefore, the cell atmosphere at times was badly contaminated with air.

Briefly, the cell consisted of a rectangular Ni shell surrounded by mild steel air jackets for controlled cooling. The crucible was centrally located within the shell and constructed of graphite slabs. Carbon black was tamped to a density of approximately 40 lb/ft^3 in the 1-in. wide annular space between the graphite crucible and the shell to serve as an insulating medium. A 1½ in. layer of carbon black was also tamped into the shell bottom. This gave a crucible with inside dimensions of 8½ in. x 9½ in. x 17 in. deep. The graphite slabs forming the crucible needed only to fit reasonably close together since they were not required to form a leakproof, impervious vessel. To complete the assembly, a 2-in. thick piece of porous graphite was positioned across the top of the crucible to reduce radiated heat losses out the cell top. Fig. 1 is a schematic view of the frozen salt crucible cell.

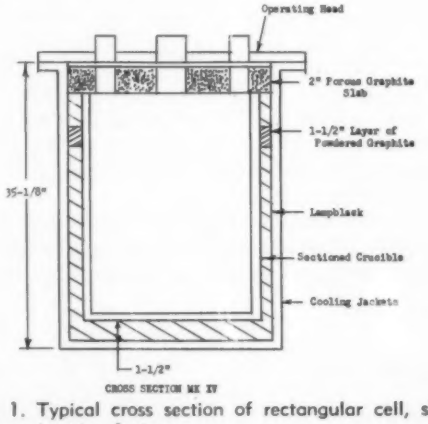

Fig. 1. Typical cross section of rectangular cell, showing major construction features.

[1] Present address: Booz, Allen and Hamilton, 380 Madison Ave., New York, N. Y.

For heating, two ¾ in. diameter graphite rods were press-fitted into the bottom of the crucible as shown in Fig. 2 and served as electrical resistors in an a-c power circuit.

In operation, it was found that the molten salt tends to leak through pores or discontinuities in the crucible walls and penetrates the carbon black slightly. Coolant flow through the air jackets was adjusted so that a portion of the liquid salt was frozen solid in the carbon black insulation; in this manner, the contents of the crucible remained molten and the entire crucible functioned as one electrode (anode) in the electrolysis.

Eleven runs were made in this unit without any major changes except for modifying the graphite heating elements. Several designs were tried, the one exhibiting the most desirable characteristics (highest resistance), consisting of a simple graphite "U" fabricated from ¾ in. diameter graphite rods. It was insulated from the crucible bottom with ½ in. thick porcelain slabs. Fig. 3 shows the graphite "U" heating element assembled. Typical circuit impedance under operating conditions at 750°C was 0.02 ohm. Total a-c heat input requirements ranged from 3 to 5 kw in order to maintain proper bath temperatures.

Cell Operation

Since the electrolytic deposition of Th was carried out in an all-chloride system, it was possible to place a thermocouple directly into the bath protected only by a quartz tube.

Prior to cell start-up, the electrolytic cell was hot-evacuated until outgassing ceased, then flushed with argon. The salt charge was melted under an argon atmosphere in approximately 7 hr. Fifty pounds of NaCl were melted first, followed by cell feed additions consisting of NaCl-$ThCl_4$. The total charge was 75 lb, initially containing approximately 15% Th by weight. The bath temperature was controlled at 790°-800°C.

A cathode consisting of a steel tip 1 in. in diameter and 5 in. long, attached to a ½-in. Ni shaft protected by graphite tubing, was immersed to a depth of 6 in. in the fused salt bath with a small d-c voltage impressed on it. When the cathode reached bath temperature (in 3-5 min), the voltage was increased to operating level (4-5 v) and current flow maintained thereafter at a cathode current density of 250 to 350 amp/dm², based on initial cathode area.

When a predetermined number of ampere hours had been passed through the electrolyte, the d-c voltage was lowered, and the cathode was raised to a position above the bath. It was maintained in this position in argon until the temperature of the entire unit was below 100°C, after which the deposit was removed. This procedure was necessary since no provisions for a removal chamber had been made. With a removal chamber, the bath could be maintained molten; theoretically, $ThCl_4$-NaCl additions could be made indefinitely without any detrimental effects on the electrolyte; thus, additional deposits could be produced with a minimal amount of down time.

The Th was deposited as dendritic crystalline metal in a matrix of salts from which it could be readily separated by water leaching. Fig. 4 shows a typical cathode and cathode deposit after removal from the cell. Fig. 5 shows the deposit broken open to reveal the characteristic internal appearance of Th metal deposits.

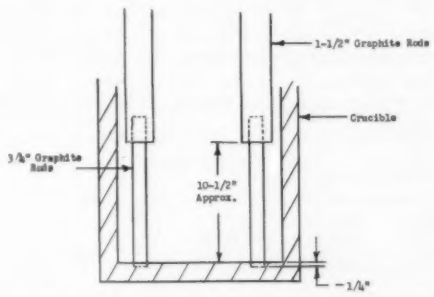

Fig. 2. View of rectangular cell, showing method of installing heating element rods.

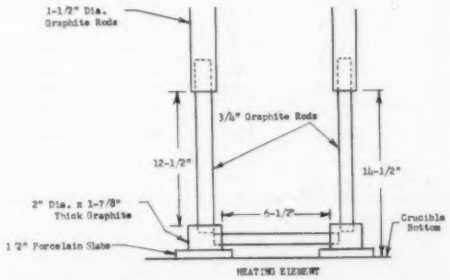

Fig. 3. Revised design of heating element for rectangular electrolytic cell.

Experimental Results

Cathode deposits produced in the electrolysis of anhydrous $ThCl_4$ in fused NaCl generally averaged 45-60% Th metal by weight. Current efficiencies averaged in excess of 75%. The Th metal produced in this campaign ranged from Rockwell B-30 to Rockwell B-58.5 in hardness. Hardness was determined on metal buttons produced by melting compacted metal powder in a water-cooled copper hearth arc furnace.

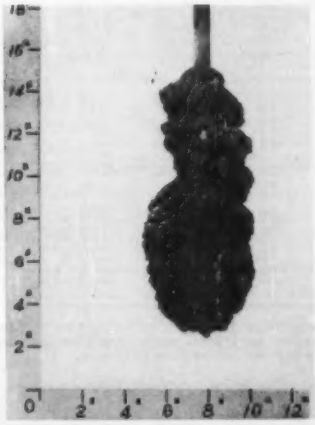

Fig. 4. Typical deposit of thorium metal produced in rectangular laboratory electrolytic cell.

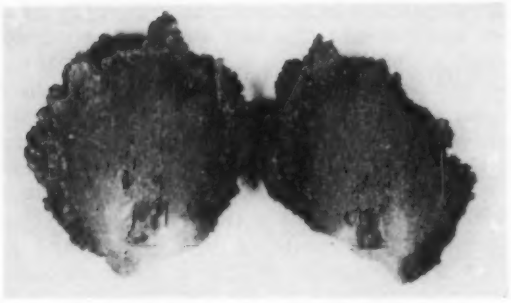

Fig. 5. Internal structure of thorium cathode deposit

The Th powder produced by fused salt electrolysis had a particle size distribution which made the metal readily amenable to powder metallurgy techniques. Generally, less than 10% of the powder was +20 mesh, and 70% was +70 mesh.

Table I presents a summary of data pertinent to the operation of the electrolytic cell.

Discussion and Conclusions

A program to evaluate fused salt electrolytic techniques for producing Th metal has been carried out in an attempt to devise a commercially feasible cell design concept. It has been demonstrated that satisfactory cell linings for Th production may be constructed of graphite slabs without regard for porosity and close tolerances, thereby eliminating problems attendant with size limitations on monolithic crucibles. The use of lampblack as an insulator, the establishment of a "frozen salt crucible" therein, and application of internal resistive heating have been incorporated experimentally in a device for the preparation of Th metal.

Observations of cell components showed no measurable deterioration, attrition, or chemical attack during the operational period, and, based on the extent of exposure time and extrapolation, it appears probable that cell linings will last at least one year. Heating element life probably will be shorter, perhaps 3-6 months. Designs, therefore, should provide for occasional replacement of the heater components.

Production of relatively good quality Th metal with high yield and acceptable current efficiency was demonstrated on a small scale, all results comparing favorably with previous work which has been carried out in monolithic cells.

Results on the small-scale program clearly demonstrated feasibility and warranted scale-up for pilot evaluation of equipment and processes on a semicontinuous basis.

Acknowledgments

The work described in this paper was carried out under the sponsorship of the Atomic Energy Commission, Contract No. AT(30-1)-1335, and grateful acknowledgment for permission to publish the data is made. Certain aspects of processes and equipment form the basis for patent applications pending at present.

The authors wish to make special acknowledgment to B. C. Raynes, J. C. Bleiweiss, J. A. DaMico, and R. Engle, present or former members of Horizons' staff, each of whom made major contributions to the program.

Permission to describe the crucible design, developed by Horizons Incorporated under contract with Horizons Titanium Corporation, is also gratefully acknowledged.

Manuscript received Jan. 23, 1957.

Any discussion of this paper will appear in a Discussion Section to be published in the June 1958 JOURNAL.

REFERENCES

1. C. A. Hampel, "Rare Metals Handbook," p. 435 Reinhold Publishing Co., New York (1954).
2. *Ibid.*, p. 433.
3. F. H. Driggs and W. C. Lilliendahl, *Ind. Eng. Chem.*, **22**, 1302 (1930).
4. B. C. Raynes, J. C. Bleiweiss, M. E. Sibert, and M. A. Steinberg, "Electrolytic Preparation of Thorium Metal," submitted to AIME for publication, 1956.
5. C. E. Fisher and J. L. Wyatt, *This Journal*, **104**, 672 (1957).

Table I. Summary of Mark-15 electrolytic runs

Run No.	Total charge wt lb	% Th in bath	Bath temp °C	D.C. current amp	D.C. v	Amp hr	Weight water washed metal g	Weight acid treat. metal g	Weight* recov. fines in overflow	% Current eff.†	Hardness R_B	% Th metal in dep.
1	80	16	800	270-335	4.4	3000	2211	2133	320	39.0	53	32.0
2	84	17	775-815	260-320	4.4	2350	3455	2814	73	69.5	50	—
3	88	15	800	280-300	4.9-4.2	2300	3191	2977	216	68.5	30-35	—
5	80	13	800	240-300	5.5-5.3	1480	2561	2534	176	85.5	35	57.5
6	75	13	810	260-280	5.6-5.3	1220	1893	1860	120	76.5	56	56.0
7	77	14	800	230-260	5.6-5.1	1655	2759	2708	140	81.0	49	54.5
8	80	10.6	785-800	170-290	5.5	1500	2773	2697	155	90.5	58	58.5
10	75	11.3	790-800	220-310	5.2-5.4	1200	2375	2298	69	94.0	43.5	55.0
11	70	12	790-800	220-275	5.8-5.5	1200	2130	1996	190	89.5	58.5	60.0

† Current efficiency has been calculated on the basis of total weight of metal recovered.
* "Fines" refers to powder metal less than 325 mesh in size that becomes suspended during washing and acid-treating operations; it is collected separately by settling or filtration.

Principles of Very Low Power Electrochemical Control Devices

Ray M. Hurd and R. N. Lane

Defense Research Laboratory, The University of Texas, Austin, Texas

ABSTRACT

A new technology utilizing electrochemical phenomena has been developed, from which it is possible to design detection and control devices requiring extremely low power consumption, in the order of 100-1000 times smaller than that of transistors. As an example, an electrochemical detector for acoustic energy operates on 10 μw in the quiescent state, delivering 300-500 μw when fully excited. Development work to date has been limited to low frequencies (0-200 cps). Reversible redox systems and working d-c electrodes are used in conjunction with such electrochemical phenomena as concentration polarization, electrokinetic effects, and the electrocapillary curve of mercury.

Use of Concentration Polarization for Flow Detection

The use of Pt wire micro-electrodes and the diffusion current for the analysis of electrolytically reducible or oxidizable substances is well known (1). A great deal of information on the effects of stirring (as, for example, with rotating Pt electrodes) has also been published in the chemical literature (2). That these phenomena can be used for detecting and measuring fluid flows will be immediately apparent to the reader. That the type of function obtainable from an electrochemical unit operating on this principle may be made to vary over a considerable range by changing the electrode design is not quite so obvious.

A typical flow detector is shown in Fig. 1. Electrodes may be of any metal which is inert to the electrolytic system used. In this particular example Pt electrodes are used in an electrolytic system of I_2 and KI in water. The cathodic reduction of I_2 is made the controlling reaction by using a low concentration of iodine ($10^{-3}N$) and a high KI (supporting electrolyte) concentration ($0.5N$). Other electrolyte systems may be used, as, for example, ferricyanide-ferrocyanide, bromine-bromide, ceric-cerous, ferric-ferrous, etc. It is only necessary that they be reversible redox systems.

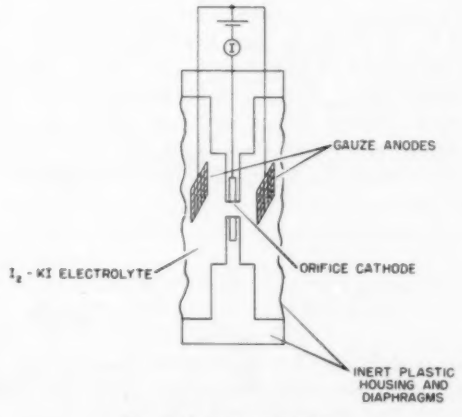

Fig. 1. Acoustic detector

Current-voltage curves for a cell of this type are shown in Fig. 2 for different values of low frequency acoustic energy incident on the diaphragms. A plot of the equilibrium current as a function of the incident pressure is given in Fig. 3. The relationship between current and pressure is expressed by equations of the type:

$$I = k P^n$$

or

$$I = k \log P$$

with the values of n and k dependent on the geometry of the cathode.

From an electrochemical standpoint, the proper operation of these units requires the following: (*a*) as nearly reversible electrode reactions as possible, so that no energy is consumed in overcoming activation polarization; (*b*) equal and opposite reactions occurring at the anode and cathode; i.e., a redox system, so that no net changes in concentration take place as current flows through the cell; it is also necessary to adjust the bias voltage to a value low enough that consecutive electrode reactions do not occur; (*c*) absence of reducible or oxi-

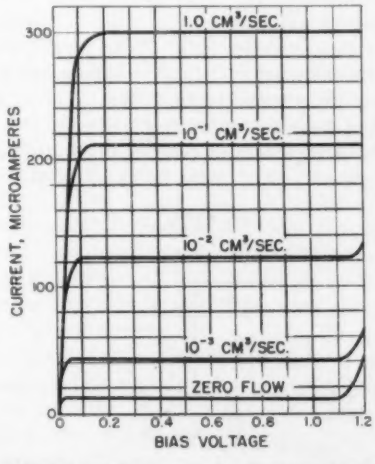

Fig. 2. Current-voltage curves for varying sinusoidal flows in acoustic detector.

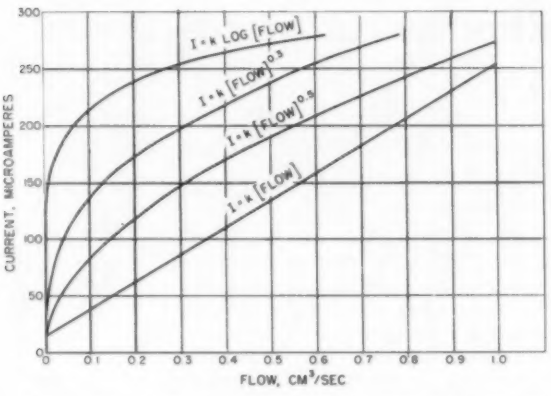

Fig. 3. Current-flow curves for acoustic detectors with different orifice designs.

dizable impurities. A reducible impurity not only yields a momentarily higher current, but builds up a permanent higher concentration of the primary reducible reactant (in this example, iodine) by the increased anodic oxidation.

Separated Detector for D-C Measurements

The cell described above was designed primarily for detection and metering of acoustic energy (a-c pressures). A more satisfactory design for d-c flows and pressures is shown in Fig. 4. In this cell an additional cathode is placed in the right-hand compartment so that the bias voltage transfers the I_2 from this side to the anode side, resulting in a final concentration of virtually zero in the cathode side. This transfer of I_2 is entirely analogous to that encountered in the simple I_2 coulometer as described by Washburn and Bates (2). In all such cells, the electrodes used primarily for separation of the I_2 are called the "main" cathode and the "main" anode.

The working cathode consists of a small piece of closely woven Pt gauze situated in an orifice between the two compartments. A small background current (of the order of 10 μa) flows continually in the detecting cathode circuit due to diffusion of I from the concentrated side. Fluid flow from left to right (concentrated to dilute) produces an electrical signal directly proportional to the magnitude of the flow. For a detector operating linearly, i. e., reducing all the I in the fluid flowing through the gauze, the current output is given by the equation:

$$I = 10^{-5} \mathbf{F} N \, dv/dt$$

where $\mathbf{F}$ = the Faraday, N = normality of the reducible substance on the anode side, dv/dt = flow rate in cm³/sec.

From this equation, assuming an I_2 normality of 10^{-1}, it can be seen that flow rates as low as 10^{-5} cm³/sec yield currents in the neighborhood of 100 μa, or some ten times the background current. Experiments have shown that, by suitable design of the detecting cathode, linear current outputs are obtainable over a range of four orders of magnitude in the flow rates.

Note that the unit shown in Fig. 4 is also a rectifier, in that fluid flow from right to left will not produce a current, since no I_2 is carried over the detector gauze. A full-wave detector may be constructed easily by using two anode compartments and two detector gauzes.

Conversion of Electrical Current to Fluid Flow

In order to perform various mathematical operations on the output currents of the devices described above, it is necessary to have a unit which carries out the reverse operation of converting these very low power electrical signals into fluid flows. In this manner, electrical and fluid flow signals may be fed from unit to unit in much the same manner that currents and voltages are fed through electronic networks. In addition to simple amplification, several mathematical operations may be carried out upon the original incident signal or signals in this manner; for example, products, ratios, derivatives, etc., may be obtained.

The simplest and most reliable method of carrying out this reverse effect is by the use of electro-osmosis, a phenomenon described in most standard textbooks on electrochemistry (4). An electro-osmotic cell (Fig. 5) consists of a fritted glass disk dividing a cell into two compartments, with electrodes on each face of the disk. The operating characteristics of such a cell can be made to vary over extremely wide ranges by control of such variables as disk porosity, thickness, and diameter, and choice of working liquid. The important point, however, is that the fluid flow produced by an applied voltage is linear with the value of voltage. If the flow is restrained, as, for example, by means of the plastic diaphragms of Fig. 5, then the electro-osmotic pressure developed is linear with the voltage. In Fig. 6 the equilibrium pressures for a typical "fine" porosity disk (about 4.0 μ pore diameter) is shown plotted as a function of applied voltage, using distilled water as the working fluid. Unrestrained fluid

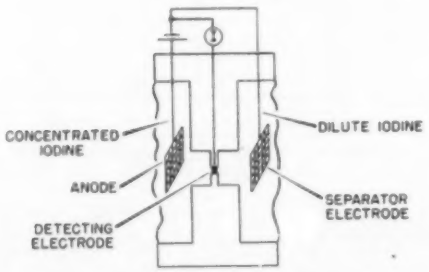

Fig. 4. Separated detector

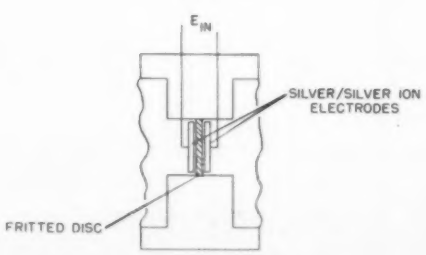

Fig. 5. Electro-osmotic cell

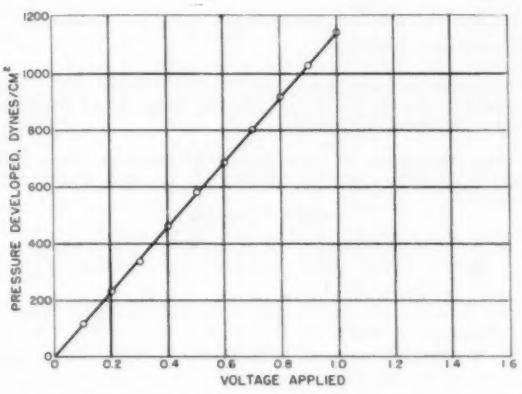

Fig. 6. Pressure-voltage curve for typical electro-osmotic cell.

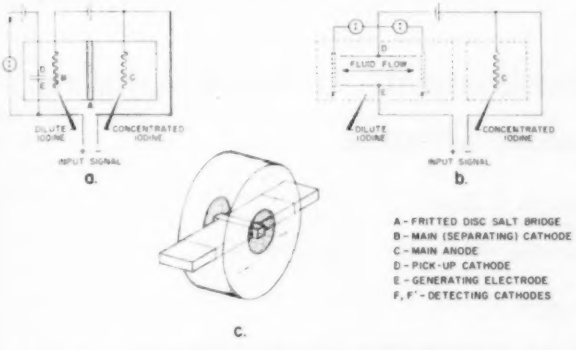

Fig. 7. Electrode arrangements for using anodically deposited iodine.

flow for a 30 mm diameter, 20 mm thick disk of this type is in the neighborhood of 10^{-8} cm³/sec at 1.0 v applied to the electrodes. It will be remembered that a flow rate of 10^{-6} cm³/sec through a separated detector will yield some 100 μa output, so that the values of flow rate produced by the electro-osmotic cell easily cover the working range of the other electrochemical units.

An idea of the power gains obtainable with these electrochemical units may be illustrated by combining the electro-osmotic cell with a linearly operating separated detector. The current drawn by the electro-osmotic cell at 1.0 v applied can be held to about 30 μa if the working fluid has a conductivity of some 10^{-6} ohm^{-1} cm^{-1}, giving a power input of 30 μw. The linear detector coupled to the cell can be designed to give an output of 10 ma dropped across a load resistor of 100 ohms, or a power output of 10 mw. This represents a power gain of some 330 fold; this could be increased easily by an additional order of magnitude.

One of the essential requirements of a properly operating electro-osmotic cell is that the working electrodes polarize as little as possible. For a-c signals this is no particular problem, but for continuous and unidirectional d-c signals, suitable electrodes are not so easily found. To date, the most satisfactory electrodes have been the simple metal/metal-ion type, particularly Ag/Ag$^+$ made by firing compressed tablets of Ag_2O.

Another method of obtaining the conversion of electrical energy into flow energy is through the use of the electrocapillary curve of Hg (5). This has not been studied as thoroughly as has the electro-osmotic cell, but its workability has been demonstrated. The most interesting aspect of the electrocapillary curve is the fact that the surface tension (and thus the fluid displacement) varies as the square of the voltage applied to the interface. Furthermore, because of the extremely low currents required to charge the Hg double layer, and the relatively large displacements obtainable by the changes in surface tension, the power gain through such a system can be higher even than the examples cited above.

Use of Anodically Deposited Iodine

The last aspect of these electrochemical devices to be described in this paper is the use of a reducible substance (I_2) formed in place by the passage of anodic current through the electrolyte solution. For example, Fig. 7a shows a small cell separated into two compartments by a fritted disk salt bridge, A. If the cell is filled with an iodine-iodide solution and electrodes B and C connected as shown, the I will be transferred to the anode side as described previously. Electrodes D and E are two closely spaced (<0.010 in.) Pt plates, insulated so that their inner faces only are exposed to the solution. Now if the battery and meter connections are made as shown, a very small (<1 μa) background current will flow in the meter circuit. However, if an input signal is applied to electrodes E and C such that iodine is generated at E and consumed at C, the iodine thus formed at E will diffuse across to D and be reduced, causing the meter current to increase. Note that the increased current is fed directly back to electrode E, so that iodine, once formed between the electrodes, cannot escape. By means of suitable relays and switches (not shown), it can be shunted back to electrode C, so that the space can be returned to its initial iodine-free condition. The current flowing in the meter circuit is proportional to the time integral of the input signal.

If electrodes D and E are made the opposite faces of a corridor through which the electrolyte solution can flow, the product of a generating current and a fluid flow may be obtained. A typical arrangement is shown schematically in Fig. 7b, and a cutaway of the corridor in Fig. 7c. In Fig. 7b, electrode E is again the generating electrode, D the pickup electrode, and C the main anode, while the two electrodes F and F' are the detecting electrodes. The separating cathode B and fritted disk A are not shown, but must be present to maintain the separated iodine condition (dilute throughout the corridor region, concentrated around C). Since there is no iodine initially inside the corridor, no current is obtained at the end electrodes, regardless of flow. If, however, an external current is applied across electrodes E and C, iodine will be formed inside the corridor, which will then either diffuse across to D, or may be forced to either of the detecting electrodes F and F'. The current in the meter circuits

is proportional to the product of the generating current and the fluid flow.

By use of the principles just described, operations other than simple integration and multiplication can be carried out.

Summary

The method in which several common electrochemical phenomena have been combined to yield a new technology for very low power detection and control devices has been described. The operation of a few of the many possible units has been described also as well as some of the characteristics cited to show the operating ranges, low power requirements, and power gains obtainable. Some of the electrochemical requirements of properly operating cells have also been mentioned. Further details on the operation of the units and of the research which has been done to bring them to the present state of development will be revealed in subsequent papers.

Manuscript received June 26, 1957. This paper was prepared for delivery before the Cleveland Meeting, Sept. 30-Oct. 4, 1956.

Any discussion of this paper will appear in a Discussion Section to be published in the June 1958 JOURNAL.

REFERENCES

1. I. M. Kolthoff and J. J. Lingane, "Polarography," Vol. I, Chap. XIX, Interscience Publishers, Inc., New York (1952).
2. H. A. Laitinen and I. M. Kolthoff, *J. Phys. Chem.*, **45**, 1079 (1941).
3. E. W. Washburn and S. J. Bates, *J. Am. Chem. Soc.*, **34**, 1341 (1912).
4. For example, G. Kortüm and J. O'M. Bockris, "Electrochemistry," Vol. II, Chap. X, Elsevier Publishing Co., New York (1951).
5. G. Lippmann, *Ann. chim. et phys.*, **5**, 494 (1875).

Impedance and Polarization Measurements in Fused Lithium Chloride-Potassium Chloride

H. A. Laitinen and H. C. Gaur[1]

Department of Chemistry and Chemical Engineering, University of Illinois, Urbana, Illinois

ABSTRACT

Impedance measurements with a platinum microelectrode in fused eutectic mixture of potassium chloride (41 mole %) and lithium chloride (59 mole %) are described. The residual resistance and capacitance showed frequency dispersion; probable causes are discussed.

Most of the metal ions showed a tendency for "predeposition." The faradaic admittance in the reduction of Pb^{++}, Co^{++}, Ni^{++}, Zn^{++}, and Cd^{++} ions had a phase angle of the combination greater than 45°, which has been ascribed to the adsorption of metal ions on the electrode surface. After application of an empirical correction for this effect, the faradaic admittance became normal and was used to calculate the rate constants for the above processes.

The current-potential curves showing the polarization behavior in the vicinity of equilibrium potential are described. By a curve fitting method the values of α, the transfer coefficient for the cathodic process, and i_o, the exchange current, are computed. These values of i_o are, however, much lower than those calculated by using the rate constants obtained from impedance measurements.

In a previous communication (1) impedance measurements for solid microelectrodes in a fused eutectic mixture of LiCl (59 mole %) and KCl (41 mole %) at 450°C were reported. It was found that the residual capacity (apparent double layer capacity) of Pt showed a large frequency dispersion. In the presence of Ni(II) and Co(II), a pronounced increase of capacitance was found for a Pt microelectrode even at potentials considerably anodic to the reversible equilibrium potentials of Ni or Co in the solutions. This effect was attributed to "predeposition."

The present investigation was undertaken with several objectives: (*a*) to determine whether the frequency dispersion of residual capacity would be decreased by improved techniques of melt dehydration (2); (*b*) to ascertain whether the dispersion is sensitive to roughness of the electrode; (*c*) to find whether predeposition occurs quite generally with metals of high and low melting points; (*d*) to attempt a quantitative estimate of rate constants of electrode reactions from impedance data; and (*e*) to compare such values with those obtained from polarization data.

Experimental

The difficulties encountered in the preparation of a suitably dry melt, and the procedure now followed in these laboratories have been described elsewhere (2-4). Before carrying out an experiment, the purity of the melt was tested by measuring the polarographic residual current and the double layer capacity of the Pt electrode in the melt. With the microelectrodes as employed (vide infra), the resid-

[1] On leave of absence from Chemistry Department, University of Delhi, Delhi, India.

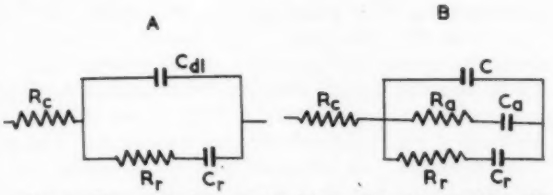

Fig. 1. The equivalent circuit (A) employed by Randles (5) and the modified circuit (B) used by Laitinen and Randles (18) to account for the adsorption of reactants at the electrode surface.

ual current up to a potential of −1.8 v vs. Pt. Ref. did not exceed 2-3 μa, and the double layer capacity at a frequency of 1000 cps of the a-c signal and at a potential of about −0.5 v vs. Pt. Ref. was of the order of 2.5-3 μF mm^{-2}.

The microelectrodes used in this investigation were prepared by sealing No. 26 B and S gauge Pt wire into Corning 0120 glass and flush grinding the tip with fine carborundum. This electrode had a rough surface (electrode A), which could be buffed with finest grade emery paper to a shiny smooth surface (electrode B). Unless otherwise stated, the electrode B has been used in this investigation. The projected area of the electrode was the cross-sectional area of the Pt wire, viz., 0.129 mm^2.

The reference electrode was a Pt foil ca. 8 x 6 mm^2 in contact with Pt(II) solution in the melt which has been shown (3, 4) to be reproducible and nonpolarizable. The concentration of Pt(II) was 0.1*M*.

For impedance measurement the conventional a-c bridge as used by Laitinen and Osteryoung (1) was employed. However, in view of the measurement with lower frequencies, a high inductance choke (3000 henries) was introduced in the d-c circuit to avoid the grounding of a.c. through this path.

By a potentiometric arrangement and employing a Pt working foil, the microelectrode was polarized, its potential with respect to Pt reference being meas-

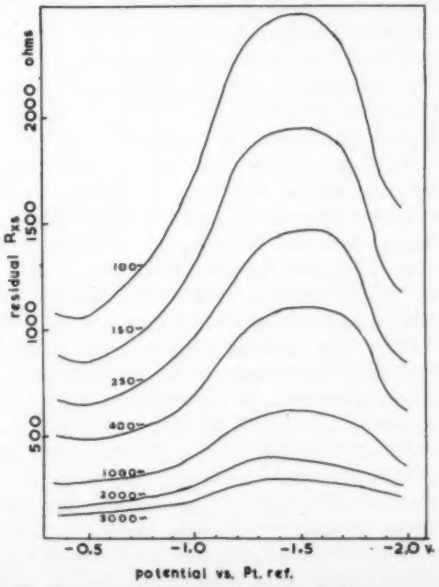

Fig. 2. Variation of residual R_{xs} with frequency of the a-c signal and at various potentials of the microelectrode. PME with smooth surface used.

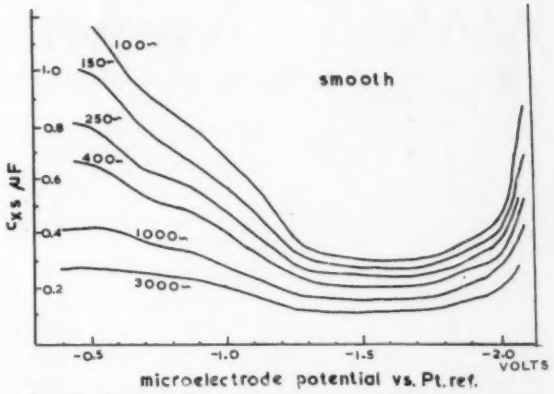

Fig. 3. Residual C_{xs} value at different frequencies of the applied signal and at various PME potentials for electrode with smooth and rough surfaces.

ured with a L&N students' potentiometer. At a given microelectrode potential the over-all impedance of the system was measured at frequencies ranging from 100 to 3,000 cps of the a-c signal applied to the bridge; the current passing through the cell was also measured. Measurements were repeated at various potentials, anodic as well as cathodic to the equilibrium potential; the latter being the open circuit potential of the metal coated electrode.

Results and Discussion

Residual C_s and R_s

The bridge measures the gross impedance of the system as a series combination of a resistance (R_s) and a capacity (C_s). If an electrochemical reaction is occurring at the electrode, the impedance will be composed of the double layer capacity at the Pt-melt interface (C_{dl}), the solution resistance (R_e) and the reaction impedance (R_r, C_r). Considering the network of Fig. 1A employed by Randles (5), in the (pure) melt, i.e., when no charge crosses the double layer, the residual C_s and R_s should correspond to C_{dl} and R_e, respectively, and the values of both should be independent of the frequency of the a-c signal applied to the bridge. However, both have been reported (1) and found in this study to be frequency dependent. Similar frequency dispersion in residual impedance has been observed with solid microelectrodes in aqueous systems also (6-11) and have been ascribed to roughness of the electrode surface or due to the presence of impurities in the solution. It is difficult to ascribe, at present, the cause(s) of this dispersion in the present case but the various possibilities are discussed.

The gross impedance for electrodes A and B was measured; only the observations for electrode B are shown in Fig. 2 and 3, since no substantial difference in R_s or C_s was observed between electrodes A and B in spite of the fact that electrode A appeared "rough" under the microscope and therefore appeared to have a larger true area than electrode B which appeared "shiny". Likewise the dispersion expressed as a ratio of the value of R_s or C_s at a given frequency to its value at 1000 cps is only slightly higher for the rough electrode than for the smooth electrode. This suggests that the smooth surface is not of smaller true area than the rough one.

Fig. 4. Rough (left); smooth, right. (Same length of cutting edge in both figures.)

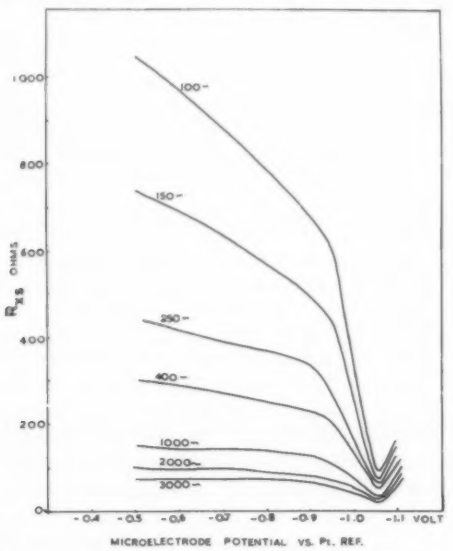

Fig. 5. The R_{xs} values in the reduction of 0.02604M Co^{++} in KCl-LiCl at 450°C at various a-c frequencies and microelectrode potentials.

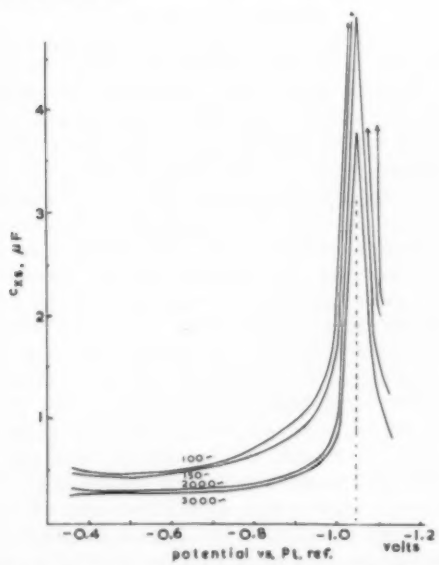

Fig. 6. The C_{xs} values in the reduction of 0.02604M Co^{++} in the melt at 450°C at various microelectrode potentials and at frequencies ranging from 100 to 3000 cps of the a-c signal.

This is clear from the following consideration.[2] If a saw tooth is made finer (Fig. 4) the actual length of the cutting edge is not thereby decreased. The same idea applies on a three dimensional surface. Only if the depth of the groove becomes comparable to or smaller than the thickness of the double layer does the smooth surface look smaller to an impedance measuring device. No very pronounced trends of dispersion with potential over the range −0.5 to −1.0 (vs. Pt. reference) were noted. In contrast, Osteryoung and Laitinen (1) reported that the residual capacity at low frequencies increased rapidly from −0.8 to −1.0 v, while at frequencies of 1000 or 2000 cps it remained sensibly constant in this range. This difference in behavior can no doubt be attributed to the fact that water was more completely removed by the technique used in the present study.

Recent work of Hillson (6) and Grahame (9) with a solid microelectrode in aqueous medium has shown that the impedance behavior of such electrodes is extremely sensitive to traces of surface active impurities. Although the most important category of surface contaminant, namely traces of organic matter, is presumably absent under our conditions, one cannot rule out the possible adsorption of impurities. Indeed, the detailed behavior of impedance in the presence of an electrode reaction is discussed below in terms of an adsorbed layer of metal atoms or ions. Traces of water, or more likely hydroxyl ions resulting from the hydrolytic decomposition of the melt, may be surface active, as may traces of various impurities present in reagent grade salts used for the solvent.

Several investigators (12, 13) have observed frequency dispersion with metal electrodes coated with oxide films. The formation of an oxide layer on a surface during abrasion of the surface in air, as employed at present, has been observed for some metals (14), and it is not unlikely that such a film is present on the electrode surface, and causes the observed dispersion, which has been interpreted (12) in terms of an equivalent circuit composed of a condenser with a relatively low parallel "leakage resistance" in series with the ordinary electrolytic resistance and the frequency independent double layer capacity. Such a model would account satisfactorily for the higher R_s values at low frequencies in the present case also but would lead to C_s values lower than the double layer capacity at high frequencies and increasing to that value at low frequencies. The true double layer capacity is probably actually approached at high frequencies. This concept therefore is inadequate to account for the high C_s values experimentally observed.

A faradaic admittance (15, 16) properly accounts for high C_s values but such a process should be highly dependent on the applied potential.

Recently Bockris, *et al.* (17) suggested that a dielectric loss could be associated with a firmly attached layer of solvent, which has a relaxation time comparable with the applied frequency. In a molten salt one may be dealing with a layer of adsorbed hydroxyl ions which operate in a similar way. This dispersion, however, is remarkably insensitive to refinements in the purification scheme, and may be characteristic of even a pure molten salt system.

Over the potential range of −0.5 to −1.5 v (vs. Pt. reference) the value of residual C_s, extrapolated to infinite frequency, which would approximate closely to the double layer capacity, varied between 0.05 and 0.10 μF, and considering as an approximation the area of the electrode as equal to its projected area, the C_d would correspond to 38-77 μF

[2] The authors are grateful to Dr. David C. Grahame who kindly suggested this idea.

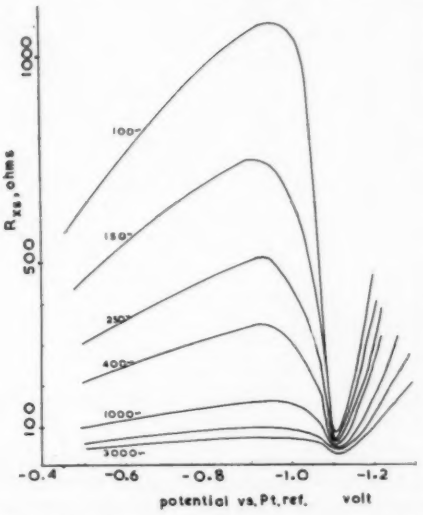

Fig. 7. Pb^{++} in KCl-LiCl at 450°C: the variation of R_{xs} at different frequencies and microelectrode potentials. The equilibrium potential for 0.0432M solution is —1.11 v vs. 0.1M Pt/Pt(II) reference.

cm^{-2}. It would appear that residual C_{xs} may be regarded as consisting of a relatively small frequency independent C_{dl} and a large frequency dependent value arising out of the cause(s) discussed above.

Impedance Measurements

Impedance measurements in the reduction of several metal ions as Co^{++}, Zn^{++}, Pb^{++}, Bi^{+++}, Ni^{++}, Cd^{++} were carried out. In the typical plots in Fig. 7-10, the gross C_{xs} and R_{xs} values are plotted against the electrode potential. Since the maximum change in impedance arises primarily from the electrode process involving the reduction of metal ion, the change in reaction impedance is reflected in these plots. The

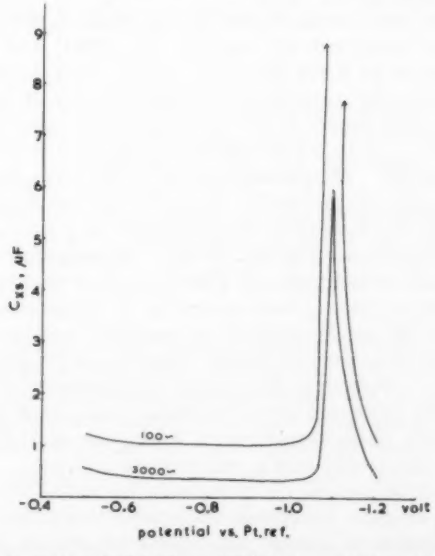

Fig. 8. Pb^{++} in KCl-LiCl at 450°C: the variation of C_{xs} at different frequencies and microelectrode potentials. Only curves for 100 and 3000 cps are shown; for intermediate frequencies the curves lay between these two. The equilibrium potential is —1.11 v vs. 0.1M Pt/Pt(II) reference.

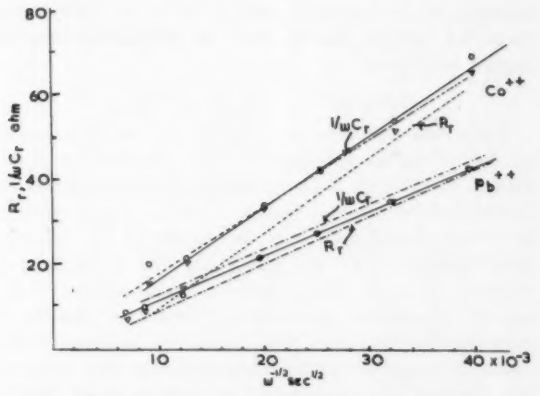

Fig. 9. The broken lines are uncorrected plots for R_r and $1/wC_r$ against $1/\sqrt{w}$. The solid line was obtained after correcting for the admittance due to adsorbed reactants; open circle for R_r and open triangle for $1/wC_r$ for the corrected plots. The concentration of Co and Pb solutions were 2.604 x 10^{-6} and 4.32 x 10^{-6} moles cm^{-3}, respectively.

plots are essentially similar: the C_{xs} passes through a maximum value (pseudo capacity) and R_{xs} through a minimum at the equilibrium potential; there is a tendency for predeposition in most of the cases. For example, in the reduction of Co(II) ion, there is an increasing tendency in C_{xs} from about —0.75 v vs. 0.1*M* Pt. Ref. which gradually develops into a maximum at the equilibrium potential (—1.05 v vs. Pt. Ref.). Since the pseudo capacity could only arise from the reduction of Co^{++} at the electrode, the gradually increasing maximum indicates the deposition and discharge of Co^{++} occurring at potentials at least 0.25 v anodic to the equilibrium potential. Such undervoltages were observed in all the cases studied and varied from 0.035 v for Pb^{++} to 0.45 v for Zn^{++}.

It may be pointed out that predeposition in dilute aqueous media has been observed by Rogers, *et al.* (19, 24), Haissinsky (25), and others (26, 27); it

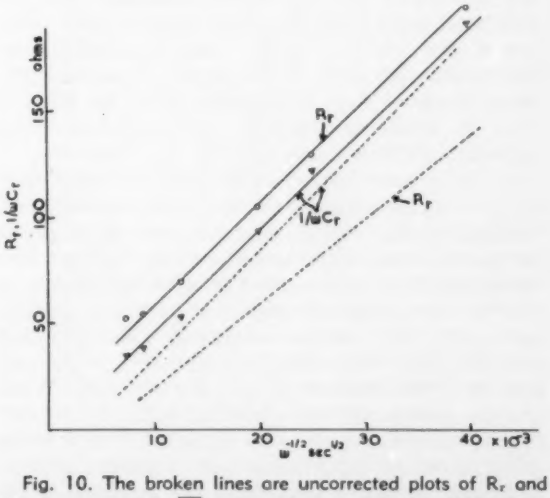

Fig. 10. The broken lines are uncorrected plots of R_r and $1/wC_r$ against $1/\sqrt{w}$ for the reduction of Zn^{++} in KCl-LiCl at 390°C; the solid lines represent the plots after a correction for admittance due to adsorbed ions was introduced. The Zn concentration was 7.16 x 10^{-6} moles cm^{-3}.

appears to be more common in fused salt media however and is shown even in relatively concentrated solutions.

Calculation of Rate Constants

From the observed R_s, and C_s, values in presence of metal ion at the equilibrium potential and the values of C_{dl} and R_c, the reaction impedance can be calculated by several series → parallel and parallel to series transformations as employed by Laitinen and Randles (18). To allow for the dispersion in residual C_s, for the purpose of calculations of reaction impedance, at a given frequency, the C_s, as measured in the melt was employed instead of any value obtained by extrapolation to infinite frequency; the residual R_s, values are in general much higher and these could not be used; the solution resistance was obtained by extrapolating the observed R_s, values to infinite frequency.

For the deposition of a metal ion on an inert electrode the reaction impedance, in terms of the electrical analogy, a resistive (R_r) and capacitative (C_r) component in series is given by:

$$R_r = \frac{RT}{n^2\mathbf{F}^2AC}\left[\sqrt{\frac{2}{wD}} + \frac{1}{k}\right] \qquad \text{(I)}$$

$$\frac{1}{C_r} = \frac{RT}{n^2\mathbf{F}^2AC}\left[\frac{2}{wD}\right] \qquad \text{(II)}$$

so that

$$\Delta = R_r - \frac{1}{wC_r} = \frac{RT}{n^2\mathbf{F}^2AC} \cdot \frac{1}{k} \qquad \text{(III)}$$

where $w = 2\pi f$, f being the number of cycles per second of a-c signal fed to the bridge; n is the number of electrons involved in the rate-determining step; A is the area of the electrode in cm^2; C is the concentration of the reducible ion in moles cm^{-3}; k is the rate constant for the electrode process in cm sec^{-1}; R, T, and $\mathbf{F}$ have their usual significance.

It is seen that a plot of R_r and $1/wC_r$ against $1/\sqrt{w}$ should give two straight and parallel lines; the resistance plot lying over the reactance plot and the latter passing through the origin; their separation given by Eq. (III) being dependent, *inter alia*, on the rate of the electrochemical reaction. The phase angle of the combination ϕ given by tan $\phi = 1/wC_rR_r$ would be less than $\pi/4$, this value being approached for an immeasurably fast reaction.

In the present study ϕ was always greater than $\pi/4$ so that the impedance plots were reversed and furthermore the reactance plot missed the origin. A similar situation was encountered by Laitinen and Randles (18) in the study of faradaic admittance to a. c. of a dropping mercury electrode in a solution containing *tris* (ethylenediamine) cobaltous and -cobaltic ions. The effect was ascribed to the adsorption of the reactant ions at the electrode. These authors considered the admittance due to the adsorbed reactants to be pure capacitance or a series combination of capacitance and resistance and as additional to that arising from the electrochemical reaction. After making an empirical correction for this effect, the faradaic admittance was used for calculating the rate constant for the electrode process.

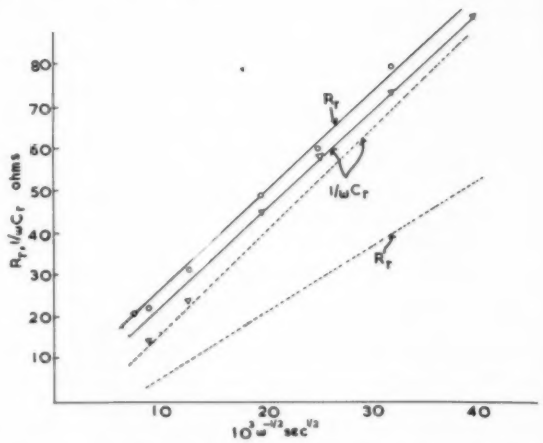

Fig. 11. The broken lines are the uncorrected reaction impedance plots for the reduction of $CdCl_2$ in KCl-LiCl at 450°C. The solid lines represent the plots obtained after correcting for the admittance due to the adsorbed ions. The Cd concentration was 5.95×10^{-5} moles cm^{-3}.

Corrections of similar nature were also applied in the present case, suitable values being found by several trials. The equivalent circuit for the process is given in Fig. 1(b).

In the reduction of Pb^{++}, Ni^{++}, and Co^{++} ions the uncorrected plots were very close to each other and only a capacitative correction of 1.1, 0.3, and 1.3 μF, respectively, was needed for the reactance plot to pass through the origin; this correction also shifted the resistance plot and the two overlapped, as would be the case for an immeasurably fast reaction. For the reduction of Cd^{++} and Zn^{++} the correction needed was a series combination of a resistance and capacitance, and furthermore the corrected plots were separated from each other (Fig. 11, 12, and 13).

The rate constants for the reduction of these ions were calculated by use of Eq. (III) and were found to be 0.686 and 1.27 cm sec^{-1}, corresponding to exchange currents of 172 and 31.8 amp at the hypothetical concentration of 1 mole cm^{-3}. Taking the value $\alpha = 0.5$ the exchange currents at a concentration of 0.1M are calculated to be 1.72 amp and 0.32 amp, respectively, for our electrode area.

The significance of the correction may be clarified by the following considerations. A frequency-independent admittance, such as that applied as an empirical correction, was shown by Laitinen and Randles (18) to correspond to a surface electron exchange reaction occurring without a diffusion step which introduces frequency dependence. An infinitely rapid electron exchange would give rise to a purely capacitative correction, whereas one of finite rate would add a resistive component.

Considering the heterogeneous nature of the electrode surface, it appears reasonable to postulate the adsorption of heavy metal ions on certain active sites at potentials anodic to the equilibrium potentials and the conversion of such adsorbed ions by electron exchange to adsorbed (predeposited) metal atoms. As the equilibrium potential is approached

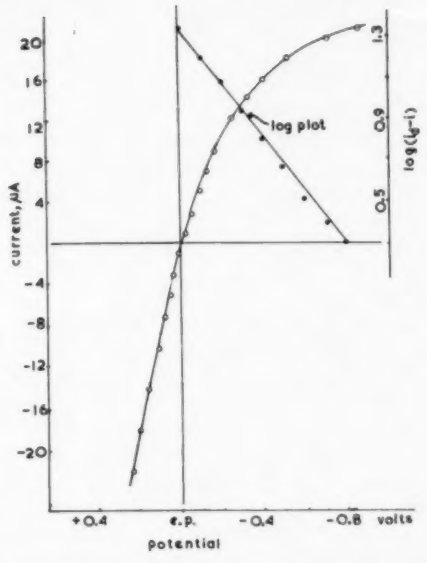

Fig. 12. The polarization curve for Pb^{++} in KCl-LiCl eutectic at 450°C. The Pb^{++} concentration was 4.32×10^{-5} moles cm^{-3}. The equilibrium potential at this concentration was −1.11 v vs. 0.1M Pt/Pt(II) reference. The potentials are referred to the equilibrium potential. The log plot has a slope of 0.077 v.

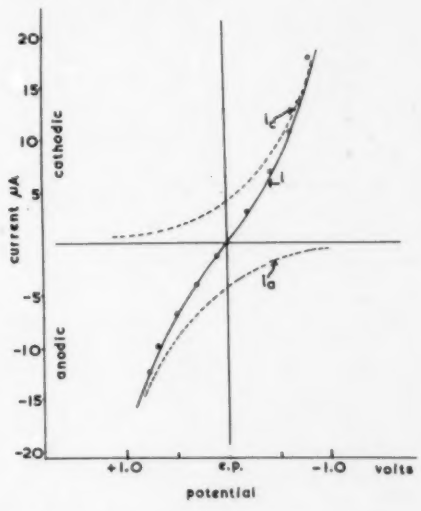

Fig. 14. The current-potential curve for the system Zn^{++} in KCl-LiCl at 390°C. The solid line is calculated curve for $\alpha = 0.53$ and $i_o = 4 \times 10^{-6}$ amp for the area of the electrode used (0.13 mm^2) and the dots are the experimental points. The potentials are referred to the equilibrium potential (−1.47 v vs. 0.1M Pt/Pt^{++}). Current (i) is the algebraic sum of the cathodic (i_c) and anodic (i_a) currents.

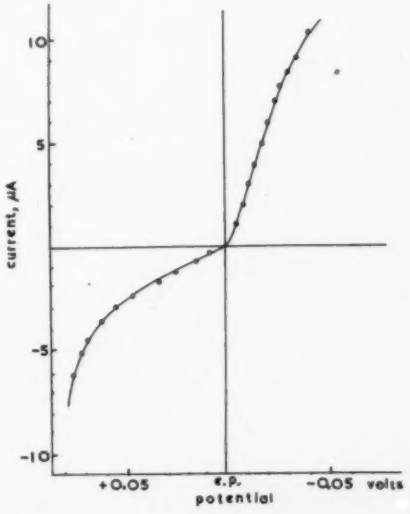

Fig. 13. The c.v. curve for Co^{++} in KCl-LiCl at 450°C. The concentration of Co was 2.604×10^{-5} moles cm^{-3} and the equilibrium potential −1.05 v vs. 0.1M Pt/Pt(II) reference. The potentials are referred to the equilibrium potential.

from the anodic direction, a greater fraction of the total area of Pt is called into play, so that a greater amount of electron exchange between adsorbed ions and atoms, and therefore a greater pseudocapacity, is observed. At cathodic potentials, the normal decrease due to concentration polarization occurs.

Polarization Studies

These studies describe the current-potential behavior on cathodic and anodic polarization of Pt microelectrode with respect to its equilibrium potential for several metal ions. The results are summarized in Fig. 12 to 16. In agreement with the polarographic practice the cathodic currents are regarded as positive and the cathodic potentials are plotted on the abscissa axis from left to right.

The current-potential curve for Pb^{++} is the nearest ideal case: a well-defined reduction wave with a diffusion current plateau is obtained at appreciable cathodic overpotentials; on reversing the polarization the current retraces the path, passes through zero value at equilibrium potential, and, at anodic potential, an anodic current is drawn due to the dissolution of metal from the electrode. Using the value of 22.6 μa for i_d, a plot of $-E_{mc}$ vs. log $(i_d - i)$ for the small voltage span had a slope of 0.077 v as compared to 0.0717 v for a reversible two electron reduction. In the Ni curve the limiting cathodic current was not well defined and the value varied somewhat with time; this has been the experience in a majority of the cases where the metal deposits onto the electrode in the solid state. In both these cases, the electrode processes are very fast, a conclusion which is in accord with the one arrived at by the impedance technique. The anodic portion of the Co^{++} curve (Fig. 13) has an unusual shape. Instead of a sharp increase in anodic current with increase of anodic overvoltage, as would be expected of a process involving only the dissolution of the metal, there is a gradual increase at first which at appreciable anodic overpotentials increases rapidly. This part of the curve is reproducible although the actual current varied somewhat in different experiments. This anomalous shape could be explained due to the formation of a film of an insoluble material which introduces a slow step in the dissolution of the metal into the solution. At appreciable anodic overpotentials the film is partially or completely dissolved and then the normal shape of the curve follows. The passivity of the freshly

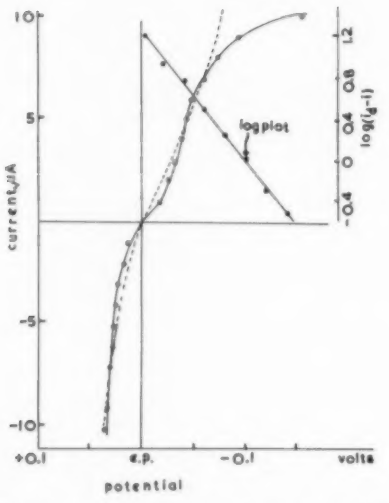

Fig. 15. The c.v. curve for the Bi^{+++} ion in KCl-LiCl at 450°C. The potentials are referred to the equilibrium potential. The broken line is calculated for $i_o = 3.5 \times 10^{-6}$ amp and $\alpha = 0.30$. The log plot has a slope of 0.0239 v. The details are in the text.

formed metal on the electrode surface could also be responsible for such an observation.

The Zn, Bi, and Cd polarization curves have definite inflections in the equilibrium potential region indicating that the electrochemical reaction proceeds with a measurable speed. For the deposition of a metal ion on an inert electrode and for a process involving a single rate-determining step, the current potential relationships are given by:

$$i = n\mathbf{F}Ak\left[\, C\exp\left\{\frac{-\alpha n\mathbf{F}\eta}{RT}\right\} - \exp\left\{(1-\alpha)\,\frac{n\mathbf{F}\eta}{RT}\right\}\right] \qquad \text{(IV)}$$

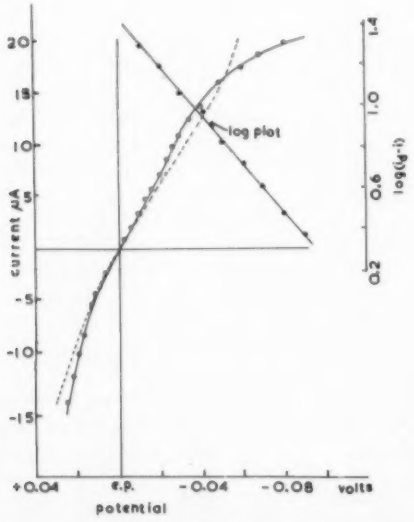

Fig. 16. The polarization curve (solid line) for Cd^{++} in KCl-LiCl at 450°C. The Cd concentration was 5.95×10^{-6} moles cm^{-3}, and the open circuit potential for the metal coated electrode (equilibrium potential) was —1.278 v vs. 0.1M Pt/Pt(II). The potentials are referred to the equilibrium potential. The dotted line is calculated for $i_o = 12 \times 10^{-6}$ amp and $\alpha = 0.30$. The slope of log plot is 0.0864 v.

$$i_o = n\mathbf{F}AkC^{1-\alpha} \qquad \text{(V)}$$

and

$$i = i_o\left[\exp\left\{\frac{-\alpha n\mathbf{F}\eta}{RT}\right\} - \exp\left\{(1-\alpha)\,\frac{n\mathbf{F}\eta}{RT}\right\}\right] \qquad \text{(VI)}$$

where i is the current in amperes for an overvoltage η; i_o is the exchange current, and α is the transfer coefficient for the cathodic process; n is the number of electrons in the rate-determining step; A is the area of the electron in cm^2; C is the concentration of the metal ion in moles cm^{-3} and $\mathbf{F}$, R, T have their usual significance.

Equation (VI) involves two experimentally controllable variables i and η and hence direct determination of the two unknown variables i_o and α by this is not possible since, over the narrow potential range, the current due to reverse process cannot be neglected. By several trials values of i_o and α were so chosen that for a given curve the values of i for different values of η calculated from (VI) corresponded as nearly as possible to the observed values of i. In Fig. 14 the dots are experimental points for the zinc curve while the curve is theoretical for $\alpha = 0.53$ and $i_o = 4\,\mu a$.

For the cadmium and bismuth curves (Fig. 15, 16) the dotted lines are for $\alpha = 0.30$, and i_o is equal to 12 and 3 μa, respectively.

An attempt was made to compare the exchange current from the polarization curve with those computed by use of Eq. (V) and employing the rate constants from the impedance measurements. Taking as an example the reduction of Cd^{++} and Zn^{++} ions for a concentration of 10^{-4} mole cm^{-3}, and $\alpha = 0.5$, the exchange current would be 1.72 and 0.318 amp, respectively, for our electrode area. These are of the order of 10^5 larger than those computed from the polarization curves. In calculating the values from impedance data it was necessary to apply an empirical correction for adsorption and a considerable uncertainty is thus introduced in the value of rate constant by the necessity of this correction. However, no adjustment of empirical parameters could possibly change the values more than a power of ten because the impedance plots would then have impossible shapes.

Alternatively a tenfold increase in the exchange current would completely remove the inflection from the region of origin of the polarization curves. Therefore, the two sets of values must be regarded as incompatible.

The weight of evidence appears to favor the impedance method because of the appearance of unexplained inflections in several of the polarization curves. The matter will not be completely settled, however, until independent methods of kinetic studies are carried out.

Acknowledgments

The authors are grateful to the Office of Ordnance Research and the Diamond Ordnance Fuse Laboratory for the financial support of this project and for the research associateship held by one of them (H. C. G.).

Manuscript received March 11, 1957. This paper is based on a Technical Report submitted to the Office of

Ordnance Research and Diamond Ordnance Fuse Laboratory, Jan. 15, 1957.

Any discussion of this paper will appear in a Discussion Section to be published in the June 1958 JOURNAL.

REFERENCES

1. H. A. Laitinen and R. A. Osteryoung, *This Journal*, **102**, 598 (1955).
2. H. A. Laitinen, W. S. Ferguson, and R. A. Osteryoung, **ibid., 104**, 516 (1957).
3. R. A. Osteryoung, Ph.D. Thesis, University of Illinois (1954).
4. W. S. Ferguson, Ph.D. Thesis, University of Illinois (1956).
5. J. E. B. Randles, *Disc. Faraday Soc.*, **1**, 11 (1947).
6. P. J. Hillson, *Trans. Faraday Soc.*, **50**, 385 (1954).
7. W. Lorenz, *Z. Elektrochem.*, **58**, 912 (1954).
8. W. D. Robertson, *This Journal*, **100**, 194 (1953).
9. D. C. Grahame, R. E. Ireland, and R. C. Peterson, ONR Tech. Rep. No. 22, Research Contract N8-ONR-66903 (March 1956).
10. J. J. Vetter, *Z. physik. chem.*, **199**, 300 (1952).
11. J. N. Sarmousakis and M. J. Prager, *This Journal*, **104**, 454 (1957).
12. J. E. Lillienfield and C. Miller, *ibid.*, **100**, 222 (1953).
13. L. Young, *Trans. Faraday Soc.*, **51**, 1250 (1955).
14. R. T. Foley, B. T. Stark, and C. J. Guare, *This Journal*, **103**, 534 (1956).
15. D. C. Grahame, *Chem. Rev.*, **41**, 441 (1947).
16. D. C. Grahame, *This Journal*, **99**, 370C (1952).
17. J. O'M. Bockris, W. Mehl, B. E. Conway, and L. Young, *J. Chem. Phys.*, **25**, 776 (1956).
18. H. A. Laitinen and J. E. B. Randles, *Trans. Faraday Soc.*, **51**, 54 (1955).
19. L. B. Rogers and A. F. Stehney, *J. (and Trans.) Electrochem. Soc.*, **95**, 25 (1949).
20. L. B. Rogers, D. P. Krause, J. C. Griess, and D. B. Ehrlinger, *ibid.*, **95**, 33 (1949).
21. J. C. Griess and L. B. Rogers, *ibid.*, **95**, 129 (1949).
22. J. C. Griess, Jr., J. T. Byrne, and L. B. Rogers, *ibid.*, **98**, 447 (1951).
23. J. T. Byrne and L. B. Rogers, *This Journal*, **98**, 457 (1951).
24. L. B. Rogers, *Rec. chem. Progress*, **16**, No. 3, 197 (1955).
25. M. Haissinsky, *J. Chim. Phys.*, **43**, 21 (1946).
26. T. Berzins and P. Delahay, *J. Am. Chem. Soc.*, **75**, 555 (1953).
27. M. M. Nicholson, *ibid.*, **79**, 7 (1957).

Technical Note

The Influence of Surface Pretreatment on the Atmospheric Oxidation of 2S (U. S. Alloy 1100) Aluminum

Philip M. Aziz and Hugh P. Godard

Aluminium Laboratories Limited, Kingston, Ontario, Canada

In the course of an experimental study of the room temperature atmospheric oxidation of aluminum and its alloys the influence of a variety of surface pretreatments on the oxidation rate was investigated. This work was carried out on 5 x 20 x 0.025 cm samples of Alcan 2S (U. S. 1100) aluminum in the H-18 temper. The oxidation process was followed by determining the change in weight of the sample with a Mettler constant load microbalance. All weighings were corrected for atmospheric buoyancy taking into account the influence of barometric pressure, temperature, and relative humidity. The samples were given the desired pretreatment, then immediately weighed and transferred to a desiccator containing a saturated sodium carbonate solution which maintained a relative humidity of 87% within the desiccator at ambient room temperature. Weighings were continued over a period of time providing a weight gain-time curve. The experimental results presented in Fig. 1 are representative of the large number of such curves obtained. Since the weight gains observed on duplicate samples were reproducible to ± 5 μg, the observed differences are not due to experimental error.

The chemically polished samples (phosphoric-nitric acid type bath) were subsequently washed, dipped into acetone, and air dried prior to weighing. The surfaces which had been scratch brushed under kerosene were washed with acetone and air dried before weighing, while the surfaces which had been abraded with emery were washed with fresh kerosene between changes of paper and finally washed with acetone. The initial weighing was completed within 10 min of the cessation of the surface treatment. Scratch brushing was carried out by hand using a steel wire brush.

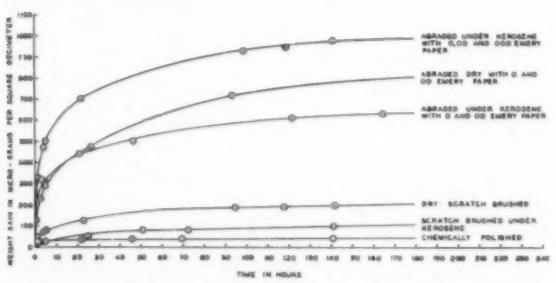
ABRADED UNDER KEROSENE WITH 0,00 AND 000 EMERY PAPER
ABRADED DRY WITH 0 AND 00 EMERY PAPER
ABRADED UNDER KEROSENE WITH 0 AND 00 EMERY PAPER
DRY SCRATCH BRUSHED
SCRATCH BRUSHED UNDER KEROSENE
CHEMICALLY POLISHED
TIME IN HOURS

Fig. 1. Atmospheric oxidation of Alcan 2S alloy (US1100-H18) relative humidity of 87% as a function of surface treatment.

The difference in weight gains between the chemically polished and dry scratch brushed surfaces can probably be accounted for by the difference in true surface areas of the samples. The former surface has a roughness factor of about 1-2 whereas the latter is about 3-4. This can account for the observed difference within the limits of reproducibility from sample to sample for the same pretreatment.

The reason for the influence of the kerosene lubricant on the scratch brushed surface is not clear. It is possible that the presence of kerosene may influence the degree of surface roughness obtained or it may react with the surface producing an initial film influencing the subsequent reaction.

The large difference in weight gains as shown by the lower and upper three curves is more difficult to explain. It is hard to conceive of surface roughness having any major effect since it is very difficult to picture large differences in surface roughness between abraded and scratch brushed surfaces and in addition it is difficult to conceive of roughness factors greater than 3-4 on metal surfaces. Also both methods of surface treatment, abrasion and scratch brushing, should effectively remove the initial oxide film and leave a bare metal surface.

Microscopic examination of the abraded surfaces after gentle metallographic polishing has shown that they contain a great deal of embedded emery and that the degree of oxidation that they undergo increases with the quantity of emery in the surface. This then seems to be the cause of the enhanced oxidation of the emery abraded surfaces over the scratch brushed and chemically polished surfaces.

Vernon (1) has presented data on the atmospheric oxidation of commercially pure aluminum with a dry scratch brushed surface and his measured weight gains are in good agreement with those obtained during the course of this work. In view of the difference in relative humidity between the two sets of experiments, great significance should not be

attached to the close agreement, but it is nevertheless gratifying.

These results point up the importance of surface treatment in the study of the oxidation of metals especially in the case of soft metals where abrasive particles can become embedded in the surface. Chemical etching methods are suspect because of the ever present danger of preferential etching, as is chemical polishing since, especially in the case of alloys, it could lead to an enrichment of the alloying elements in the surface. Thus it is felt that for work where the use of evaporated films is not possible and alloys are to be studied, a mechanical method of removing the surface film such as dry scratch brushing, as first introduced by Vernon, is the most satisfactory.

Manuscript received Nov. 26, 1956.

Any discussion of this paper will appear in a Discussion Section to be published in the June 1958 JOURNAL.

REFERENCE

1. W. H. J. Vernon, *Trans. Faraday Soc.*, **23**, 113 (1927).

Technical Review

Electroluminescence and Field Effects in Phosphors

Henry F. Ivey

Research Department, Westinghouse Electric Corporation, Bloomfield, New Jersey

Today the word electroluminescence is used almost universally to indicate the generation of light in a solid material when it is excited solely by electric fields or currents, the light thus generated being in excess, in some spectral region, of the thermal radiation of the material. If other means of excitation, such a ultraviolet, x-rays, or cathode rays, for example, act simultaneously with the electric field or current, then some materials display more complicated phenomena which here for the moment are classified simply as "field effects". Today a wide variety of these phenomena are known and it is the main purpose here to differentiate these various effects, to explain them qualitatively, and to discuss something of their history.

It should be pointed out that the definition suggested above for electroluminescence is not one that has always been used consistently in the past by various workers in the field of luminescence. Thus, Leverenz writes (1) that "electroluminescence is obtained during electric discharges in gases", while on page 148 of the same book he indicates that electroluminescence is the same as cathodoluminescence, i. e., the light generated when a solid is bombarded with electrons or cathode rays.[1] These definitions would make both neon signs and television picture tubes examples of electroluminescence. It was because of such previous wide use of the word electroluminescence that Destriau in his early publications (2) used the word "electrophotoluminescence" to indicate what is now meant by the shorter word. "Electroluminescence" was first used in the modern sense by Payne, Mager, and Jerome in 1950 (3). Modern terminology completes the confusion by using the word electrophotoluminescence to describe a case in which the material is subjected simultaneously to the action of an electric field and to photoexcitation. With time, this distinction and the restriction of electroluminescence to the case of a solid excited only electrically, without external irradiation (either electromagnetic or corpuscular), seems to have become crystallized and is today the common usage.[2]

Although here electroluminescence is considered as restricted to purely solid systems, it is of interest that a similar effect in liquid systems has been known for a much longer time. The fact that electrodes immersed in electrolytes through which an electric current was passed often showed luminescence was known to Braun in 1898 (5) and may be of even more ancient vintage; the emission probably originates in an oxide layer on the electrode. This phenomenon is today called "galvanoluminescence", a name apparently first used by Sullivan and Dufford (6) in 1931.[3]

It should also be noted that modern usage is to confine the words "light" and "luminescence" to radiation in the visible region of the spectrum; this usage has been approved by the American Standards Association, the Illuminating Engineering Society, and the Optical Society of America. It is thus necessary to have a different word to describe the process which differs from electroluminescence only in that the emitted radiation lies outside the visible region. Since materials emitting in the ultraviolet and infrared regions are now known, one of the Task Groups of the AIEE-IRE Subcommittee on Dielectric Devices has tentatively suggested the name "electroradiescence" for this phenomenon. In this connection there comes to mind the old "Reboul effect".[4] In 1920 Reboul (9) found that, if a high electric field is applied to certain semiconductors by means of perforated electrodes, the air in the vicinity of the anode becomes ionized by some kind of radiation emitted by the solid. From latter experiments it seems that this radiation is composed of electrons, soft x-rays, and ultraviolet radiation and is thus, at least in part, electroradiescence.

Recombination Electroluminescence

The first observation of what would today be called electroluminescence was made in Russia in 1923 by Lossew (10). It seems unusual that the Russians have not emphasized this priority in their usual style; as a matter of fact, since this early work there has apparently been very little activity on

[1] It is also of interest that on page 392 of the same book Leverenz expresses doubts as to the existence of true electroluminescence as defined here!

[2] There are, however, still unfortunate exceptions to this terminology. Thus, for example, in a paper (4) published in March, 1957, the word "electrofluorescence" is used to describe the light emission of dynodes in a photomultiplier under electron impact.

[3] In an earlier paper Dufford (7) states, "The name electroluminescence naturally suggests itself for a luminescence produced in this way; but unfortunately this term, along with anodoluminescence and cathodoluminescence, has been appropriated for the description of the effects observed in the discharge through gases."

[4] The only reference to the Reboul effect known to the writer in the modern literature is the book by Zwikker (8). There seems to have been no work on this effect for the last twenty years.

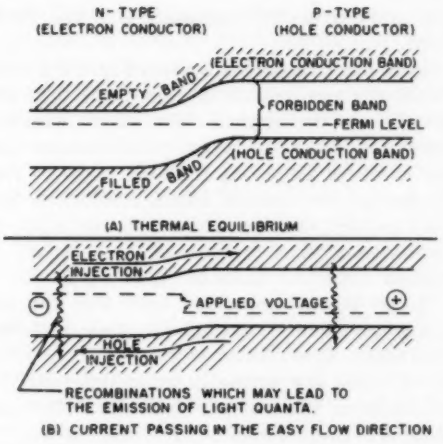

Fig. 1. Energy diagrams for a p-n barrier in the absence of an applied field (A) and for current flow in the forward direction with consequent injection of minority charge carriers (B). In addition to direct radiative recombination of holes and electrons as shown, recombination may also occur via luminescence activator centers or in a radiationless manner.

electroluminescence in Russia. Lossew found that when point contacts were applied to certain SiC crystals (used for radio detection at that time) and current passed through the crystal, light was often emitted.

In recent times this emission in SiC has been studied by Lehovec, Accardo, and Jamgochian (11), who also gave the currently accepted explanation, which was not possible before the advent of modern solid-state physics and semiconductor theory. In Fig. 1A is shown the energy level diagram for a p-n junction in the absence of an applied voltage. By definition, in the n-type region the density of negatively charged carriers (electrons in the "empty" conduction band) exceeds that of positively charged carriers (positive holes in the "filled" valence band); here electrons are the majority carriers and holes the minority carriers. In the p-type region the situation is reversed. In each region there is continual thermal production and subsequent recombination of electron-hole pairs. The system is thus in a state of dynamic equilibrium. Some of the recombinations occur with the emission of radiation; the emission generated in this way simply contributes to the normal thermal radiation characteristic of the material at the ambient temperature and is quite small.

If a voltage is applied to such a junction in the so-called forward direction or direction of easy flow (Fig. 1B), then electrons are injected into the p-type region and positive-holes into the n-type region; this then corresponds to minority carrier injection. The increased minority carrier concentration produced in this way obviously leads to an increased rate of recombination; if part of these recombinations are radiative, then one has electroluminescence. In principle this is the type of electroluminescence discovered by Lossew. In the case of SiC, where the emitted radiation is in the yellow region of the spectrum although the energy gap between conduction and valence bands corresponds to an energy in the blue region, the recombination does not occur directly band-to-band but indirectly through intermediate impurity or activator levels. A similar kind of emission has been observed in CdS, Ge, Si, diamond, and some of the so-called III-V compounds, particularly indium antimonide; in the case of Si and Ge the emission is in the infrared region of the spectrum and corresponds, at least in part, to band-to-band transitions. In this discussion the picture of a p-n junction has been used. From transistor experience it is known that point contacts can also produce minority carrier injection in much the same way as area junctions.

It is of value here to emphasize the characteristics of this kind of electroluminescence which distinguish it from another type to be discussed later. These are:

1. There is no high electric field required to excite the emission; the field in the junction is actually lower when the voltage is applied than in its absence.
2. The fundamental controlling quantity is the injected current, not the voltage producing this current.
3. The charge carriers of importance are minority carriers.
4. Once these carriers are injected, they are able immediately to recombine with carriers of the opposite sign to produce radiation without the necessity of gaining further energy from the field. Because of these characteristics this type of luminescence has been or might be called "recombination electroluminescence", "minority carrier injection electroluminescence", or "current-controlled electroluminescence". It has also been called "d-c electroluminescence", but since it can also be excited by a.c., at least on alternate half-cycles, this does not seem to be a good description.

Not all electron-hole recombinations following minority carrier injection are of the radiating variety. As a matter of fact at the present time, with perhaps the exception of the infrared-emitting indium antimonide, this is most often not the case. As a result, the efficiency of materials emitting in the visible due to recombination electroluminescence is comparatively low.

The Destriau Effect

In 1936 Destriau (12) observed a different kind of electroluminescence. Here the experimental arrangement consisted of a zinc sulfide phosphor powder suspended in a dielectric and subjected to an intense alternating electric field (of the order of 10^5 v/cm). The purpose of the dielectric is to exclude air, breakdown of which under the intense fields will produce u. v. radiation which can indirectly excite the phosphor to photoluminescence. For a time there was some doubt that such indirect excitation could be completely avoided and hence doubt as to the existence of true electroluminescence in the solid state. Today, however, there can be no question as to existence of this effect. Within the past ten years the Destriau effect has been investigated extensively. Limitation of space does not permit a discussion of the wide variety of experimental observations;

these have, however, been reviewed elsewhere (13-15). Today the brightnesses and efficiencies obtained with the Destriau effect far exceed those of recombination electroluminescence.

Consider the possible physical effects of such intense fields on a phosphor material. The energy-level diagram of such a material consists in general, in addition to the valence and conduction bands, of isolated, normally filled levels lying above the valence band (the activator or luminescence centers) and isolated, normally empty levels lying below the conduction band (electron trapping centers). Under conditions of excitation some of the normally filled luminescence centers are, of course, emptied and some of the normally empty traps filled. The various possibilities are:[5]

1. The field may induce the transfer of an electron from the valence band to the conduction band by quantum-mechanical tunneling, thus simultaneously producing a free electron and a free hole. Such a Zener effect (17) does indeed occur in some materials, but it is most unlikely in normal phosphors at the field strengths utilized in electroluminescence because of the wide energy gap (forbidden zone) in these materials.

2. The field may induce the transfer of an electron from a filled luminescence center to the conduction band by quantum-mechanical tunneling. This process has been studied theoretically by Franz (18), but again it is unlikely at normal field strengths in electroluminescence.

3. The field may cause the transfer of an electron from the valence band to an empty luminescence center. Since the energy difference in this case is comparatively small (a few tenths of an electron volt) this is much more likely than the effects discussed above. Since such transfer can in addition be produced thermally, the transition may also occur under the combined action of field and temperature; the field in this case serves to lower the thermal activation energy for the transition. Since this process fills empty luminescence centers, it is obviously a de-exciting rather than an exciting effect. Evidence that field filling of empty centers occurs will be discussed later.

4. The field may cause the release of an electron from a filled trap. Here again, as in the previous case, the effect may be due to field action alone (tunneling) or to lowering of the trap barrier by the field and subsequent thermal release.[6] The release of trapped electrons by an electric field has been directly observed by Böer and Kümmel (22) in their experiments on "electrical glow curves". Here the phosphor is excited at low temperatures and then the electric field is continually increased; the resultant release of carriers can be observed by conduction effects in a manner analogous to the usual thermoluminescence experiment where the temperature is continually increased and the emission observed.

5. Once electrons are introduced into the conduction band (by any conceivable method) they can be accelerated by the electric field. Such accelerated electrons may excite or ionize luminescence centers as well as cause emptying of filled traps or ionization of the lattice material itself. Avalanche formation and carrier multiplication may occur. Such an acceleration-collision process is well-known from the field of dielectric breakdown of solids.

6. Under the action of the field, free carriers of both signs are swept toward the surface of the phosphor particles. Recombination rates and the concentration of traps are normally quite different (higher) at surfaces than in the bulk, and this action therefore serves as a means of de-excitation.

It remains to be discussed which of these mechanisms are important in the Destriau effect and, in latter sections, in the other field effects related to electroluminescence.

Destriau in his early papers (2) made the suggestion that the observed dependence of electroluminescent brightness on applied field strength could be explained either on the basis of a field emission process or an acceleration collision process. Because of the extremely high fields necessary for field emission, it is now commonly agreed that the acceleration-collision model is the correct one. Garlick (23) was apparently the first to realize the importance of field emptying of traps in electroluminescence. In 1949 he wrote, "There are always a few electrons in traps in unexcited phosphors which can be freed by the field and accelerated to produce excitation of luminescence centers." The details of the theoretical treatment of this kind of electroluminescence have been presented by Curie (24), Piper and Williams (25, 26), Zalm (14), and Alfrey and Taylor (27), among others. The essential steps in the process are shown in Fig. 2.

One essential feature of the current explanation of the mechanism of the Destriau effect is the existence within the phosphor particles of localized regions within which the field strength is much higher than the average or applied field strength. In these special regions the field strengths may be as high

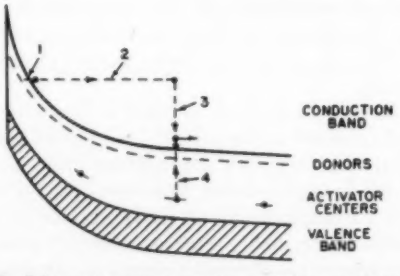

Fig. 2. Schematic representation of the acceleration-collision mechanism of electroluminescence. Electrons from traps in the localized high field region are liberated by the action of the high electric field and/or temperature [1], are then accelerated by the field [2] to acquire energies above the bottom of the conduction band, and collide with activator centers whereby they lose their energy [3] and the activator center is ionized [4] or excited. Emission usually occurs later in the cycle when the applied potential is reversing.

[5] Some of these possibilities were reviewed in the keynote speech of F. E. Williams at the Symposium on Luminescence held by this Society in Cincinnati two years ago and in a subsequent paper by Piper and Williams (16).

[6] Frenkel (19) has used this concept in a discussion of dielectric breakdown. The hydrogenic model for electron traps has, of course, been used extensively (20). Lanczos (21) has discussed the effect of electric fields on the hydrogen atom but this quantitative treatment does not seem to have been extended to the solid-state case.

as 10^6 or 10^7 v/cm. If such fields extended throughout the bulk of the particle, dielectric breakdown would probably occur as a result of avalanche formation. It is generally believed that in most normal electroluminescent phosphors, which are almost universally of the ZnS class, these regions of enhanced field arise from the presence of a second chemical phase, usually copper sulfide or ZnO. The exact location of these important regions inside or on the particles and the details of the mechanism of their operation is still, however, open to discussion (13, 28-30). Destriau's early phosphors contained large amounts of ZnO. Zalm, Diemer, and Klasens (29) showed that small amounts of copper sulfide deposited on the surface of ZnS made it electroluminescent. Lehmann (30) has found that a wide variety of normally nonelectroluminescent phosphors become electroluminescent if they are simply mechanically mixed with metal or semiconductor powders. The creation of these localized regions of high field is the key to the production of the relatively small number of known efficient electroluminescent phosphors compared to the comparatively large number of available photoluminescent systems.

In the presence of the applied field and the resultant excitation, the electroluminescent particles become polarized. The influence of this polarization on the details of the light emission has been investigated by various workers (14, 31-33). One important result is that the electroluminescent emission is "delayed emission"; the charges excited during one half-cycle of the applied voltage can recombine and emit only during the subsequent half-cycle (at least for ZnS:Cu phosphors). This has been shown strikingly by Zalm (14). During the charge separation trapping occurs and is responsible for many of the experimentally observed aspects of electroluminescence (14, 27, 34-36), including the dependence of average brightness on frequency and temperature, the nature of the variation of output during one cycle of the applied voltage ("brightness waves"), and the growth in output after application of the field and before equilibrium is reached ("buildup"). The emptying of electron traps by the combined action of field and temperature and the collision excitation of luminescent centers by accelerated electrons (processes 4 and 5 in the list given previously) are the predominant mechanisms in the Destriau effect; the statement of Garlick quoted earlier still contains the essence of the process as it is understood today. The role of traps has been recently reviewed by Haake (37).

Let us now summarize the characteristics of the Destriau effect which distinguish it from recombination electroluminescence as discussed earlier. These are:

1. The phenomenon is a field-dominated one, although thermal effects also play a role.

2. The charge carriers of importance are majority carriers.

3. After these carriers are introduced they must be accelerated by the field in order to obtain sufficient energy to excite luminescence centers by collision.

Because of these characteristics this type of luminescence has been or might be called "acceleration-collision electroluminescence", "majority-carrier injection electroluminescence", or "field-controlled electroluminescence". It has sometimes been called "a. c. electroluminescence" but since in the case of single crystals or thin phosphor films it can be excited by static fields, this does not seem to be a good description. The present writer (13) is responsible for the term "intrinsic electroluminescence". This was an attempt to specify the fact that the process is confined to the phosphor particles and does not depend on external carrier injection by means of electrodes. In view, however, of the present knowledge of the complexity of electroluminescent phosphors and the fact that the segregated second phase essentially corresponds to internal electrodes, this terminology should probably be abandoned.

If instead of a phosphor powder separated from electrodes by an insulator, a powder (38, 38a), a thin continuous film (39), or a single crystal (40-42) in contact with electrodes is employed, then sometimes there are observed additional experimental details which are due to carrier injection from the electrodes. As long as the carriers, however, correspond to majority carriers, acceleration will be necessary to achieve excitation and the process is similar in principle, although different in detail, to that observed in powders embedded in an insulator. Although it has been hoped that experiments on single crystals would clarify some of the results obtained with powders, this does not seem to be the case in reality because of the various difficulties or ambiguities involved.

In the previous section the recombination electroluminescence resulting when a p-n junction is biased in the forward direction was discussed. In the case of Si, for example, this radiation lies in the infrared region of the spectrum. If, however, such a junction is biased in the reverse or blocking direction so that high electric fields are produced in the junction, then a visible emission may be observed (43). An apparently similar emission was indeed observed by Lossew (10) in his earliest experiments on SiC and called by him Luminescence I in distinction to the other type which he called Luminescence II. Since this emission occurs when high fields are developed and when the polarity is such as to cause injection of majority carriers, it is believed that here also one has a process involving an acceleration-collision mechanism. Chynoweth and McKay (44) have also reported an emission in reverse-biased very narrow Si p-n junctions which is believed to result from internal field emission (Zener emission) rather than from an avalanche mechanism.

In concluding this section on the excitation of phosphors by electric fields alone, it is perhaps of interest to mention that Diemer (45) has observed what seems to be a third kind of electroluminescence in CdS crystals. His observation paralleled in many respects the characteristics of a gas discharge; it was also apparent that the local temperature of the specimen increased remarkably and played a role in the process. It has been suggested that this

type of excitation be called "breakdown electroluminescence". It should perhaps also be mentioned that Smith (46) has observed recombination electroluminescence in CdS crystals.

Electric Field Effects in Excited Phosphors

Now turn from a consideration of the effects produced by applying an electric field to a phosphor to the more complicated situation where the field is applied simultaneously with or subsequent to excitation by some other means.[7]

The Gudden-Pohl Effect (Transient Stimulation of Luminescence)

The earliest discovery of an electrophotoluminescent[8] effect was that of Gudden and Pohl (47) in 1920, even before the discovery of electroluminescence itself. Here the phosphor is first excited (by u. v. radiation, for example) and then an electric field (of the order of 10^5 v/cm) is applied during the afterglow or phosphorescence of the phosphor, or even after the emission has decayed below the limit of detection. A burst of emission is observed with some materials, even those which do not exhibit electroluminescence. During normal phosphorescence the electrons recombining with empty luminescence centers are provided by thermal emptying of electron traps. In the Gudden-Pohl effect the obvious effect of the field is to facilitate this trap emptying process. Curie (24) has also suggested that the field might accelerate electrons released from traps, either by the field alone (tunneling) or by the joint action of field and temperature, so that they acquire sufficient energy to cause emptying of additional filled traps by impact; the amount of energy required in this case is not very great. Although this effect may indeed occur, it is very difficult to distinguish experimentally from a direct action of the field on the traps.

When a static field is applied to a phosphor powder, polarization charges develop in the material and the effective internal field eventually becomes quite small. Under some cases this polarization may persist for very long times after the field has been removed; this subject has been studied extensively by Kallmann and Rosenberg (48). Because of these polarization effects the effective field in the Gudden-Pohl effect rapidly becomes zero if a static field is applied; this may, of course, be avoided by removing and applying the field periodically or by using an alternating field. Correspondingly, if a static field is applied to the phosphor during excitation and then removed during the afterglow, i. e., the reverse of the procedure for observing the normal Gudden-Pohl effect, a result similar to the normal effect is obtained (49). In this case, removal of the external field actually causes the effective internal field to increase, so that in reality there is no difference between the two methods of inducing the effect.

[7] The experimental details have been reviewed in a number of places (2, 13, 15).

[8] F. E. Williams in his keynote speech for the Luminescence Symposium of this Society in 1955 suggested that the terminology in these field effects gives the controlling agency as the first prefix and the source of power as the second prefix, although the two are difficult to unscramble in some cases. The terminology in this field has not always been consistent, however.

The Déchêne Effect (Field Quenching of Luminescence)

Many of the early experiments on electrophotoluminescence were, unfortunately, not carried out under very simple conditions and are often very difficult to interpret. For example, in 1934 Coustal (50) subjected a previously excited phosphor layer to an electrical glow discharge in air. Depending upon circumstances he obtained either quenching (presumably due to the field of the discharge) or enhancement (presumably due to u. v. radiation generated in the discharge) of the phosphorescence.

In 1935 Déchêne (51) performed an electrophotoluminescent experiment under slightly better conditions. He wet a sulfide phosphor powder with water and placed it between electrodes to which was applied a high direct voltage. Under these conditions the ionic conductivity of the water was sufficient to maintain a current of the order of microamperes per square centimeter, sufficient to counteract the polarization of the phosphor particles and maintain a field across them. Actually the field in Déchêne's experiments was strongest near the electrodes and the effects he observed were also greatest there. (It may be mentioned that this arrangement was also used by Déchêne to study the Reboul effect.) By the use of a slightly conducting medium for the phosphor Déchêne was able to observe field effects on phosphors with sustained fields and not simply during the short interval before polarization built up.

Déchêne made his observations both during the phosphorescence and with simultaneous u. v. excitation. At the moment of field application he observed a momentary increase in emission—the Gudden-Pohl effect. This, however, was followed, by a sustained quenching of the emission. This quenched emission in the afterglow might be only 24% of the normal value; for simultaneous excitation and field action, however, the quenching observed was fairly small (only to 82% of normal). Upon removal of the applied voltage a second Gudden-Pohl stimulation was observed. Fig. 3 shows the general results obtained by Déchêne for the case of continuous excitation. In 1943 Destriau (52) reported on field quench-

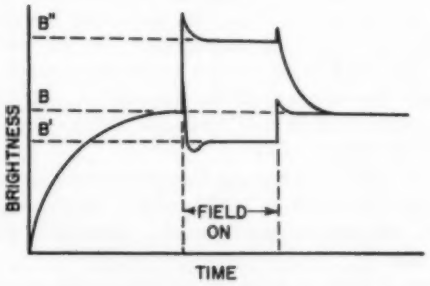

Fig. 3. Schematic representation of field quenching and enhancement effects on the brightness of an excited phosphor. Upon application of the field the brightness B may be either, depending on the material and on the experimental conditions, depressed to a new value B' or raised to a new value B". At the times the field is applied or removed there are also usually transient effects as shown; the short flashes of light observed at these times are due to the Gudden-Pohl effect and may not always be observed.

ing experiments on phosphors using powders imbedded in an insulator and alternating fields,[9] i. e., the arrangement used by him in electroluminescence. This method of avoiding polarization effects has obvious advantages over that used by Déchêne in that higher and uniform fields may be obtained. In this way the luminescence may be quenched almost to zero.

Two possible causes for the quenching effect suggest themselves: (*a*) the field may cause filling of empty luminescent centers from the valence band, or (*b*) the electrons are forced by the field to the surface of the crystals where nonradiating transitions are favored or they become deeply trapped. The fact that quenching occurs more readily in ZnS:Ag than in ZnS:Cu, as observed by Steinberger, Low, and Alexander (53, 54), gives some evidence for the former effect, but both may occur. It may be noted that Déchêne himself suggested the second explanation (although naturally not in modern parlance). He reported that thermoluminescence experiments on phosphors after quenching indicated a more intense emission persisting at higher temperatures (indicating the presence of electrons in deeper traps) but also a smaller total emission (fewer total number of filled traps, indicating that some nonradiating transitions had occurred). The kinetics of the quenching effect have been discussed by Matossi (55).

Field Effects on Infrared Stimulation or Quenching of Emission

In the preceding sections it is apparent that an electric field applied to a previously excited phosphor may empty filled traps, leading to stimulated emission, or fill empty luminescence centers, leading to emission quenching. Exactly similar effects may be induced by infrared radiation and have been known since the time of Lenard and even earlier. In 1937, one year after his discovery of acceleration-collision electroluminescence, Destriau (56) discovered that in some cases infrared quenching could be enhanced by the simultaneous application of an electric field. Correspondingly, in 1954, Low, Steinberger, and Braun (57) discovered that the response of some infrared stimulable phosphors could be enhanced by electric fields. In these cases the action of field and infrared radiation is combined.

Photoelectroluminescence and Cathodoelectroluminescence (Field Enhancement of Luminescence)

In 1954 Destriau and his son reported on a completely new effect (58-60). If certain phosphor powders, primarily ZnS:Mn, Cl and ZnCdS:Mn, Cl, are excited by x-rays and then an alternating electric field is applied, it is found that the luminescence intensity is increased (see Fig. 3). This has been called field enhancement of luminescence or the electroenhancement effect; according to Williams' nomenclature it is photoelectroluminescence. The materials showing this effect are only weakly electroluminescent and the enhancement effect can be observed at field strengths below those at which any detectable electroluminescent output is obtained.

Destriau found that the same phosphors which showed field enhancement of the x-ray excited luminescence showed, on the contrary, field quenching if excited by u. v. radiation. Recently Gobrecht and Gumlich (61) have shown, however, that although quenching is observed at low field frequencies and low u. v. intensity, at high frequencies and high exciting intensities enhancement is observed with the same materials.[10] Thus it appears that the enhancement effect and the quenching effect can occur simultaneously; depending on circumstances, one or the other may predominate. Cusano (62, 63) has also found that transparent films of ZnS:Mn, Cl show enhancement for either kind of excitation; in this case the effect may also be obtained with direct rather than alternating voltage since electrodes may be applied directly to the film. In photoelectroluminescence the energy emitted may exceed the controlling radiant energy so that radiation amplification is achieved.

Low (64) in 1955 suggested that field enhancement should also exist for luminescence excited by nuclear particles and suggested the effect as a radiation detector. The effect was actually first observed, for the case of alpha-particle excitation, in 1956 by Mattler (65) using the same phosphors used by Destriau for x-ray excitation.[11] Jaffe (67) reported that the same phosphors also show enhancement when bombarded with electrons.[12] The differences in the detailed performance of the same materials under the three types of excitation are presumably due to the differences in penetration depth and density of ionization in the three cases. Woods and Wright (69) also reported in 1955 that the cathodoluminescence of MgO could be enhanced by static electric fields. According to Williams' nomenclature, these last two effects are both examples of cathodoelectroluminescence, although in his abstract Jaffe called the effect electrocathodoluminescence.

Williams (70) in 1955 presented an explanation of all these field enhancement effects which today seem to be generally accepted. His picture is that enhancement of luminescence is really externally controlled electroluminescence as distinguished from normal electroluminescence which is self-sustained. Thus in the usual type of acceleration-collision elec-

[9] Déchêne also mentions the use of alternating fields and the electroluminescence experiments of Destriau. In an earlier paper (13) it was stated incorrectly that Déchêne worked only in the afterglow region. The correct picture of the situation was first given by Matossi (15).

[10] It has recently been brought to the writer's attention by C. H. Haake that Schmidt (49) in his 1923 paper (page 174) mentions the existance of an enhancement effect. Schmidt says, "It is a remarkable fact that phosphors excited while in an electric field sometimes luminesce noticeably brighter than during normal excitation. This can be easily demonstrated if one makes two cells of the same phosphor and applies to one a high voltage while both are irradiated with the 365 mμ Hg line and the brightness observed." There is no further information given in the paper. It may be that with the field applied, u.v. radiation generated in the powder provided the additional excitation. In any case, it was 22 years before anyone duplicated this observation despite the fact that many people studied field effects in phosphors in the interim.

[11] Earlier, in 1944, Destriau (66) looked for field enhancement of the scintillations produced by alpha particles, but was unable to find the effect in the materials then available.

[12] Note added May 24, 1957: Since the above was written it has been brought to the writer's attention that in a recent publication Cusano (68) mentions that he has obtained field enhancement of the luminescence of thin phosphor films of ZnS:Mn, Cl under cathode-ray excitation; no details of these experiments have been published, however.

troluminescence there are three steps in the excitation process (*see* Fig. 2):

1. Production of the initial free electrons by action of the field.
2. Acceleration of these electrons by the field.
3. Impact excitation of luminescence centers.

In photoelectroluminescence or cathodoelectroluminescence the initial electrons are supplied, either directly or indirectly, by the external radiation so that step [1] above is modified, but thereafter the process is essentially unchanged. In the opinion of the writer, this theory does not explain to complete satisfaction why sulfides containing Cu as an activator (which are very good materials for pure electroluminescence) do not show photoelectroluminescence, but only the quenching effect. Most phosphors which show photoelectroluminescence are activated by Mn, although Cusano (71) has recently reported the effect with As and P as activators. In addition, it should be noted that with alternating fields, the effect of frequency, field strength, and temperature is quite different in electroluminescence and in photoelectroluminescence. (See note on page 748.)

Thermoelectroluminescence and Electrothermoluminescence

In a normal thermoluminescence experiment, the phosphor is excited at low temperatures so that electron traps are filled. The excitation is then removed and the temperature allowed to increase; thermal detrapping results in emission of radiation. Reference has already been made to the experiments of Böer and Kümmel (22), who maintained the phosphor at the low temperature following excitation and applied a field of increasing magnitude. Trap emptying by the field was detected by changes in electrical conductivity.[13] It would appear that radiation resulting from the freed charges should also be detectable, but this apparently has not yet been observed.

Neumark (73) has studied the effects of applying an electric field to phosphor single crystals during a thermoluminescence experiment. She found, in the case of crystals which showed electroluminescence, that electrons released thermally from traps can be accelerated to give emission greater than the sum of the normal thermoluminescence and the electroluminescence at that temperature. The effect is thus quite similar to that of photoelectroluminescence discussed above; it is temperature-controlled electroluminescence or thermoelectroluminescence. Strangely, however, Neumark found no evidence for appreciable field release of trapped electrons in these crystals. This is in contradiction to the results of Johnson, Piper, and Williams (34) who also used single crystals in their experiments on the effect of temperature on electroluminescent brightness; these workers, however, did not study thermoluminescence with applied fields.

[13] Jensen and Cashman (72) have also observed what they called "electrical glow curves"; they, however, used increasing temperature rather than increasing field strength and measured the conductivity. Since there are two quantities which may be varied (the temperature and the field strength) and two which may be observed (luminescence and conductivity), there are obviously four possible experimental arrangements.

Prior to Neumark's work, Gobrecht, Hahn, and Gumlich (74), and later Hahn (75), observed effects on the temperature dependence of the brightness of electroluminescent powders which they interpreted in a manner similar to that given above for Neumark's experiments. On cooling the samples they obtained a smooth curve, but on heating they obtained a series of maxima and minima; this effect they called "electrothermoluminescence". Most good electroluminescent powders do not display this behavior, however, and even in those that do, Hahn reports that the nature of the embedding medium has a profound influence so that the effect may not be characteristic of the phosphor itself.

Other Field Effects in Phosphors

The use of photoelectroluminescence or the electroenhancement effect as a radiation amplifier has been described above. Halsted (76) recently described an amplification effect utilizing electrophotoluminescence. He makes use of the fact that in ZnS, for example, 2537Å radiation is very strongly absorbed compared to 3650Å radiation. Thus, for 2537Å excitation the excited luminescent centers are very nonuniformly distributed in the material and are concentrated near the side of the material on which the radiation impinged. If an alternating field is applied, carriers periodically will be swept out of and into the excitation region so that the luminescence output will be modulated at the field frequency.[14] Modulation levels of 50% may be achieved in this way with quite low fields (100 v/cm). Under proper conditions, the energy content of the modulated component of output may exceed the electrical input so that in this sense amplification is obtained. This effect differs from the photoelectroluminescent amplifier, however, in that the input and output are not both radiation.

Destriau (77) recently described a new storage or memory effect in conjunction with the field enhancement of x-ray excited luminescence. The material is first subjected simultaneously to x-ray excitation and to a field and then the x-rays are turned off before the field; this constitutes the sensitization. If now after an interval of time during which the phosphor is stored in the dark (experiments have been performed up to 17 hr) x-rays are again applied, without the field, the emission will rise to an enhanced value and then decay to an equilibrium. The effect of the sensitization by the field has thus been stored in the material. If the intensity of x-rays striking the phosphor during the sensitization period varies over its area, as is the case if an object is placed before the phosphor, then an image of this object will be obtained at the second irradiation even though the object has been removed and the second irradiation done with uniform excitation; the phosphor has stored a latent image of the object which is revealed by the subsequent irradiation. Under suitable conditions the contrast in the image may be enhanced in this way.

The explanation of this storage effect of Destriau seems to be the following. During the sensitization

[14] In the usual electrophotoluminescence experiment with more or less uniform excitation (penetrating radiation) the output is also modulated, but at a frequency twice that of the applied field (15).

period the degree of excitation is greater than that corresponding to the x-ray excitation alone since the material shows electroenhancement. During sensitization, the field draws off some of the electrons to the surfaces of the particles where they are held in deep traps.[15] In the dark these stored charges will be retained for long periods. When the x-ray beam is reapplied, without field, electrons are excited from these deep traps as well as from luminescence centers and the output rises to a transient value higher than the equilibrium value. As the traps are emptied, the emission decays to its normal value. As the x-ray intensity at the second irradiation may be made greater than that used for sensitization, the image may be displayed at high output levels; this may be of value if it is not desired to expose the object itself to intense x-irradiation.

Alburger (79) has also discussed materials which he calls "electroflors". These are liquids which show no luminescence under u. v. excitation in the absence of a voltage but which become luminescent when a voltage is applied. No information has been published on the composition of these substances, but B. Rosenberg has suggested to the writer that they involve organic materials whose luminescence is sensitive to pH value. This material is dissolved in a solvent containing an ionized salt and the local pH is controlled by polarization produced by the applied voltage. Since they are liquid, they bear no connection with normal inorganic phosphors, but their existence is at least of general interest.

Conclusion

As has been shown by the preceding discussion, the variety and the ramifications of the effects of electric fields on phosphors and the number of possible experimental arrangements are exceedingly great. It seems, however, that the observations may usually be explained by a combination of a few fairly simple basic physical processes. These are:

1. Field emptying of traps (Gudden-Pohl).

2. Field quenching of photoluminescence (Déchêne). This may occur either by field induced filling of empty luminescence centers from the valence band or by the action of the field in sweeping electrons away from the excitation region to regions where trapping and/or nonradiating recombination are favored.

3. Acceleration-collision electroluminscence (Destriau). Majority carriers may be accelerated by sufficiently high fields to excite luminescence centers by collision. The initial electrons may be supplied by the field itself (self-sustained electroluminescence) or by external action (photoelectroluminescence, etc.).

4. Recombination electroluminescence (Lossew). Minority carriers injected from contacts or over p-n barriers may immediately recombine, often with the emission of radiation.

From these basic processes there have come a wide variety of experimental effects. In the future many others will undoubtedly be discovered.

Acknowledgments

The writer is indebted for valuable discussion to Dr. Lehmann, Dr. Thornton, Dr. Rosenberg, and Mr. Jaffe, and especially to Dr. Haake, all of the Westinghouse Phosphor Research Section in Bloomfield, and to Professor Destriau and Dr. Mattler, our consultants, of the Faculty of Sciences in Paris.

Manuscript received June 14, 1957. This paper was prepared for delivery before the Washington Meeting, May 12-16, 1957.

Any discussion of this paper will appear in a Discussion Section to be published in the June 1958 JOURNAL.

REFERENCES

1. H. W. Leverenz, "An Introduction to Luminescence of Solids," p. 152, John Wiley & Sons, Inc., New York (1950).
2. G. Destriau, *Trans. Faraday Soc.*, **35**, 227 (1939); *Phil. Mag.*, **38**, 700, 774, 880, 885 (1947).
3. E. C. Payne, E. L. Mager, and C. W. Jerome, *Illum. Eng.*, **45**, 688 (1950).
4. R. Gerharz, *J. Electronics*, **2**, 409 (1957).
5. F. Braun, *Ann. der Phys.*, **65**, 361 (1898).
6. R. R. Sullivan and R. T. Dufford, *Phys. Rev.*, **37**, 1019 (1931).
7. R. T. Dufford, *J. Opt. Soc. Amer.*, **18**, 17 (1929).
8. C. Zwikker, "Physical Properties of Solid Materials," p. 279, Interscience Publishers Inc., New York (1954).
9. G. Reboul, *Compt. rend.*, **171**, 1052 (1920); **172**, 210 (1921); **173**, 222 (1921); *J. Phys. Rad.*, **2**, 86 (1931); **5**, 329 (1934).
10. O. W. Lossew, *Telegrafia i Telefonia*, No. 18, 61 (1923); No. 26, 403 (1924); *Wireless World*, **15**, 93 (1924); *Phil. Mag.*, **6**, 1024 (1928).
11. K. Lehovec, C. A. Accardo, and E. Jamgochian, *Phys. Rev.*, **83**, 603 (1951); **89**, 20 (1953).
12. G. Destriau, *J. Chim. Phys.*, **33**, 620 (1936); **34**, 117 (1937).
13. G. Destriau, and H. F. Ivey, *Proc. IRE*, **43**, 1911 (1955).
14. P. Zalm, *Philips Res. Repts.*, **11**, 353, 415 (1956).
15. F. Matossi, "Elektrolumineszenz und Elektrophotolumineszenz," Vieweg, Braunschweig (1957).
16. W. W. Piper and F. E. Williams, *Phys. Rev.*, **98**, 1809 (1955).
17. C. Zener, *Proc. Roy. Soc.*, **A145**, 523 (1934).
18. W. Franz, *Ann. der Phys.*, **11**, 17 (1952).
19. J. Frenkel, *Phys. Rev.*, **54**, 647 (1938); *Tech. Phys. USSR*, **5**, 685 (1938).
20. D. Curie, *J. Phys. radium*, **17**, 16 (1956).
21. C. Lanczos, *Z. Physik.*, **62**, 518 (1930); **65**, 413 (1930); **68**, 204 (1931).
22. K. W. Böer and U. Kümmel, *Z. Naturforsch.*, **9a**, 177 (1954).
23. G. F. J. Garlick, "Luminescent Materials," p. 150, Oxford Univ. Press (1949).
24. D. Curie, *J. Phys. Radium*, **14**, 510, 673 (1953).
25. F. E. Williams, in "Advances in Electronics," Vol. V, p. 137, Academic Press, New York (1953).
26. W. W. Piper and F. E. Williams, *Brit J. Appl. Phys.*, Suppl. No. 4, p. 39 (1955).
27. G. F. Alfrey and J. B. Taylor, *Proc. Phys. Soc. (London)*, **66B**, 775 (1955).
28. L. Burns, *This Journal*, **100**, 572 (1953).
29. P. Zalm, G. Diemer, and H. A. Klasens, *Philips Res. Repts.*, **9**, 81 (1954).
30. W. Lehmann, *This Journal*, **104**, 45 (1957).
31. J. F. Waymouth and F. Bitter, *Phys. Rev.*, **95**, 941 (1954); **102**, 686 (1956).

[15] Neumark (73) has presented experimental evidence for the filling of traps by electric fields and has shown that the effect is greater with alternating than with static fields. Kallmann and Mark (78) have discussed the de-exciting effects of electric fields on the photoconductivity of phosphors.

32. F. Matossi, *ibid.*, **98**, 434 (1955).
33. F. Matossi and S. Nudelman, *ibid.*, **99**, 1100 (1955); *This Journal*, **101**, 546 (1954).
34. P. D. Johnson, W. W. Piper, and F. E. Williams, *ibid.*, **103**, 221 (1956).
35. W. A. Thornton, Phys. Rev., **102**, 38 (1956).
36. C. H. Haake, *J. Appl. Phys.*, **28**, 117, 245 (1957); *This Journal*, **104**, 291 (1957).
37. C. H. Haake, *J. Opt. Soc. Amer.*, **47**, 881 (1957).
38. G. Destriau, *Illum. Eng.*, **51**, 197 (1956).
38a. D. Hahn and F. W. Seemann, *Z. Physik*, **146**, 644 (1956).
39. R. E. Halsted and L. R. Koller, *Phys. Rev.*, **93**, 349 (1954).
40. W. W. Piper and F. E. Williams, *ibid.*, **87**, 151 (1952).
41. D. R. Frankl, *ibid.*, **100**, 1105, 1790 (1955).
42. G. Diemer, *Philips Res. Repts.*, **10**, 194 (1955).
43. R. Newman, W. C. Dash, R. N. Hall, and W. E. Burch, *Phys. Rev.*, **98**, 1536 (1955).
44. A. G. Chynoweth and K. G. McKay, *ibid.*, **106** 418 (1957).
45. G. Diemer, *Philips Res. Repts.*, **9**, 109 (1954).
46. R. W. Smith, *Phys. Rev.*, **98**, 1169 (1955); **105**, 900 (1957).
47. B. Gudden and R. W. Pohl, *Z. Physik.*, **2**, 192 (1920).
48. H. Kallmann and B. Rosenberg, *Phys. Rev.*, **97**, 1596 (1955).
49. F. Schmidt, *Ann. Physik.*, **70**, 161 (1923).
50. R. Coustal, *Compt. rend.*, **198**, 1403, 1596 (1934).
51. G. Déchêne, *ibid.*, **201**, 139 (1935); *J. Phys. Radium*, **9**, 109 (1938).
52. G. Destriau, *ibid.*, **4**, 32 (1943).
53. I. T. Steinberger, W. Low, and E. Alexander, *Phys. Rev.*, **99**, 1213 (1955).
54. E. Alexander, W. Low, I. T. Steinberger, and S. Z. Weiss, *J. Phys. Radium*, **17**, 737 (1956).
55. F. Matossi, *Phys. Rev.*, **94**, 1151 (1955); *This Journal*, **103**, 662 (1956).
56. G. Destriau, *J. Chim. Phys.*, **34**, 327 (1937); *J. Phys. Radium*, **4**, 77 (1943).
57. W. Low, I. T. Steinberger, and E. A. Braun, *J. Opt. Soc. Amer.*, **44**, 504 (1954).
58. M. Destriau, *Compt. rend.*, **238**, 2298 (1954).
59. G. Destriau and M. Destriau, Paper presented at ECS Meeting, Chicago, 1954.
60. G. Destriau, J. Mattler, M. Destriau, and H. E. Gumlich, *This Journal*, **102**, 682 (1955).
61. H. Gobrecht and H. E. Gumlich, *J. Phys. Radium*, **17**, 754 (1956).
62. D. A. Cusano, *Phys. Rev.*, **98**, 546 (1955).
63. D. A. Cusano and F. E. Williams, *J. Phys. Radium*, **17**, 742 (1956).
64. W. Low, *Phys. Rev.*, **98**, 556 (1955).
65. J. Mattler, *J. Phys. Radium*, **17**, 758 (1956).
66. G. Destriau, *Comp. rend.*, **218**, 791 (1944).
67. P. M. Jaffe, Paper presented at ECS Meeting, Washington, 1957.
68. D. A. Cusano, *IRE Trans. Nuclear Sci.*, Vol. NS-3, No. 4, November (1956).
69. J. Woods and D. A. Wright, *Proc. Phys. Soc. (London)*, **68B**, 566 (1955).
70. F. E. Williams, *Phys. Rev.*, **98**, 547 (1955).
71. D. A. Cusano, *ibid.*, **106**, 604 (1957).
72. H. C. Jensen and R. J. Cashman, *ibid.*, **96**, 798 (1954).
73. G. Neumark, *ibid.*, **103**, 41 (1956); *Sylvania Technologist*, **10**, 29 (1957).
74. H. Gobrecht, D. Hahn, and H. E. Gumlich, *Z. Physik*, **136**, 623 (1954).
75. D. Hahn, *J. Phys. Radium*, **17**, 748 (1956).
76. R. E. Halsted, *Phys. Rev.*, **99**, 1897 (1955); *Bull. Am. Phys. Soc.*, **2**, 155 (1957).
77. G. Destriau, Meeting Physical Society, Berlin, March 15, 1957.
78. H. Kallmann and P. Mark, *Phys. Rev.*, **105**, 1445 (1957).
79. J. R. Alburger, *Electronic Indus. and Tele-Tech.*, p. 50, February, 1957.
80. D. Curie, "Progress in Semiconductors," Vol. 2, p. 249, John Wiley & Sons, Inc., New York (1957).
81. J. Mattler, Abstract 28, Washington Meeting, ECS, May 1957.

NOTE Added in Proof: In a recent article (80) Curie has concluded that the field-enhancement effect observed by Cusano does not have the same mechanism as that observed by Destriau. He comes to this conclusion because of the quite different effects of field strength and temperature in the two cases. In Destriau's experiments the output increases only slowly as the field strength is increased and approaches a limiting value; in Cusano's experiments, on the other hand, the output increases more or less exponentially with applied voltage above a threshold voltage. Mattler (81) has also shown that the enhancement ratio (with x-ray excitation) increases as the temperature is increased despite the fact that the electroluminescence of the same material (at higher field strengths) decreases with increasing temperature. Curie concludes that excitation by accelerated electrons does not occur in the enhancement experiments of Destriau.

Discussion Section

This Discussion Section includes discussion of papers appearing in the JOURNAL of The Electrochemical Society, 103, No. 9 (September 1956), and 104, No. 1-6 (January-June 1957). Discussion not available for this issue will appear in the Discussion Section of the June 1958 JOURNAL.

Oxidation of Copper to Cu_2O and CuO

D. W. Bridges, J. P. Baur, G. S. Baur, and W. M. Fassell, Jr.

(pp. 475-478, Vol. 103)

J. Paidassi[1]: We are studying the oxidation of OFHC copper in air under atmospheric pressure between 300° and 1050°C and thought that it might be interesting to summarize our results so that they could be compared with those obtained by the authors.

Our preparation of the specimens consisted of grinding on metallographic polishing papers to a fineness of 4/0, washing with toluene, and finally annealing in vacuum (10^{-4} mm Hg) at 900°C for 4 hr. The specimens were oxidized in a vertical, open furnace, where the atmosphere was renewed and finally quenched in air. The minimum duration of the oxidation varied between 1 and 60 min, the maximum between 4 and 200 hr, depending on the temperature. In each sample Δm, the increase of weight per cm^2 of the initial surface, and e, e_1, e_2, the total thickness of the scale, and the thickness of the CuO and Cu_2O layers, respectively, were determined. We restrict ourselves below to a summary of the results obtained between 600° and 1000°C.

At all the temperatures one obtains, with a good approximation, the following relations:

$$\Delta m = k_m \sqrt{t}\ (\mathrm{I});\ e = k \sqrt{t}\ (\mathrm{II});\ e_2 = k_2 \sqrt{t}\ (\mathrm{III})$$

where t is the time, and k_m, k, k_2 are constants.

The formulation of the law of growth of the thickness of the CuO layers is more complicated. In the 600°-800°C range and durations of oxidation up to 48 hr, it is of the following type:

$$e_1 = k_1 \sqrt{t} + k'_1 \qquad (\mathrm{IV})$$

where k_1 and k'_1 are two positive constants. Between 850°-1000°C the growth rate at first follows a law of type (IV), but subsequently its growth is retarded and the thickness e_1 finally reaches a limiting value for a time of oxidation, which varies between 16 and 2 hr depending on the temperature. (We believe that the above particularities of the law of growth of the CuO layer at temperatures exceeding 850°C may be explained by dissociation of the CuO in the course of oxidation.)

It follows that the relative thickness $e_{1/e}$ of the CuO layer in relation to the total thickness of the scale, strictly speaking, is not constant at any temperature. Nevertheless, because of the smallness of k'_1 of Eq. (IV) at any temperature throughout the 650°-800°C range, $e_{1/e}$, with the exception of the shortest times of oxidation, does not vary more than 20%, the limiting value being reached after from 16 to 32 hr, depending on the temperature. For temperatures higher than 800°C the diminution of the relative value of this ratio is of the same order of magnitude, although the absolute variations remain very small due to the low values of $e_{1/e}$ (from 0.3 to 3%) within the 800°-1000°C range. Fig. 1 shows the relative variations of the thickness of the CuO layer with the duration of oxidation at temperatures of 600°, 800°, and 1000°C, respectively, and Fig. 2 the variation with temperature of the limit of the $e_{1/e}$ ratio corresponding to "steady" rate of oxidation.

If we compare the above results with those of the authors it may be concluded that, on the whole, agreement is satisfactory. The observed differences may be due partly to the different surface preparation of the specimens. On the other hand, we believe that the considerable dispersion of results recorded

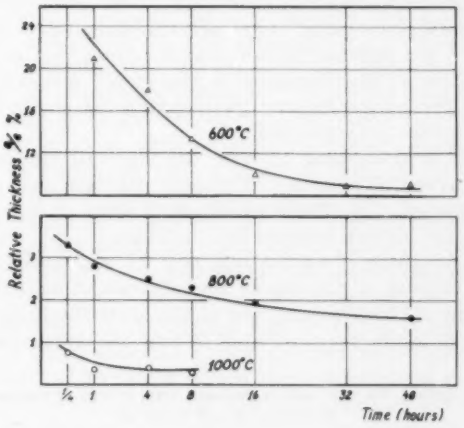

Fig. 1

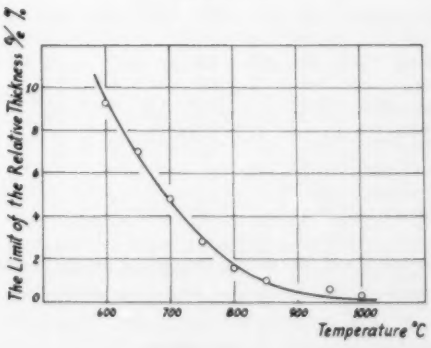

Fig. 2

[1] Dept. of Metallurgy, School of Chemical Engineering, University of Concepción, Concepción, Chile.

The partial results reported in this discussion are relative to the research corresponding to Contract No. 43 between the discussor and the "Consejo de Investigación Científica" of the "Universidad de Concepción," Chile.

by the authors may be due principally to the method used for the determination in the scales of the CuO/Cu_2O ratio, which was fundamentally a bulk x-ray analytical procedure and for this reason did not take into account the localized irregularities of the thickness of the scale. In any case, we would like to know if the authors checked the precision of the x-ray method proper through analyses of synthetic mixtures. For the determination of the layers in the scale we preferred a refined technique of the micrographic method, as used by us in the solution of a similar problem previously.[2]

D. W. Bridges, J. P. Baur, G. S. Baur, and W. M. Fassell, Jr.: We wish to thank Prof. Paidassi for his comments and interest in our work. In the last paragraph of his discussion, Professor Paidassi comments on the advisability of the use of quantitative x-ray diffraction techniques to determine the amounts of CuO and Cu_2O present, and whether or not such a method was checked through analysis of synthetic mixtures. The method as outlined in the paper consisted of mixing known weights of CuO (Baker & Adamson reagent grade) and Cu_2O (made by oxidation of OFHC copper at 1000°C and 20 mm-Hg oxygen pressure) with a known weight of high grade CaO. This technique, known as the "addition of an internal standard" has long been accepted as a most satisfactory method of quantitative analysis. Its relative merits as compared to the photomicrographic method described by Professor Paidassi and other methods[2,4] is at present speculative. However, the authors believe that the "localized irregularities of the thickness of the scale" would affect the photomicrographic method as much if not more than the x-ray method.

It is interesting to note the over-all agreement between the results of Professor Paidassi and those of the authors. These results with those of other investigators are summarized in Table I.

The authors' results can best be summarized by rephrasing a portion of the abstract. Quantitative x-ray diffraction analysis of the scale disclosed approximately 4% CuO at high and low pressures for temperatures above 800°C. Below 750°C, high pressure coatings contained 10% CuO while subatmospheric coatings continued to assay about 4% CuO. The effect of the relative amounts of the oxides present on the parabolic rate constant is shown in Fig. 1 [of the paper]. Average values of the parabolic rate constants at temperatures and oxygen pressures at which the relative amount of CuO is 4% can be connected with a "fair" straight line, while deviations occur for those points at temperatures and oxygen pressures where the amount of CuO present is greater. This evidence is believed to further the postulate that diffusion of cuprous ions through the Cu_2O layer is the rate-determining step.

Table I. Per cent CuO in the oxide layer formed at various temperatures and 1 atm air

	Temp, °C							
Investigation	600	650	700	750	800	850	900	950
Valensi[3]	60		30			7	5	
Tylecote[4]	30	20	15			10		
Paidassi	9	7	4.5		1.8	1.0		0.5
Bridges, *et al.*	3.6*		2.4*	6.6*	4.1*	3.7*	3.2*	
Average of 2-hr oxidation period experiments	10.0**		11.5**	7.3**				

* Average % CuO for samples oxidized at oxygen pressures less than 1 atm.
** Average % CuO for samples oxidized at oxygen pressures in excess of 1 atm.

[2] J. Paidassi, *Rev. mét.*, 52, 869 (1955).

[3] G. Valensi, Proceedings of the Pittsburgh International Conference on Surface Reactions, p. 156, Corrosion Publishing Co., Pittsburgh (1948).

[4] R. F. Tylecote, *Metallurgia*, 53, 191 (1956).

Cathode Ray Tube Screen Charging and Conditions Leading to Positive Ion Deterioration

A. B. Laponsky, M. J. Ozeroff, W. A. Thornton, and J. R. Young (pp. 498-507, Vol. 103)

A. B. McFarlane[5]**:** The authors give results showing that the sticking potential of the luminescent screen used in television tubes exceeds 25 kv. Early screens for this purpose were known to stick at various potentials up to 15 kv[6,7,8] but usually well below this value. Therefore, these latest results show a very great improvement. They apparently attribute this improvement to the "roughness" of the surface, but early screens also had rough surfaces. It is, therefore, difficult to explain the improvement merely in terms of "roughness" and I should like the authors' comments on this point.

I would add that the *British Journal of Applied Physics* has published a paper entitled "The Movement of the Second Crossover Potential of Insulators."[9] In it I give results showing that by suitable treatment[10] of luminescent screen the second crossover potential (about 7 kv for zero field) may be made very field dependent, so much so that negligible signs of sticking are apparent up to 20 kv and possibly beyond. I have not yet established the exact explanation of this phenomenon, and therefore I am particularly interested in the authors' comments.

Contact Electroluminescence

Willi Lehmann (pp. 45-50, Vol. 104)

W. Lehmann: In the paper I unfortunately omitted reference to the fact that Mr. Luke Thorington, formerly of this laboratory,[11] first reported at the 1952 Spring Meeting of The Electrochemical Society in Pittsburgh that "It has been observed that a purely mechanical mixture of certain phosphors in vacuum may be electroluminescent while the separate phosphors are not." The effect observed by

[5] Kingsmead Works, Electronic Tubes Ltd., High Wycombe, Bucks, England.

[6] H. Moss, "Advances in Electronics," Vol. II, p. 1, Academic Press, Inc., New York (1949).

[7] H. W. Leverenz, "Luminescence of Solids," p. 437, John Wiley & Sons, Inc., New York (1950).

[8] A. B. McFarlane, M.Sc. Thesis, Engineering, London University (1955).

[9] A. B. McFarlane, *Brit. J. App. Phys.*, 8, 248 (1957).

[10] (a) Coating the electron-bombarded side with a layer of MgO smoke; (b) settling screen in concentrated potassium silicate solutions.

[11] Lamp Div., Westinghouse Electric Corp., Bloomfield, N. J.

Thorington was restricted to high vacuum, however, and any admission of gases or of other embedding materials either greatly reduced or completely destroyed the effect.

Electrochemical Polarization, 1. A Theoretical Analysis of the Shape of Polarization Curves

M. Stern and A. L. Geary (pp. 56-63, Vol. 104)

E. W. Haycock[12]: The paper by Stern and Geary is a welcome and timely contribution to the theoretical study of polarization phenomena at electrode surfaces. Their reference to the recent paper by Logan, however, projects the authors into the realm of practical applications of the shape of polarization curves. In this regard, the following comments are offered. These comments are made for two reasons. First, to counteract the possible impression that the "current-potential break" criterion, as widely used in cathodic protection applications, has little or no theoretical basis; second, to clarify understanding of the conditions most usually encountered in the practical application of the "break" criterion.

The choice of the word "break" to describe a discontinuity or transition region in the polarization curves perhaps is unfortunate. However, the problem is one of semantics rather than science and in cathodic protection usage no real misunderstanding exists.

The drawing of a straight line through a few experimental points is usually recognized as being scientifically hazardous. In many cases it can be explained as being due to an optimism which arises from necessity rather than misunderstanding.

The requirement for the successful application of the "break" criterion to determine complete cathodic protection has been clearly stated by Mears and co-workers.[13] This is that the corrosion system be under cathodic control.

The widest application of cathodic protection at present is in the mitigation of soil corrosion. This corrosion system, in the majority of cases, is best described as a series of differential aeration cells in a nearly neutral environment. In low resistivity soils the corrosion is cathodically controlled by the availability of oxygen at the cathodic areas. As cathodic protection current is applied and the current is reached at which complete protection is achieved, the net anode reaction changes from the solution of iron to, most probably, the evolution of hydrogen. If the system is under complete cathodic control, this also will coincide with a change in the reaction at the cathode. The oxidizing capacity of the oxygen depolarizer at the cathode is being balanced by the electron flux from an external source, and any further increase in the protection current will result in the evolution of hydrogen. Since the anode and cathode reactions both change as the system is protected, a "break" or transition region in the polarization curves is expected at this point.

If the system is under anodic rather than cathodic control, it is doubtful if the transition due to the change in anode reaction could be detected experimentally in a practical case by measuring the corrosion potential as a function of the cathodic protection current applied. Similarly, the transition corresponding to protection would be masked if the system were under resistance control and to a lesser extent if an *IR* term were incorporated in the measurement of the corrosion potential due to the position of the reference electrode. In soil corrosion systems which are nearly neutral, the hydrogen ion concentration polarization effects referred to by Stern and Geary usually occur at a low current density compared to the corrosion and protection current densities involved and hence do not interfere with the shape of the polarization curve in the region of interest.

In reviewing Logan's comparison of the criteria of protection, it is interesting to note that the other criteria considered have much less scientific basis than the "break" criterion. The discrepancies reported by Logan are most probably due to reasons other than those suggested by the paper under discussion.

M. Stern: Mr. Haycock's comments provide a welcomed opportunity to discuss one of the practical applications of polarization measurements. The author believes that there is no theoretical basis for the "current-potential break" criterion, as widely used in cathodic protection applications, and is disappointed in his ability to make the reason for this view clear to Mr. Haycock in the text of the paper under discussion. An additional paper on this subject[14] illustrates the reasoning further. In particular, Case VIII, where the corrosion rate is determined by a limiting diffusion current, can be considered close to the condition existing during corrosion in some soils. A study of this will show that any break criterion is completely inaccurate.

The work of Mears and associates referred to by Mr. Haycock requires that a system be under *complete* cathodic control. More important, however, this work contains an assumption which is not often appreciated. This assumption requires that all anodes remain anodes during application of cathodic current and suddenly revert to cathodes at the equilibrium metal potential. Such a requirement has neither a theoretical basis nor (to the author's knowledge) experimental support. Theoretical and experimental work by many investigators shows that polarizing a redox system through the equilibrium potential does not necessarily result in a discontinuity.

Concerning the practical application of the "break criterion," it is doubtful that any real system has the requirements described above. Corroding iron in soils is not under complete cathodic control, but should be considered under mixed and resistance control. Also, in field measurements, *IR* terms are often the most important part of polarization observations, and obviously have a significant influence on curve shape. The recent contribution to N.A.C.E. Committee T-2C on Minimum Current Requirements by Sudrabin and Ringer[15] supports the au-

[12] Shell Development Co., Emeryville, Calif.

[13] *See*, for example, R. B. Mears and J. M. Bialosky, "Cathodic Protection," p. 37, National Association of Corrosion Engineers (1947).

[14] M. Stern, *This Journal*, **104**, 645 (1957).

[15] L. P. Sudrabin and F. W. Ringer, *Corrosion*, **13**, 351 (1957).

thor's contention that this method is not reliable. It is significant to note that this committee report actually refers to the method as the "apparent" break relation.

There are so many reported cases where the "apparent" break method does not work, and there are so many conditions where the method cannot work, that it is difficult to understand why it is used. Other criteria are available which are more accurate, have a sounder foundation in theory, and are easier to use.

Thermogalvanic Potentials and Currents at Aluminum Surfaces in Industrial Water

Edgar C. Pitzer (pp. 70-74, Vol. 104)

R. A. Hine[16]: This investigation is of great interest since we have made rather similar measurements of potentials in studying the formation of Boehmite films on Al immersed in distilled water at elevated temperatures. In this case the potential difference between the Al specimen and a Pt electrode also immersed in the water was measured directly. At 20°C the potential of the Al was of the order of −0.5 to −0.6 v, and slowly became more base with increasing temperature until at 80°-90°C a rapid change took place to a maximum of −1.25 v at boiling; on continued boiling, the potential became slightly less base, and after ½ hr remained fairly steady at about −0.95 v. The maximum current densities on the anode were about 3×10^{-4} amp/cm^2.

There obviously is some correspondence between these results and those of the author using supply water. The formation of Boehmite films on Al has been extensively studied by Altenpohl.[17] In distilled water, reaction visibly appears to start at about 80°-90°C and is accompanied by evolution of hydrogen. The corrosion product has been definitely established as Boehmite, $Al_2O_3 \cdot H_2O$ (or $AlO \cdot OH$), by x-ray diffraction. It is formed as a continuous adherent film, and hence its growth rate is of an exponential type; after 1 hr's immersion at boiling, the thickness is usually of the order of 0.5 μ, and immersion for many hours is required to obtain a thickness of 2 μ, this being about the maximum thickness obtainable. It is also clear that the Boehmite film produced in distilled water is protective in nature, and Al utensils processed to produce such a film have markedly increased resistance to corrosion. In less pure water, such as supply waters, Boehmite films are also produced, but usually they are more porous and less protective than with distilled water and they may be discolored by the inclusion of small particles of unoxidized Al metal in the film; in tap water buffered to about pH 10, for example with ammonia, very much thicker Boehmite films are produced.

In view of these facts it is difficult in the case of distilled water to regard the phenomenon of the potential change to a value some 0.6 v more negative as an impairment of the protective film on the surface; on the contrary, in fact, it is known that the change is accompanied by the formation of a highly protective film. The formation of this film is probably indicated by the potential change from −1.25 v to −0.95 v during continued immersion at the boiling point observed in our results. Further, the potential of the Al after formation of the film, and after allowing to cool again to 20°C, was some 0.1 v more noble than at the commencement of the experiment. In the author's experiments the films produced in supply water were probably not protective since no potential change in the positive direction was noted on prolonged exposure. Altenpohl states that in such cases the Boehmite produced is more in the nature of a corrosion product than a protective film.

There are many questions unanswered about the mechanism of this reaction of Al with heated water, but it is generally assumed that Al^{+++} ions diffuse through the film to react with OH^- ions, and it is clear that the change of K_w with temperature may have an important bearing on this aspect of the matter.

[16] Aluminium Labs. Ltd., Banbury, Oscon, England.

[17] D. Altenpohl, *Aluminium*, 33, [2], 78 (1957).

Electrochemical Properties of a Cation-Transfer Membrane

N. W. Rosenberg, J. H. B. George, and W. D. Potter (pp. 111-115, Vol. 104)

Reinhard H. Beutner[18]: Drs. Rosenberg, George, and Potter explain the electromotive forces by ion transfer and ion mobilities in the hypothetical pores. They disregard the possibility that potential differences exist at the phase boundary (or contact) surface of the Nepton membrane on both sides where the membrane is in contact with aqueous solutions.

N. W. Rosenberg and J. H. B. George: Dr. Beutner has two reservations with respect to the membrane model suggested by the authors: namely, mass transfer through pores, and emf caused by such mass transfer.

A membrane of the type under discussion is formed from a cross-linked organic polymer, which, prior to sulfonation, has substantially no permeability to water or to ions. After sulfonation, which provides negative exchange sites on the polymer, the membrane will swell in aqueous systems, by absorption of water, to an extent determined by the cross-linking. Thus, previous workers in the field (and the authors) describe the resin as a network of hydrocarbon chains, "welded" at intervals of 10-20Å by cross chains, and permeable to water and to ions through the interstices of the network, defined as pores. The level of porosity in ion exchange resins has been reported by Kressman[19] and Partridge and Brimley[20] by measurement of capacity for a series of ions of increasing size, and noting a complete loss of capacity for ions of greater than 10-20Å diameter.

With respect to selective mass transfer as a source of emf, we have used the conventional Nernst equation for electrochemical potential of a cell with membrane transference, recently critically re-ex-

[18] Des Moines Still College of Osteopathy and Surgery, Des Moines 9, Iowa.

[19] T. R. E. Kressman, *J. Phys. Chem.*, 56, 118 (1952).

[20] S. M. Partridge and R. C. Brimley, *Biochem. J. (London)*, 51, 628 (1952).

amined by Scatchard[21] in view of water transport. Potential differences (other than those considered by the Nernst equation) may well exist at a single-phase boundary surface but cannot be measured since a membrane separating two solutions has two such surfaces and an equal and opposite potential will, of course, exist at the second surface, cancelling that at the first surface.

Current Distribution in Galvanic Cells Involving Natural Convection

Carl Wagner (pp. 129-131, Vol. 104)

E. M. Sparrow[22]: Professor Wagner's interesting paper is a clear demonstration of the advances which may be made by application of results which were initially derived in a rather different field of scientific research. By using the analogy between the transfer processes involved, results for free convection heat transfer were applied to the mass transfer problem.

It is the purpose of this discussion to present some additional results, initially found for heat transfer, which may be useful in extending Professor Wagner's analysis. Suppose that instead of treating the case where the rate of mass transfer of Cu ions (j) is uniform over the electrode, the more general situation where $j \sim x^r$ is considered. (The notation is identical to that of the discussed paper.) Then, the value of Δc at a distance x from the leading edge of the electrode is[23]

$$\Delta c = 1.31 \frac{jx}{D} \left[\frac{\left(\frac{35}{12} Sc + 1\right)(r+1) + \frac{4}{3}}{(r+1)\, Sc^2\, Gr_x} \right]^{1/5} \qquad \text{(I)}$$

When $r = 0$, this equation corresponds to Eq. (IV) in the discussed paper.[24] It is expected that Eq. (I) will be sufficiently accurate for most applications for $r > -0.5$.

Another situation of possible interest is that in which Δc is prescribed and it is desired to compute j. For the case where $\Delta c \sim x^n$, the variation of j with x is given by[23]

$$j = 0.715 \mid \Delta c \mid \frac{D}{x} \left[\frac{\left(\frac{5n+3}{4}\right)^2 Sc^2\, Gr_x}{\left(\frac{35}{12} Sc + 1\right)\left(\frac{5n+3}{4}\right) + \frac{4}{3}} \right]^{1/4} \qquad \text{(II)}$$

where

$$Gr_x = \frac{g\beta' \mid \Delta c \mid x^3}{\nu^2}$$

Eq. (II) is expected to be of adequate accuracy for $n > -0.2$.

[21] G. Scatchard, *J. Am. Chem. Soc.*, 75, 2883 (1953).

[22] NACA Lewis Lab., Cleveland 11, Ohio.

[23] M. Tribus, Discussion of A.S.M.E. paper 57-SA-3, "Similar Solutions for Free Convection from a Nonisothermal Vertical Plate" by E. M. Sparrow and J. L. Gregg, to be published in *Trans. A.S.M.E.*, 80 (1958).

[24] There is a printing error in Eq. (IV) of the discussed paper in that $(0.8 + Sc)/Sc^2\, Gr_x^4$ should be raised to the one-fifth power.

Notes on Hydrogen Overvoltage, I. Maximum Concentration of Atomic Hydrogen on the Surface of a Working Cathode

Hugh W. Salzberg and Sigmund Schuldiner (pp. 319-321, Vol. 104)

H. W. Salzberg and S. Schuldiner: The following corrections should be made to the equations on page 320 of the paper.

(*A*) Eq. (I): change F^2_H to f^2_H.

(*B*) t in equations should be changed to T.

(*C*) Expressions on right-hand sides for r_{mobile} should be multiplied by 2.

(*D*) The term $H^2\, \sigma\, (kT/h)^{1/2}$ immediately following Eq. (II*a*) should be changed to read $2H^2\, \sigma\, (kT/m)^{1/2}$.

Preparation of Thorium Bismuth Dispersions from Electrolytic Thorium

M. E. Sibert and M. A. Steinberg (pp. 374-378, Vol. 104)

R. P. Marshall[25]: Reference is made to the conditions required for electrolysis to yield a fine particle size, viz., high current density, low temperature, and high Th content. In the next paragraph reference is made to the melt being exhausted of Th content. Therefore these two statements are incompatible because, even though a high starting Th content is used, ultimately this is to be nearly all removed, when the progressively lowering Th content should affect the particular size of the deposit.

The authors refer to a temperature of 550°-650°C. This probably is satisfactory in the presence of 10% of Th, but, when the melt has been stripped of $ThCl_4$, pure NaCl will be left which has a melting point of 801°C. It is therefore not clear from the authors' comments for how long they maintained the temperature of 550°-650°C to which they refer.

The term "high current density" is correlated to a cathode current density of 200-300 amp/dm^{-2}. In my opinion, the cathode current density can only effectively apply to the starting current density and is very rapidly altered as the dendritic deposit grows. Therefore the starting cathode current density cannot have a serious influence on the particular size of the deposit if any appreciable quantity of Th is being deposited. Incidentally, I was surprised that the authors consider a cathode current density of the above magnitude to be high, since from my practical experience cathode current densities of 1000 amp/dm^{-2} are normal and frequently current densities much in excess of this have been applied to fused alkali chloride electrolytes.

I shall be interested in the authors' comments on the mechanism of the purification of $ThCl_4$ melts by the passing of HCl gas through them.

M. E. Sibert: In reference to the statement concerning exhaustion of Th content of the bath during electrolysis at 550°-650°C, this was possible for the majority of runs where eutectic melts such as KCl-NaCl or NaCl-$CaCl_2$ were employed. Obviously, if NaCl were used alone as a solvent, the temperature

[25] T. A. Dept., Impregnated Diamond Products Ltd., Tuffley Crescent, Gloucester, England.

would rise to 801°C (mp of NaCl) when the Th content is exhausted as Mr. Marshall states. In most cases the melt was not exhausted of Th content; melts contained 110-225 g Th, and, in general, 55-165 g were deposited out.

Mr. Marshall is correct in his statement regarding cathode current density. All figures shown are starting cathode current densities based on initial cathode areas. The values of 200-300 amp/dm^2 are termed "high" only in comparison with the "low" range of <50 amp/dm^2 also employed in the work.

Starting cathode current density does have a marked effect on average particle size of the deposit. Raising the starting cathode current density from 50 to 250 amp/dm^2 will reduce the average particle size of the deposit by 50% or more.

The apparent mechanism of purification of $ThCl_4$-bearing melts by HCl sparging is a straightforward one although the actual mechanism is possibly quite complex. It appears that oxidic impurities in the melt (e.g., ThO_2, $ThOCl_2$, etc.) are chlorinated and moisture eliminated (at 800°-900°C)

$$\text{e.g., } ThOCl_2 + 2HCl \rightarrow ThCl_4 + \overline{H_2O}$$

This has been indicated by melt analyses plus analysis and dew point measurements on effluent gases from the cell during sparging.

Manuscripts and Abstracts for Spring 1958 Meeting

Papers are now being solicited for the Spring 1958 Meeting of the Society, to be held at the Statler Hotel in New York City, April 27, 28, 29, 30, and May 1, 1958. Technical Sessions probably will be scheduled on Electric Insulation, Electronics, Electrothermics and Metallurgy, Industrial Electrolytics, and Theoretical Electrochemistry (including a symposium on "Electrokinetic and Membrane Phenomena").

To be considered for this meeting, triplicate copies of abstracts *(not to exceed 75 words in length)* must be received at Society Headquarters, 1860 Broadway, New York 23, N. Y., *not later than January 2, 1958. Please indicate on abstract for which Division's symposium the paper is to be scheduled.* Complete manuscripts should be sent to the Managing Editor of the JOURNAL at 1860 Broadway, New York 23, N. Y.

* * *

The Fall 1958 Meeting will be held in Ottawa, Canada, September 28, 29, 30, October 1, and 2, 1958, at the Chateau Laurier.

Current Affairs

News Notes in the Electrochemical Field

Nominations for 1958 Acheson Award

Charles L. Faust, Chairman of the Acheson Medal Award Committee, would like to receive suggestions for possible candidates for the next Acheson Medal Award, to be made in the fall of 1958.

The procedure to be followed by the membership, taken from the Rules Governing the Award of the Acheson Medal, is given below.

1. Nominations shall be accepted from the membership at large.

2. All nominations, whether made by a member of the Nominating Committee or by any other member of the Society, must be accompanied by a full record of qualifications of the nominee for the award. Such supporting documents from friends of the candidate or from his organization shall be in order.

3. The nominator must assume the responsibility for providing the Chairman of the Nominating Committee with nine copies of the supporting documents, one for each member.

Nominations must be sent to the Chairman not later than March 1 of the year in which the medal is awarded and nominations will be considered closed after that date.

All nominations of candidates for the medal shall be continued in force for a period of two consecutive awards of the medal. Any unsuccessful candidate may be renominated in the usual manner for any subsequent Medal award.

Correspondence should be addressed to Charles L. Faust, Battelle Memorial Institute, 505 King Ave., Columbus 1, Ohio.

Aluminum Soldering Simplified

Simple and effective techniques for soldering aluminum and its alloys as well as galvanized metals have been developed by G. M. Bouton and P. R. White, metallurgists at Bell Telephone Labs. These techniques employ an inexpensive and stable zinc base alloy as a preferred solder, and no flux or vigorous abrasion is necessary. Joints in aluminum made by these methods are stronger than commercial aluminum itself.

Because of their simplicity, the techniques are expected to find widespread applications both in industry and in the home workshop.

Long-term stability of the soldered joint is assured by the rigid exclusion from the high purity zinc base alloy of deleterious elements such as lead, tin, bismuth, and cadmium to prevent intergranular corrosion. A fraction of a per cent of magnesium may be added to enhance its stability, and up to several per cent of aluminum may be included.

Temperature Range of *p*H Scale Extended

The National Bureau of Standards has recently extended the temperature range in which *p*H standards are certified. Formerly the *p*H scale was accurately determined only between 0° and 60°C; now standard *p*H samples are available from 0° to 95°C. This extension was made possible by the work of V. E. Bower and R. G. Bates of the Bureau's physical chemistry laboratories.

The standard *p*H scale was set up to meet the need for accurate measurement of acidity and basicity in aqueous solutions. In the manufacture of many commercial products—for example, paper, textiles, dyes, and ceramics—the rapidity and efficiency of the processes depend upon the accuracy with which *p*H can be controlled. The NBS standard *p*H scale is defined in terms of several fixed points in much the same manner as is the International Temperature Scale. The primary standards of the *p*H scale are solutions whose *p*H values are only slightly affected by dilution or by accidental contamination with traces of acid or alkali from the walls of the container or from the atmosphere. The substances from which the standard solutions are prepared are, in turn, stable materials which may be obtained as certified standard samples from the Bureau.

In order to assign values to the NBS standards, the electromotive force of cells employing the standards as electrolytes was measured. These cells are specially designed, utilizing the highly reproducible hydrogen and silver—silver chloride electrodes. Computation of *p*H is based upon several reasonable assumed relationships between ionic activities and mean activities. Until recently, data for the standard potential of the silver—silver chloride electrode above 60°C were not available, so, in spite of the demands of industry, an extension of the *p*H scale to temperatures beyond 60° was not possible.

A recent determination of the standard potential of the silver—silver chloride electrode included measurements from 0° to 95°C. With these new data it became possible to assign *p*H values over the extended range of temperatures to five of the six substances used as standards. The sixth substance recently recommended as a highly alkaline standard was not certified for the extended temperature range.

Applications for Science Fellowships Invited by National Science Foundation

The National Science Foundation has announced that applications are being accepted in four National Science Foundation fellowship programs for advanced study and research in the natural sciences. The four fellowship programs are: *(a)* a predoctoral fellowship program for which college seniors and graduate science students may apply; *(b)* a postdoctoral fellowship program for scientists who have already received the doctoral degree; *(c)* a senior postdoctoral fellowship program for candidates who have held the science doctorate for a minimum of five years; and *(d)* a science faculty fellowship program for college teachers of science who wish to improve their competence as teachers.

Approximately 1000 awards will be made in the Foundation fellowship programs in March 1958. National Science Foundation fellowships are awarded to American citizens who have shown special aptitude in science and who will begin

or continue their studies at the graduate or postdoctoral level. Under the broadened program, fellowships will be awarded in the mathematical, physical, medical, biological, engineering, and other sciences, including anthropology, psychology (other than clinical), geography, certain interdisciplinary fields, and areas of convergence between the natural and social sciences.

Fellows will be selected on the basis of ability as evidenced by letters of recommendation, academic records, and other evidence of attainment. Applicants for the predoctoral fellowships are required to take the Graduate Record Examination. Candidates' qualifications will be evaluated by carefully chosen panels of scientists established by the National Academy of Sciences—National Research Council and the Association of American Colleges. Final selection of Fellows will be made by the National Science Foundation.

Stipends for National Science Foundation fellowships vary with the academic status of the Fellows. First year Fellows, students entering graduate school for the first time or those who have had less than one year of graduate study, will receive annual stipends of $1600. Fellows who need one final academic year of training for the doctor's degree will receive annual stipends of $2000. Fellows between these groups will receive stipends at the rate of $1800 annually. The stipends for regular postdoctoral Fellows will be $3800 per year. Dependency allowances will be made to all married Fellows. Tuition and laboratory fees and limited travel allowance will also be provided.

Senior postdoctoral Fellows and Science Faculty Fellows are awarded stipends adjusted to match as closely as feasible the regular salaries of the award recipients up to a maximum of $10,000 per year. A travel allowance is also usually made available.

National Science Foundation Fellows may attend any accredited nonprofit institution of higher education in the United States or similar institution abroad.

Applications for the 1958-59 National Science Foundation graduate and regular postdoctoral fellowship program may be obtained from the Fellowship Office, National Academy of Sciences—National Research Council, 2101 Constitution Ave., N.W., Washington 25, D. C. The closing dates for receipt of applications are December 23, 1957, for postdoctoral applicants, and January 3, 1958, for graduate students working toward advanced degrees in science. The selections will be announced on March 15, 1958.

Applications for the Senior Postdoctoral and the Science Faculty fellowships may be obtained from the Division of Scientific Personnel and Education, National Science Foundation, Washington 25, D. C. Completed material must be received not later than January 13, 1958. Selections will be announced on March 18 and 20, 1958.

Linde Continues Expansion of Tonawanda Laboratories

Plans for extensive new facilities for the company's Tonawanda Research Labs. have been announced by Linde Co., Div. of Union Carbide Corp.

At the present time a high-pressure laboratory, metallurgical laboratory,

Now Available

the 1955 Issue of

Semiconductor Abstracts

Abstracts of Literature on Semiconducting and Luminescent Materials and Their Applications

Compiled by Battelle Memorial Institute and Sponsored by The Electrochemical Society, Inc.

The Electrochemical Society is pleased to announce the availability of the 1955 Issue of Semiconductor Abstracts. This issue represents the third year of sponsorship of the Abstracts by the Society. For 1955 the Abstracts have been bound in a hard cover which is more in keeping with its intended use as a desk reference book.

In addition, the coverage has been extended to include all of the papers presented at the Society's two annual meetings. More information is presented in this issue on applications of materials (transistors, rectifiers, cathodes, TV tubes, etc.). This added coverage, plus the increased volume of published literature, has increased the size of the 1955 Issue. For 1955 there are 1258 abstracts and 322 pages, as compared to 753 abstracts in 1954.

To assist in locating specific subjects, a comprehensive cross index, subject index, and an author index are provided. Subjects covered include: germanium, silicon, selenium, compound semiconductors (InSb, GaAs, AlSb), sulfides, selenides, tellurides, oxides, halides, phosphors, organics, and theory.

To obtain your copy of the 1955 Semiconductor Abstracts, please fill in the coupon below and mail direct to the publisher, John Wiley & Sons, Inc., 440 Fourth Ave., New York 16, N. Y. *A 33 1/3% discount is offered to Electrochemical Society members only and can be obtained by mailing the coupon to Society Headquarters, 1860 Broadway, New York 23, N. Y.*

The 1953 and 1954 Issues of the Abstracts are also available and can be obtained at the member discount.

Electrochemical Society Abstracts Series

Please send me the following volume(s) of SEMICONDUCTOR ABSTRACTS:

(33 1/3% discount offered to ECS Members only)

☐ 1955 Issue, Volume III, $10.00

☐ 1954 Issue, Volume II, $ 5.00

☐ 1953 Issue, Volume I, $ 5.00

Name .....

Address .....

City ..... Zone ..... State .....

a new hydrocarbon storage building, and a new services building are to be constructed.

Union Carbide Announces Plans for Graphite Electrode Plant Near Monterrey, Mexico

A new graphite electrode plant being built near Monterrey, Mexico, by Electrodos Nacionales, S.A., an affiliate of Union Carbide Corp., is scheduled to start production in 1958. Company representatives met recently with the Governor of the Mexican State of Nuevo Leon to report completion of arrangements for power, water, and gas requirements, as well as progress on site preparation and equipment procurement. The 200-acre plant site of Electrodos Nacionales, S.A., is located in Apodaca, a small town approximately nine miles from Monterrey.

The new factory will serve the electric-furnace steel, ferroalloy, and electrochemical industries as well as provide materials essential to the nuclear power development of Mexico. Plant capacity will be capable of meeting Mexican requirements for these graphite products for a number of years to come. It is anticipated that a portion of the production will be exported, thus improving Mexico's foreign exchange position.

American Potash Participates in High Energy Fuel Program

Formation of a new company to participate in the Government's high energy fuel program has been announced by American Potash & Chemical Corp.

The new company, AFN, Inc., is owned one-third each by American Potash, Food Machinery & Chemical Corp., and National Distillers & Chemical Corp. American Potash has been appointed operator of the company, whose initial work will be carried on at Henderson, Nev.

AFN, Inc., has been awarded an Air Force contract covering process development and semi-pilot plant work in the high energy fuel field. The fuel will be boron-based, but details beyond that are classified.

Hooker, Foote Jointly Explore High Energy Fuel Venture

Hooker Electrochemical Co., Niagara Falls, N. Y., and Foote Mineral Co., Philadelphia, Pa., have jointly announced that they are together exploring possibilities for the development, production, and sale of components of high energy fuels. Currently, their interests are confined to lithium perchlorate and ammonium perchlorate, materials which act as oxidizers in fuels for rockets and missiles, but studies may be extended to other high energy fuel components later. The joint announcement was made by R. Lindley Murray and Gordon H. Chambers, board chairmen of Hooker and Foote.

Allied Chemical & Dye Doubles Production of Chlorine and Caustic Soda

Completion of the expansion program doubling the capacity of its Brunswick, Ga., mercury cell chlorine-caustic soda plant recently was announced by Solvay Process Div., Allied Chemical & Dye Corp.

With the start-up of the new facilities, Solvay Process Div. is in a position to supply additional chlorine and caustic soda from its new chemical producing center at Brunswick to meet the current heavy demand for these products, particularly in the South. Liquid caustic soda (50% NaOH) is available in both regular and rayon grades, and shipments are being made by tank car or barge.

Pennsalt Chemicals Selects Canadian Plant Site

Pennsalt Chemicals Corp. has selected a ten-acre area near Oakville, Ont., as the site of its first plant in Canada, President William P. Drake has announced. As a component of Pennsalt Chemicals of Canada, Ltd., a wholly owned subsidiary, the new unit will facilitate the distribution of Pennsalt chemical specialties not now available in eastern Canada and will make possible the extension and improvement of customer services. Initial product lines will include metal processing chemicals, sanitizing agents used in food processing and dairy plant operations, laundry and dry cleaning chemicals, and numerous other Pennsalt and "Sharples" brand specialty products.

Correction

The following corrections should be made in the article by H. P. Rothbaum, "The Composition of Copper Complexes in Cuprocyanide Solutions," which appeared on pp. 682-686 of the November 1957 JOURNAL.

Page 682, line 3 of the Abstract: $Cu(Cn)^{=}_{3}$ should read $Cu(CN)^{=}_{3}$.

Page 684, column 1, equation on line 3: πo should read E_o.

Page 684, column 2, line 3: $k_1 \times 10^{16}$ should read $k_1 = 10^{16}$.

Page 684, column 2, lines 35 and 40: πo should read E_o.

Volumes Wanted

If any member of the Society wishes to sell his copies of Bound Volumes of the JOURNAL for 1950 (Vol. 97) and 1951 (Vol. 98), please communicate direct with Col. George C. Cox, 3711 Washington Ave., S.E., Charleston 4, W. Va.

Division News

Theoretical Electrochemistry Division

Spring 1958 Symposium

A symposium on **Electrokinetic and Membrane Phenomena** is being arranged by the Theoretical Electrochemistry Division for the meeting of the Society to be held in New York, N. Y., April 27 to May 1, 1958. The program is to include invited and contributed papers.

The committee arranging this program is: *Chairman*, Dr. Paul Delahay, Louisiana State University, Baton Rouge, La.; Professor J. J. Hermanns, Rijks University, Leiden, Netherlands; Dr. R. M. Hurd, University of Texas, Austin 12, Texas; Dr. T. Shedlovsky, The Rockefeller Institute for Medical Research, New York 21, N. Y.

Abstracts (not exceeding 75 words in length) of contributed and invited papers for this symposium and papers for the general sessions of the Theoretical Division should be submitted to the Secretary's Office, 1860 Broadway, New York 23, N. Y., in triplicate, *not later than January 2, 1958.*

Ralph Roberts, *Secretary-Treasurer*

Section News

Niagara Falls Section

On August 8, 9, and 10, the Niagara Falls Section was host to 15 French electrochemical students from the University of Grenoble. The students were taken into the homes of Society members to become better acquainted with the American way of life. Plant trips were arranged to the Metals Research Labs. of Union Carbide Co., Electro Metallurgical Co., Hooker Electrochemical Co., Carborundum Co., and generation facilities Ontario Hydroelectric Power Commission and North American Cyanamid.

L. A. Stoyell

New York Metropolitan Section

The Metropolitan Section held its first meeting of the year in New York on October 2. Mr. Kenneth B. Smith of the Bell Telephone Labs. spoke on "Transistor Materials." He first dis-

cussed the properties of various semiconductor materials. He stressed the growing importance of intermetallics, particularly In-P and Ga-As. The latter two materials have energy gaps comparable to that of Si and electron mobilities comparable to that of Ge. The speaker discussed the cost, applications, and properties of six available grades of Si. An extended discussion of methods of forming *N-P* and *N-P-N* junctions led to a presentation of recent Bell developments. Among these are application of thermo-compression bonding, and development of transistors with 700 megacycle cut-off and 10 db gain over a 200 megacycle bandwidth, yet occupying a volume of only 40 × 50 × 10 mils.

E. B. Saubestre

San Francisco Section

The speaker at the September meeting of the San Francisco Section was Dr. E. R. Parker, Professor of Metallurgy, Dept. of Mineral Technology, University of California at Berkeley. Dr. Parker spoke about "Ductile Ceramics."

In the 1930's it was shown that sodium chloride crystals could be deformed without breaking if they were immersed in water. From this and other experiments conducted at about the same time, the investigators were led to believe that immersing the crystals caused a solution of the surface layer of the crystals, this layer containing the surface cracks which were the nuclei for fracture formation. In some recent work, Dr. Parker has shown that materials like NaCl, KCl, and CsCl, when formed into nearly perfect crystals, would be ductile at room temperature, when the crystals were freshly cleaned. On exposure to air these same crystals became brittle within a very short period of time (of the order of 30 sec). Apparently this brittleness is related to an adsorbed surface layer of some materials, shown in many cases to be nitrogen. Magnesium oxide can be made either brittle or ductile depending on the purity of the starting material. The mechanism of this ductile-brittle change is not understood at the present time. Freshly cleaned crystals held in a vacuum, in argon, or under oil do remain ductile indefinitely. Samples of these materials, approximately 0.1 in. x 0.1 in. x 1 in. long, were shown at the meeting after having been twisted or bent into an S-shape while they were still in the ductile form.

This work opens up an entirely new field for use of materials, i.e., by machining the ductile ceramics one could make many pieces of apparatus which cannot now be made with the same material in the usual brittle form. Dr. Parker is continuing the investigation into the basic causes of this ductile-brittle change in materials. Commercial applications of this material will be left to others to investigate.

Bernard Porter,
Vice-Chairman

New Members

In October 1957 the following were approved for membership in The Electrochemical Society by the Admissions Committee:

Active Members Sponsored by a Sustaining Member

Janet Vernon, Minnesota Mining & Manufacturing Co., 2301 Hudson Rd., St. Paul 6, Minn. (Electro-Organic)

Active Members

Seward E. Beacom, General Motors Tech. Center; Mail add: 801 No. Edison St., Royal Oak, Mich. (Electrodeposition)

Francis J. Bourassa, U. S. Dynamics Corp., 1250 Columbus Ave., Boston, Mass. (Electronics)

Nelson P. Bosted, Mellon Institute, Pittsburgh 13, Pa. (Electronics)

Richard C. Bourke, Battelle Memorial Institute, 505 King Ave., Columbus 1, Ohio (Electrothermics & Metallurgy)

Walter R. Buck, III., Virginia Institute for Scientific Research; Mail add: 326 No. Blvd., Richmond 20, Va. (Corrosion)

Alberto M. Campos, University of Santo Tomas; Mail add: 34 Malindang, Quezon City, Philippines (Theoretical Electrochemistry)

Albert P. Centolella, Sumner Chemical Co.; Mail add: 625 E. Lincoln Ave., Zeeland, Mich. (Electro-Organic)

Richard A. Crago, Electro Metallurgical Co.; Mail add: Mineral Springs Rd., Ashtabula, Ohio (Electrodeposition, Electrothermics & Metallurgy)

Willard J. Croxall, Sumner Chemical Co., Elkhart, Ind. (Electro-Organic)

Ward Dickover, National Bureau of Standards; Mail add: 7709 Granada Dr., Bethesda, Md. (Battery)

Fredrick C. Disque, Alpha Metals Inc.; Mail add: 1440 Boynton Ave., Westfield, N. J. (Electronics)

Laurence M. Downes, General Electric Co.; Mail add: RD 3, Doyle Rd., Baldwinsville, N. Y. (Electronics)

Samuel M. Draganov, U. S. Borax & Chemicals Co.; Mail add: 322 No. Vine St., Apt. "A," Anaheim, Calif. (Theoretical Electrochemistry)

Joseph F. Dytrt, Naval Research Lab., 147 Ivanhoe S.W., Washington 24, D. C. (Electrodeposition)

John A. Ewart, Jr., Sumner Chemical Co., 70 W. Ninth St., Holland, Mich. (Electro-Organic)

Robert L. Featherly, Dow Chemical Co.; Mail add: 406 W. Meadowbrook, Midland, Mich. (Battery)

Peter G. Forrester, Glacier Metal Co., Ltd., Kirkstyle, Kilmarnock, Ayrshire, Scotland (Electrodeposition)

Siddhartha Ghosh, Central Electro-Chemical Research Institute, Karaikudi, S. Ry., India (Battery, Electronics, Electrodeposition, Theoretical Electrochemistry)

Errol Goss, Oldham & Sons (Aust.) Pty. Ltd., 15 Catherine St., St. Ives, N.S.W., Australia (Battery)

William R. Harding, Jr., Westinghouse Electric Corp., Youngwood, Pa. (Electronics)

Edward A. Heintz, Metals Research Lab.; Mail add: 76 Blackmon Rd., Grand Island, N. Y. (Electrodeposition, Theoretical Electrochemistry)

Thomas H. Leary, Jr., Sprague Electric Co., Pembroke Rd., Concord, N. H. (Electronics)

Frank J. Lysaght, Electric Storage Battery Co., Box 83, Station H, Toronto 13, Ont., Canada (Battery)

Ralph T. Mead, Wurlitzer Co.; Mail add: 309 McKinley Ave., Kenmore 23, N. Y. (Battery, Theoretical Electrochemistry)

Christian E. Michelson, General Electric Co., 162 Birch Lane, Scotia, N. Y. (Corrosion, Electrodeposition)

Emil M. Murad, Stromberg Carlson Co., Div. of General Dynamics Corp., 76 Turpin St., Rochester 21, N. Y. (Electronics)

Joseph S. Palermo, Mass. Institute of Technology, Project Lincoln, 101 Russell St., Woburn, Mass. (Electronics)

Howard S. Pattin, National Carbon Research Labs.; Mail add: 2191 Wyandotte Ave., Lakewood 7, Ohio (Electronics)

By action of the Board of Directors of the Society, all prospective members must include first year's dues with their applications for membership.

Also, please note that, if sponsors sign the application form itself, processing can be expedited considerably.

Robert S. Peterson, Delco Radio Div., General Motors; Mail add: 1514 W. Walnut St., Kokomo, Ind. (Electrothermics & Metallurgy)

Ann G. Piken, Bendix Research Lab., Box 5115, Detroit 35, Mich. (Electrodeposition, Electronics)

Richard C. Pinkerton, Ethyl Corp., Mail add: 1510 Lee Dr., Baton Rouge, La. (Electro-Organic)

Charles A. Prawdzik, Industro Transistor Corp.; Mail add: 20 Riker Hill Rd., Livingston, N. J. (Electronics)

C. Daniel Richard, Jr., Superior Tube Co., Norristown, Pa. (Electronics)

Frank W. Rudolph, Wurlitzer Co.; Mail add: 342 Traverse Blvd., Kenmore 17, N. Y. (Battery, Electrodeposition)

Anthony S. Rugare, General Electric Co.; Mail add: 1803 W. High Terrace, Syracuse 9, N. Y. (Electronics)

Bernard Selikson, 138 Voorhees St., W. Englewood, N. J. (Electronics)

Sumner Sheff, Mass. Institute of Technology, Lincoln Lab., P.O. Box 73, Lexington 73, Mass. (Theoretical Electrochemistry)

James E. Slager, Sumner Chemical Co.; Mail add: 112 Cambridge, Holland, Mich. (Electro-Organic)

Ambrose W. H. Smith, P. R. Mallory & Co.; Mail add: 402 No. Delaware, Indianapolis 2, Ind. (Battery, Corrosion, Electronics)

Earl L. Steele, Motorola Inc., 5005 East McDowell, Phoenix, Ariz. (Electronics)

Gordon K. Storin, International Graphite & Electrode Div., Speer Carbon Co.; Mail add: 3 Forest Rd., Lewiston Heights, Lewiston, N. Y. (Industrial Electrolytic)

Joseph B. Story, Ethyl Corp.; Mail add: 10576 No. Harvey Dr., Baton Rouge 6, La. (Electro-Organic)

William H. Wise, Electro Metallurgical Co.; Mail add: 7 Kingsbury Lane, Tonawanda, N. Y. (Electrothermics & Metallurgy, Industrial Electrolytic, Theoretical Electrochemistry)

Lawrence Young, B. C. Research Council; Mail add: 56 W. Fairview Ave., U. B. C., Vancouver, B. C., Canada (Electronics, Theoretical Electrochemistry)

Chester S. Zukowski, Wurlitzer Co.; Mail add: 4 Weiss St., Buffalo 6, N. Y. (Electronics, Theoretical Electrochemistry)

Associate Members

David E. Basket, Sumner Chemical Co.; Mail add: 165 W. 17 St., Holland, Mich. (Electro-Organic)

Lawrence C. Kenausis, Harrison Chemistry Lab., University of Pennsylvania, Philadelphia 4, Pa. (Theoretical Electrochemistry)

Transfer from Associate to Active Membership

Ramesh C. Misra, Electro-Chemical Lab., TDE (Electronics), P.O. Box 1504, Bangalore-6, India (Battery, Corrosion, Electrodeposition)

Transfers from Student Associate to Active Membership

Ralph S. Cooper, University of California; Mail add: 4555A Ridgeway Dr., Los Alamos, N. Mex. (Theoretical Electrochemistry)

Norbert D. Greene, Metals Research Labs., P.O. Box 580, Niagara Falls, N. Y. (Corrosion, Theoretical Electrochemistry)

Peter F. King, Dow Chemical Co.; Mail add: 2419 Damman Dr., Apt. 202, Midland, Mich. (Battery, Corrosion, Theoretical Electrochemistry)

Deceased Members

John G. Cashell, Pittsburgh, Pa.
James M. Lohr, Morristown, N. J.

Personals

Walter J. Moore of Indiana University has been appointed Advisory Editor in the field of Chemistry by Dodd, Mead & Co., Inc., New York City. Under Professor Moore's editorship, Dodd, Mead & Co. will seek to publish a selection of textbooks of intellectual and literary distinction in the field of chemistry.

Morton Schwartz has been added to the staff of Kelite Corp.'s Research and Development Labs. in Los Angeles, Calif. Mr. Schwartz will be working in the capacity of senior electrochemist.

Roy E. Heath, a member of the chemistry department faculty at the Michigan College of Mining and Technology, Houghton, Mich., has been promoted to the rank of full professor.

Notice to Members

By now you have received your official voting ballot from Society Headquarters. If you have not already done so, please return the ballot by *December 15* so that your vote can be included in the final election count.

Ralph F. Wehrmann has been appointed assistant director of chemical research at Fansteel Metallurgical Corp., North Chicago, Ill.

Junius D. Edwards

Junius D. Edwards, Assistant Director of Research (Retired), Aluminum Co. of America, New Kensington, Pa., died on August 5, 1957 at the age of 66.

Mr. Edwards was born in Minneapolis, Minn., on March 17, 1890. He studied at the University of Minnesota, receiving his B.S. degree in 1912 and his Chemical Engineering degree in 1913.

He was affiliated with the National Bureau of Standards from 1913 to 1919. From there he went to the Aluminum Co. of America as a physical chemist in 1919, and in 1921 he was appointed Assistant Director of Research. He remained with the company until his retirement in 1955.

Mr. Edwards became a member of The Electrochemical Society in 1925 and served as Society Vice-President during the years 1931-33, 1935-37, and 1939-41. He was also a member of the Institute of Chemical Engineers, Society of Heating and Ventilating Engineering, Illuminating Engineers Society, and the Pennsylvania Chemical Society.

He is survived by his wife, Florence R. Edwards of Delray Beach, Fla.

Alfred J. Liebmann

Alfred J. Liebmann, President of Schenley Research Institute, died on October 11, 1957. He was 71 years old.

Dr. Liebmann was born in Zurich, Switzerland, on August 4, 1885. He received his B.A. degree at the Technische Hochschule there and his Ph.D. degree in chemistry at the University of Zurich.

He came to the United States in 1909 as a research chemist for General Electric in Lynn, Mass., and Harrison, N. J. He returned to Munich and Vienna two years later, but came back to this country in 1912 as general manager and director of the Independent Lamp & Wire Co. in Weehawken, N. J., a post he held for eight years. From 1921 to 1926 he was manager of the Elkon Works for General Electric in Weehawken.

Dr. Liebmann had been with Schenley Industries, Inc., since 1933 as technical director and head of research. His chief fields of interest were in fermentology, antibiotics, and distillation. In 1942 he helped organize the Schenley Research In-

stitute which pioneered the commercial production of penicillin for the Allied forces. During World War II he served the War Production Board as a member of Penicillin Producers Industry Advisory Committee.

In addition to The Electrochemical Society, which he joined in 1910, Dr. Liebmann held memberships in the American Chemical Society, the Society of American Bacteriologists, the New York Academy of Sciences, and others.

He is survived by his wife, Mrs. Edna K. Liebmann, of New York City; three sisters, and a brother.

Letter to the Editor

Dear Sir:

This is a note of appreciation and congratulation for your courage in publishing the October Editorial in Interlingua.

I suppose I represent an average reader and, as such, it is a pleasure to report that I was able to read the entire editorial without difficulty and without reference to a dictionary.

I am looking forward to reading further articles in the JOURNAL published in Interlingua.

Carleton C. Long
St. Joseph Lead Co.
Monaca, Pa.

Book Reviews

Chromium. Vol. II, Metallurgy of Chromium and Its Alloys, by Marvin J. Udy. Am. Chem. Soc. Monograph No. 132; published by Reinhold Publishing Corp., New York, 1956. 402 pages + VIII, with about 70 figures and numerous tables in the text. $11.00, clothbound.

Vol. II consists of 19 chapters, each written by one or several authors; it is edited by Marvin J. Udy, who also wrote 3 of the chapters.

It is subdivided into 3 sections: I. Recovery of chromium from its ores; II. Physical properties of chromium, its alloys and metallurgical use; and III. Chromium in refractories.

Although the book has so many authors, its style is fairly uniform, and the text, with a few pleasant exceptions (e.g., p. 65), is very brief and technical. This makes the references at the end of each chapter valuable, although they refer mainly to the literature written in English. The uniformity of the book is somewhat disturbed by the figures, which differ in style and lettering from chapter to chapter. There is some duplication—for instance, information about chromium carbide and its physical properties is given on pp. 22 and 23; a more detailed description of properties can be found on pp. 114 and 115; the diagram Cr-C is on p. 124. There are no cross references, but the respective places can be found from the subject index.

Twenty-five binary phase diagrams of systems involving chromium are given without further explanation. However, the role of chromium in austenitic steels, in ferritic steels, and in cast iron is treated in three separate chapters in greater detail. The properties of these alloys (e.g., resistance to corrosion) are also described, and the compositions of the alloys are given in tables.

The resistance of chromium nickel-base alloys to oxidation and to high temperature oxidation (in resistance alloys) is also discussed. The chapters on chromium in cobalt, aluminum, copper, and titanium alloys are much shorter.

The chapter on chromium refractories is interesting but somewhat outside the scope of the volume on metallurgy of chromium, except that the refractories are used in metallurgical furnaces.

There are some mistreatments of names in the book; for instance, the names of Hidnert and Tofaute are misspelled (Hindert, p. 146, Ref. 28, 29; Tofante, p. 206, Ref. 43). The reviewer got the impression that in many chapters the literature cited ends with the year 1950, although occasionally articles of a later date, even of 1956 (p. 98), are mentioned. The reliability of the references was not checked.

Aside from these small drawbacks, the volume has a vast amount of useful information, compiled by top experts in the respective fields. It is of importance as a source of information and reference to chemists, metallurgists, and to a lesser degree to solid state physicists.

M. E. Straumanis

The Metallurgy of Zirconium. Edited by B. Lustman and F. Kerze, Jr. Published by McGraw-Hill Book Co., Inc., New York, 1955. First Edition, 776 pages + XVIII. Price $10.00. National Nuclear Energy Series, Division VII, Vol. 4.

It is said in the preface that the book could be published only because of suggestion, support, and encouragement by Rear Admiral H. G. Rickover, and "the objective of the present book is to provide a critical presentation of the many aspects of zirconium technology." Consequently, "as much as possible of the classified data on zirconium which could be declassified has been included in this book." It is not a textbook, but shows in detail the present status of development of zirconium metallurgy in a very broad sense. Each chapter of the book was written by one or several authors, whose critical and authoritative knowledge of the subject was gained during the intense period of nuclear research development sponsored by the Atomic Energy Commission and U. S. Navy.

The introductory chapter deals with history, nuclear properties, and application of zirconium in reactors. The application of the metal for other uses is discussed in Chap. 2. Then only come the descriptions of occurrence (Chap. 3) and of zirconium production methods (Chap. 4). Here, the theories of reduction processes, production techniques, the Kroll process, and the separation of hafnium from zirconium are described in detail. Even more thoroughly (on 80 pages) the iodine-decomposition process for zirconium production is discussed (Chap. 5).

Notice to Subscribers

Your subscription to the JOURNAL of The Electrochemical Society will expire on *December 31, 1957.* Avoid missing any issue. Send us your remittance now in the amount of $18.00 for your 1958 subscription. (Subscribers located outside the United States must add $1.00 to the subscription price for postage, and payment must be made by Money Order or New York draft, not local check.) A final expiration notice has been mailed to all subscribers.

A bound volume of the 1958 JOURNALS can be obtained at a prepublication price of $6.00 by adding this amount to your remittance. However, no orders will be accepted at this rate after *December 1, 1957,* when the price will be increased to $18.00 subject to prior acceptance. Bound volumes are *not* offered independently of your JOURNAL subscription.

The various kinds of zirconium melting, the recovery of scrap, the fabrication (shaping) of the metal, powder metallurgy, joining and refinishing of zirconium are treated in Chap. 6 and 7. The physical metallurgy of zirconium and its alloys is given in Chap. 8, the binary equilibrium diagrams in Chap. 9, and the mechanical properties of the metal (and alloys) in Chap. 10. The corrosion properties of zirconium and its alloys under various conditions of corrosion, including attack by liquid metals, are discussed in the extensive Chap. 11. It was interesting to note that hydrofluoric acid, which destroys zirconium with great rapidity, is not mentioned at all in the article. Chap. 12 deals with the analytical chemistry of zirconium, and in the appendix the metallography of the metal and the industrial hygiene and safety are discussed.

Since at the end of each chapter there is an extensive review of literature (mostly up to 1953), the book is very valuable for all those working with or exploring zirconium, its alloys, and compounds, and will also be useful to those who are merely interested in zirconium and its properties.

It is a question whether the arrangement of the material in the book is suitably appropriate and systematic; however, the investigator will still find it useful. The outer appearance of the book, which is lithoprinted by Edwards Brothers, Inc., Ann Arbor, Mich., is good; the numerous figures, diagrams, and pictures are clear. Extensive name and subject indexes conclude the book.

M. E. Straumanis

Passivierende Filme und Deckschichten—Anlaufschichten—Mechanismus ihrer Entstehung und ihre Schutzwirkung gegen Korrosion (Passivating Films and Protective Layers—Tarnish Coatings—Mechanism of Their Production and Protective Action Against Corrosion). Edited by H. Fischer, K. Hauffe, and W. Wiederholt. Published by Springer-Verlag, Berlin, 1956. XI + 400 pages, 169 figures. Price DM43.50 (about $10.35).

This book is made up of a series of papers presented at a meeting of the Corrosion Division of the German Society for Metallurgy in Frankfurt on October 13 and 14, 1955, together with the discussion. The scaling of metals at high temperatures was not included. The papers were in two groups, one Theoretical and the other Practical, although not well marked in this manner in the book. Good Author and Subject Indexes are provided, the editing appears excellent, and the book is well bound. The titles of the papers are as follows:

Theoretical

K. Hauffe: Scientific and Industrial Problems of Metal Oxidation and Corrosion, pp. 1-21.

P. Kofstad: The Use of Radioactive Isotopes in the Study of High Temperature Oxidation of Metals (In English), (Discussion to Hauffe), pp. 22-42.

E. Fitzer: On the Protective Layer Formation in the Oxidation of Molybdenum Disilicide, (Discussion to Hauffe), pp. 43-54.

H. J. Engell: Oxidation Processes with Non-Parabolic Time Law, pp. 55-66.

K. Nagel: Variation of the Chemical, Electrical, and Electrochemical Potentials in a Solid Corrosion Cell, (Discussion to Engell), pp. 67-71.

K. J. Vetter: On the Mechanism of Electrical Passive Film Formation, pp. 72-91.

K. Nagel: The System Iron—Aqueous Solution as a Multiple Electrode, (Discussion to Vetter), pp. 92-98.

H. Fischer: On the Concept and Mechanism of Inhibition, (Discussion to Vetter), pp. 99-105.

S. Raether and K. Hauffe: On the Mechanism of the Internal Oxidation of Alloys, pp. 106-128.

J. Block: Phase Boundary Reactions in the Oxidation of Metals, pp. 129-159.

W. Jaenicke: The Formation of Porous Protective Films in Corrosion, pp. 160-203, Discussion pp. 208-216.

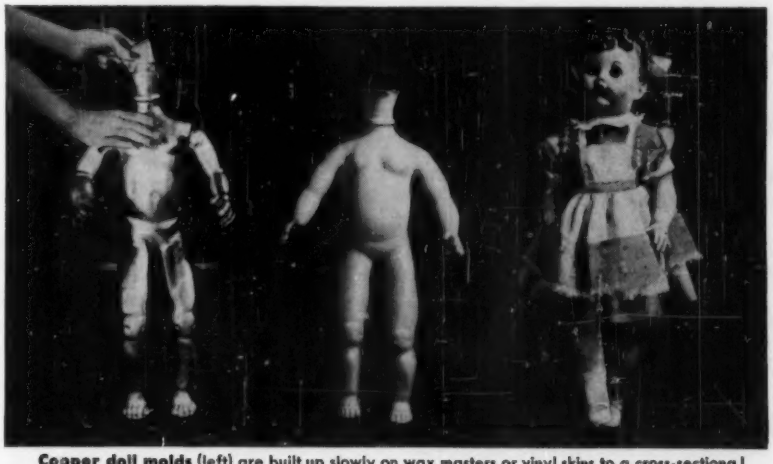

Copper doll molds (left) are built up slowly on wax masters or vinyl skins to a cross-sectional thickness of about .125". Slush-cast vinyl doll skin made in the mold. Finished doll at the right.

"Plus-4" Anodes make superior molds for slush-casting vinyl doll skins

"Electroforming copper molds for producing vinyl doll 'skins' is a tricky business," says Herbert L. Walker, president of The Plastiplate Co., South River, N. J. Details, right down to the toenails, must be reproduced accurately. The molds must be light, yet have the strength and toughness to withstand the strains of production. The deposited copper must be uniform and nonporous to prevent the seepage of water and solvents.

Plastiplate has been using "Plus-4"® Anodes, (Anaconda's phosphorized copper anodes) for about two years. Molds made with "Plus-4" Anodes meet all requirements and are far superior to those formed from ordinary copper anodes. In addition, Mr. Walker listed these operating advantages:

1. "Plus-4" Anodes corrode uniformly, providing about 10% more platable copper.

2. "Plus-4" Anodes do not develop anode sludge—providing more uniform build-up of cathode and a cleaner plating bath.

3. "Plus-4" Anodes give a smooth build-up on the mold, without treeing—and have superior throwing power, giving a better plate on the hard-to-reach surfaces of the mold.

See for yourself how "Plus-4" Anodes can simplify acid-copper electroplating and electroforming, reduce your costs. Write for information on how you can get a test quantity to supply one tank. Address: The American Brass Company, Waterbury 20, Conn. In Canada: Anaconda American Brass Ltd., New Toronto, Ont. 67148

ANACONDA®

"Plus-4" Anodes

(PHOSPHORIZED COPPER)

made by

The American Brass Company

FOR USE UNDER PATENT NO. 2,699,216

Th. Heumann: Report on Pfefferkorn's Electron Microscope Observations on the Needle-Like Growth of Metal Oxides, pp. 204-208.

K. Hauffe: Combined Effect of a Parabolic and Linear Growth of Two Oxide Layers Superimposed Upon Each Other, (Discussion to Block and Jaenicke), pp. 217-220.

Practical

A. Politycki: Experimental Methods for the Investigation of Thin Oxide Layers on Metals, pp. 221-230.

G. Schikorr: The Protective Films Produced During the Atmospheric Corrosion of Metals and Their Protective Action, pp. 231-255.

Th. Heumann: The Role of Alloying Additions in the Formation and Deterioration of Protective Films, pp. 256-288.

E. Raub: Tarnishing Processes with Noble Metals and Their Avoidance, pp. 289-307.

E. Ulrich: The Corrosion of Iron by Steam, pp. 308-333.

H. Keller: The Production of Artificial Protective Coatings by Chemical Means, pp. 334-359.

R. Lattey: Passivation Phenomena in the Chemical Polishing of Aluminum, pp. 360-364.

H. Spähn: On the Chemical Polishing of Copper and Its Alloys, pp. 365-377.

J. Heyes: Protective Films in Electrolytic Polishing, pp. 378-385. (Discussion to Lattey, Spähn, and Heyes, pp. 385-389.)

G. Dubpernell

Handbuch der Technischen Elektrochemie, edited by Georg Eger. **Vol. IV. Part 3A. Die Anwendung des Elektrischen Ofens in der Metallurgischen Industrie, Elektroöfen in der Industrie der Nichteisenmetalle** (Electric Furnaces in the Nonferrous Metal Industry). Published by Akademische Verlagsges, Geest & Portig K.-G., Leipzig, 1956. XII + 323 pages, 143 figures. Price DM36 (about $8.60).

While not originally intended, it has now been decided to include Electrothermics in this Handbook. In addition to the book under review, the volumes of the Handbook appearing since World War II are as follows:

Vol. III, 2nd Ed., 720 pages, 1955, Fused Electrolysis [Reviewed in *This Journal*, **104**, 43C (1957)].

Vol. IV, Part 1, 327 pages, 1950, The Fundamentals of Electric Furnace Heating, by F. Walter.

Vol. IV, Part 2A, 464 pages, 1955, The Application of the Electric Furnace in the Ferrous Metal Industry.

Vol. V, Part 1, 117 pages, 1953, Calcium Carbide and the Carbide Industry, by M. Wildhagen.

The publisher states that a second edition of Vol. I, Part 1, on the Electrometallurgy of Aqueous Solutions, is in preparation and publication is expected in 1958.

The present volume includes the following chapters: Copper, Nickel, Cobalt, and Lead, by O. Barth, 96 pages; Tin—The Electric Smelting of Tin Ores, by C. Ferrante, 28 pages; The Electric Furnace Melting of Zinc Cathodes, by P. Pieper, 42 pages; The Electrothermic Working of Zinc Ores, by G. Björling, 76 pages; The Electrothermic Winning of Aluminum and Aluminum Alloys, by H. Ginsberg and P. Weiss, 49 pages; Magnesium, by E. Bauer, 24 pages.

There is a good Author and Subject Index. The treatment of the literature is for the most part nominal, with only the chapter on Zinc Ores having an extensive list of U. S. and German Patents. The covers are of inexpensive stiff paper, inconsistent with the relatively high price, but of similar appearance to earlier volumes. Vol. IV, Part 1 and V are bound in this way; Volume III is bound with heavy cloth.

G. Dubpernell

Manufacturing Processes, 4th Ed., by M. L. Begeman. Published by John Wiley & Sons, Inc., New York, 1957. 612 pages, including table, diagrams, and text; $8.00.

In the 4th edition of his book, Mr. Begeman has again managed to bring together in a comprehensive manner a variety of standard mechanical manufacturing techniques and operations which should continue to prove of great value to engineering students and practicing engineers. Topics covered include standard Foundry and Metal Casting practice, welding, heat treatment, metal cutting, shaping and working operations of all types, electroforming and coating, and others of common interest to all engineers. Emphasis has been placed on recent new developments, so that the student will gain an up-to-date acquaintance with the various operations.

The author's clarity of presentation makes it easy to use the book as a reference text, and avoids the laborious and time-consuming preparation which is so often necessary when manufacturer's literature or more exhaustive technical treatises are consulted. The book contains a wealth of photographs, schematics, and line diagrams which pinpoint the topics under discussion, thus enabling the reader to obtain a better insight into the operation.

From the standpoint of an instructor, who might wish to use the text in connection with a study of engineering materials and mechanical manufacturing practices, the book also must be commended. The topics are developed in logical sequence, and the various interrelationships are carefully delineated. Moreover, the excellent review questions which appear at the end of each chapter are quite useful and stimulate the student's imagination. In addition, numerous references are quoted, thus greatly enhancing the utility of the text.

William H. Kapfer

CHEMICAL ENGINEER

Company expansion has created the following new position:

CHEMICAL ENGINEER with an advanced degree or equivalent experience in research and development relating to the Electroplating, Electro-Chemical, and high temperature corrosion resistant coatings.

WORKING CONDITIONS are excellent in a new well-equipped laboratory with high-caliber associates.

BENEFIT PLANS are liberal and salary will be commensurate with education and experience. Southeast Michigan Area.

Reply to Box A-272, c/o Journal of The Electrochemical Society

Advertiser's Index

American Brass Company..... 255C
Enthone, Incorporated .....Cover 4
Great Lakes Carbon Corporation .....Cover 2
E. H. Sargent & Company..... 246C

Employment Situation

Please address replies to box shown, c/o The Electrochemical Society, Inc., 1860 Broadway, New York 23, N. Y.

Position Available

Principal Corrosion Engineer: Study of the fundamentals of corrosion relating to ferrous metal in environmental media of liquid metals, aqueous solutions, and gases. Applicant should be Ph.D. grade or 3 to 5 years' experience in corrosion technology. Salary commensurate with ability. Located Western Pennsylvania. Replies confidential. *Reply to Box A-273.*

The Electrochemical Society

INSTRUCTIONS TO AUTHORS OF PAPERS

Address all correspondence to the Editor, JOURNAL OF THE ELECTROCHEMICAL SOCIETY, 1860 BROADWAY, NEW YORK 23, N. Y.

FORM

Manuscripts submitted for publication should be in triplicate to expedite review. They should be typewritten, double-spaced, with 2½-4 cm (1-1½ in.) margins.

Title should be brief, followed by the author's name and his business or university connection.

Abstract of about 100 words should state the scope of the paper and give a brief summary of results.

ILLUSTRATIONS

Drawings will be reduced to column width, 8.3 cm (3¼ in.), after reduction should have lettering at least 0.15 cm (1/16 in.) high. Original drawings in India ink on tracing cloth or white paper are preferred. Curves may be drawn on coordinate paper only if the paper is ruled in blue. All lettering must be of lettering-guide quality. See sample drawing on reverse page.

Photographs must be glossy prints and mounted flat.

Captions for all figures must be included on a separate sheet. Captions and figure numbers should not appear in the body of the figure.

General—Figures should be used only when necessary. Omit drawings or photographs of familiar equipment. Figures from other publications are to be used only when the publication is not readily available, and should always be accompanied with written permission for reprinting.

REFERENCES

Literature and patent references should be listed at the end of the paper on a separate sheet, in the order in which they are cited. They should be given in the style adopted by *Chemical Abstracts*. For example:

R. Freas, *Trans. Electrochem. Soc.*, **40**, 109 (1921).

H. T. S. Britton, "Hydrogen Ions," Vol. **1**, p. 309, D. Van Nostrand Co., New York (1943).

H. F. Weiss (To Wood Conversion Co.), U. S. Pat. 1,695,445, Dec. 18, 1928.

UNITS OF MEASUREMENT

Metric units should be used throughout but, where desirable, English units may be given in parentheses.

Corrosion rates in the metric system should preferably be expressed as milligrams per square decimeter per day (mdd), and in the English system as inches penetration per year (ipy).

As regards algebraic signs of potentials, the standard electrode potential for $Zn \rightarrow Zn^{++} + 2e$ is negative; for $Cu \rightarrow Cu^{++} + 2e$, positive.

ABBREVIATIONS

Abbreviations should conform with the American Standards Association's list of "Abbreviations for Scientific and Engineering Terms."

GENERAL

Authors should be as brief as is consistent with clarity, and must omit all material which can be regarded as familiar to specialists in the particular field.

The use of proprietary names, trade-marks, and trade names should be avoided if possible. If used, these should be capitalized so that the owner's legal rights are not jeopardized.

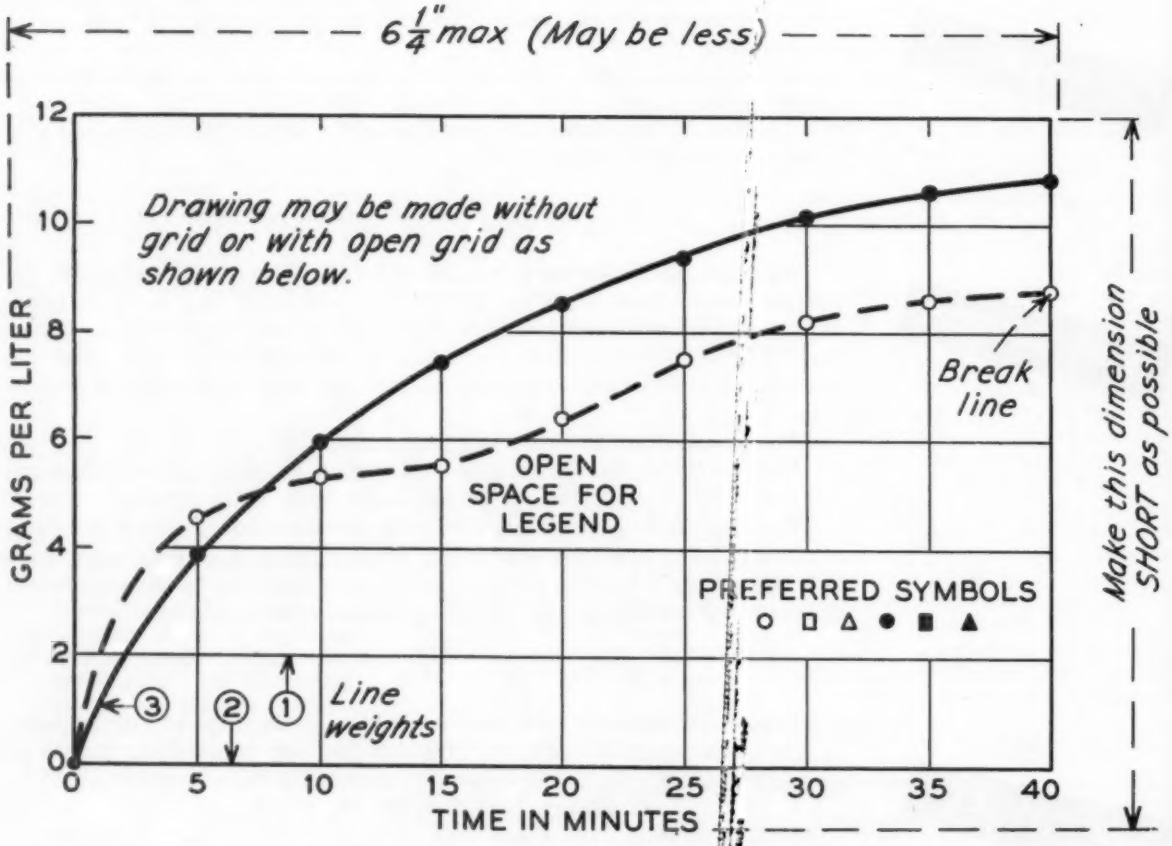

Remarks: Line weight ② is used for borders and zero lines. When several curves are shown, each may be numbered and described in the caption. Lettering is approx. 1/8".

SAMPLE CURVE DRAWING FOR REDUCTION TO $\frac{1}{2}$ SIZE

The Electrochemical Society

INSTRUCTIONS TO AUTHORS OF PAPERS

Address all correspondence to the Editor, JOURNAL OF THE ELECTROCHEMICAL SOCIETY, 1860 BROADWAY, NEW YORK 23, N. Y.

FORM

Manuscripts submitted for publication should be in triplicate to expedite review. They should be typewritten, double-spaced, with 2½-4 cm (1-1½ in.) margins.

Title should be brief, followed by the author's name and his business or university connection.

Abstract of about 100 words should state the scope of the paper and give a brief summary of results.

ILLUSTRATIONS

Drawings will be reduced to column width, 8.3 cm (3¼ in.), after reduction should have lettering at least 0.15 cm (1/16 in.) high. Original drawings in India ink on tracing cloth or white paper are preferred. Curves may be drawn on coordinate paper only if the paper is ruled in blue. All lettering must be of lettering-guide quality. See sample drawing on reverse page.

Photographs must be glossy prints and mounted flat.

Captions for all figures must be included on a separate sheet. Captions and figure numbers should not appear in the body of the figure.

General—Figures should be used only when necessary. Omit drawings or photographs of familiar equipment. Figures from other publications are to be used only when the publication is not readily available, and should always be accompanied with written permission for reprinting.

REFERENCES

Literature and patent references should be listed at the end of the paper on a separate sheet, in the order in which they are cited. They should be given in the style adopted by *Chemical Abstracts*. For example:

R. Freas, *Trans. Electrochem. Soc.*, **40**, 109 (1921).

H. T. S. Britton, "Hydrogen Ions," Vol. **1**, p. 309, D. Van Nostrand Co., New York (1943).

H. F. Weiss (To Wood Conversion Co.), U. S. Pat. 1,695,445, Dec. 18, 1928.

UNITS OF MEASUREMENT

Metric units should be used throughout but, where desirable, English units may be given in parentheses.

Corrosion rates in the metric system should preferably be expressed as milligrams per square decimeter per day (mdd), and in the English system as inches penetration per year (ipy).

As regards algebraic signs of potentials, the standard electrode potential for $Zn \rightarrow Zn^{++} + 2e$ is negative; for $Cu \rightarrow Cu^{++} + 2e$, positive.

ABBREVIATIONS

Abbreviations should conform with the American Standards Association's list of "Abbreviations for Scientific and Engineering Terms."

GENERAL

Authors should be as brief as is consistent with clarity, and must omit all material which can be regarded as familiar to specialists in the particular field.

The use of proprietary names, trade-marks, and trade names should be avoided if possible. If used, these should be capitalized so that the owner's legal rights are not jeopardized.

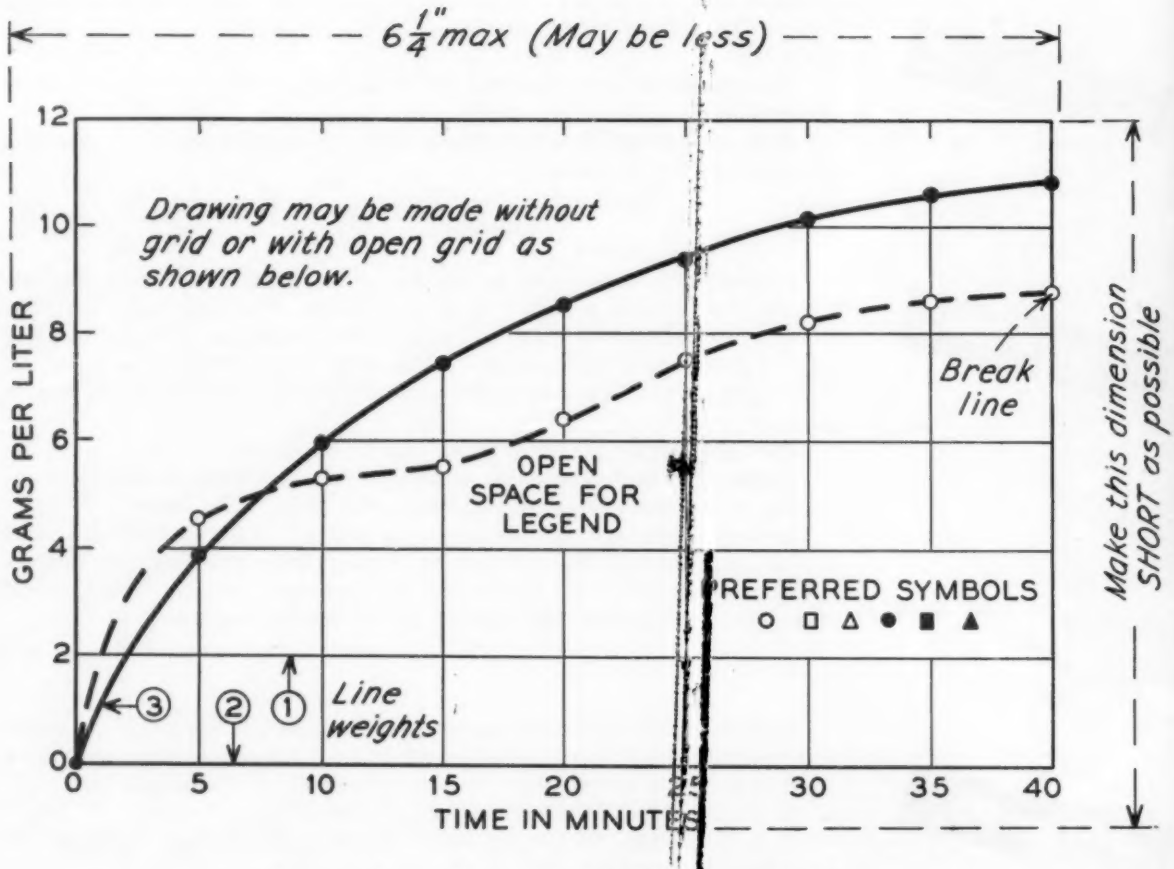

Remarks: Line weight ② is used for borders and zero lines. When several curves are shown, each may be numbered and described in the caption. Lettering is approx. 1/8".

SAMPLE CURVE DRAWING FOR REDUCTION TO $\frac{1}{2}$ SIZE

THE ELECTROCHEMICAL SOCIETY, INC.

The Electrochemical Society is an international organization of individuals and companies concerned with or interested in Electrochemistry and allied subjects.

The Society is dedicated to the advancement of the theory and practice of Electrochemistry and related subjects, as shown in the following divisions:

Battery	Electro-Organic
Corrosion	Electrothermics and Metallurgy
Electric Insulation	Industrial Electrolytic
Electrodeposition	Theoretical Electrochemistry
Electronics	

Among the means to this end are the holding of meetings for the reading and discussion of professional and scientific papers on these subjects, the publication of such papers, discussions, and communications as may seem appropriate, and cooperation with chemical, electrical, and other scientific and technical societies.

It is an incorporated society without capital stock. The affairs of the Society are managed by a Board of Directors under a Constitution and Bylaws. Officers are nominated by a nominating committee appointed by the Board of Directors and elected by the members.

Direct all general correspondence and inquiries regarding membership to Society headquarters at 1860 Broadway, New York 23, N. Y.

Officers of the Society

President	NORMAN HACKERMAN
Past President	HANS THURNAUER
Vice-President	SHERLOCK SWANN, JR.
Vice-President	W. C. GARDINER
Vice-President	R. A. SCHAEFER
Treasurer	LYLE I. GILBERTSON
Secretary	HENRY B. LINFORD